PYROLYSIS AND GASIFICATION OF LIGNIN AND EFFECT OF ALKALI ADDITION

A Thesis
Presented to
The Academic Faculty

by

Vipul Kumar

In Partial Fulfillment
of the Requirements for the Degree
Doctor of Philosophy in the
School of Chemical & Biomolecular Engineering

Georgia Institute of Technology
August, 2009

PYROLYSIS AND GASIFICATION OF LIGNIN AND EFFECT OF ALKALI ADDITION

Approved by:

Dr. Sujit Banerjee, Advisor
School of Chemical & Biomolecular Engineering
Georgia Institute of Technology

Dr. Jim Frederick, Co-Advisor
School of Chemical & Biomolecular Engineering
Georgia Institute of Technology

Dr. Kristiina Iisa
National Renewable Energy Laboratory

Dr. John D. Muzzy
School of Chemical & Biomolecular Engineering
Georgia Institute of Technology

Dr. Preet Singh
School of Material Science & Engineering
Georgia Institute of Technology

Date Approved: February 27, 2009

To my late mother

ACKNOWLEDGEMENTS

I would like to acknowledge all the people who helped me throughout this research project. I would like to thank my advisor Dr. Sujit Banerjee for his guidance and continued support. I would also like to thank Dr. Jim Frederick and Dr. Kristiina Iisa for their support and insight into my research. I would like to thank my thesis committee members, Dr. John D. Muzzy and Dr. Preet Singh for their time and effort.

I would also like to thank Dr. Haskell W. Beckham from School of Polymer, Textile and Fiber Engineering for allowing me to use Thermogravimetric Analyzer. Thanks also to Mike Buchanan, Xiaoyan Zeng, Ryan Kincer, Allan Ball, Scott Sinquefield, Tuan Le, Rallming Yang, Chuck Courchene, John Reye and the chemical analysis group for their support and advice during my research work.

Next, I would like to thank my wife for her encouragement and support through thick and thin. I would also like to thank my family members for their support. Lastly I would like to acknowledge my friends for their help. I could not have done it without help and encouragement from all of you.

TABLE OF CONTENTS

Page

LIST OF TABLES

Page

LIST OF FIGURES

Page

NOMENCLATURE

AES	Atomic Emission Spectrometry
ASAM	Alkaline Sulfite Anthraquinone Methanol
CEL	Celluloytic Enzyme Lignin
CFD	Computational Fluid Dynamics
CHP	Combined Heat and Power
DSC	Differential Scanning Calorimetry
DTA	Differential Thermal Analyzer
DTG	Differential Thermogravimetry
FTIR	Fourier Transform Infrared
G	Guaiacyl
GC	Gaschromatograph
ICP	Inductively Coupled Plasma
IFBR	Integrated Forest Biorefinery
IGCC	Integrated Gasification Combined Cycle
IR	Infrared
KBr	Potassium Bromide
LEFR	Laminar Entrained Flow Reactor
LCF	Lignocellulosic Feedstock
MWL	Milled Wood Lignin
MWV	MeadWestvaco
QC	Quebrancho Colorado
PCC	Precipitated Calcium Carbonate

S	Syringyl
SA	Sigma Aldrich
SEM	Scanning Electron Microscope
SRC	Short Rotation Willow Coppice
T_R	Characteristic Temperature
TGA	Thermogravimetric Analyzer

SUMMARY

Lignin is the second most abundant naturally occurring polymer. It is a major constituent of biomass and woody biomass typically contains 20-30% lignin. Lignin contains nearly 60 % carbon and can be used as a source of energy. Gasification is a process in which carbon based fuel is converted into gases such as H_2, CO and CH_4 that have useable heating value. Lignin is a byproduct of the chemical pulping and is currently burned in recovery boilers to recover the inorganic cooking chemicals as well as to produce steam for the mill. Lignin is also produced as a byproduct during ethanol production by fermentation of lignocellulosic biomass. It can be gasified to produce fuel gas and value-added products.

This study focused on developing a better understanding of pyrolysis and gasification of lignin. Two lignins, MeadWestvaco (MWV) lignin and Sigma Aldrich (SA) lignin, were studied using two different reactors. A laminar entrained flow reactor was used initially to determine the effect of lignin type, temperature and residence time on char yield and fixed carbon conversion during pyrolysis and gasification. During both pyrolysis and gasification, the maximum decrease in char yield took place in the initial stage of the reaction and there was little change at longer residence times. There was not much difference between pyrolysis and gasification in the residence times obtained in the LEFR, and a longer residence time is required for substantial gasification to take place. The morphology of particles changed and swelling took place during pyrolysis and gasification.

Further study was done with a thermogravimetric analyzer to study the effect of lignin type on pyrolysis and gasification. The reaction rate and char yield were affected by the lignin composition. The pyrolysis behavior of lignin showed similar behavior until 600 °C but only the high-ash SA lignin showed secondary pyrolysis reactions above 600°C. Carbon gasification reactions were delayed in SA lignin.

Na_2CO_3 was added to the lignins to understand the difference in the behavior of SA lignin and MWV lignin during pyrolysis and gasification. The effect of other alkali salts Na_2SO_4, Li_2CO_3 and K_2CO_3 was also studied. Na_2CO_3 made the primary pyrolysis reaction occur at a lower rate and enhanced the rate for secondary pyrolysis reactions.

Changes in lignin structure during pyrolysis and gasification with increase in temperature were studied using Fourier Transform Infrared (FTIR) Spectroscopy. Significant loss of spectral detail started at different temperatures for MWV lignin and SA lignin.

Finally, kinetic parameters were studied using differential and Coats – Redfern integral method. Both methods gave comparable results at lower temperatures but the results varied at high temperatures. The differential method gave overall more consistent results. The addition of Na_2CO_3 decreased the activation energy of primary pyrolysis.

CHAPTER I

INTRODUCTION

The demand for energy is increasing every day and there is a need to find new energy resources and technologies to meet this requirement. Until the discovery of low cost petroleum and natural gas, wood was used for heat and energy requirements. But as the available recourses of petroleum are shrinking and the cost is increasing, alternative and renewable fuel resources are needed. Biomass is constantly produced on earth and will play a great role as a renewable energy resource in the long term future. Sustainable heat, power, and transportation fuels generation from biomass is one of the most researched areas currently in chemical engineering.

The energy crisis along with concerns over increase in the amount of carbon dioxide in the atmosphere has made biomass a good source of "non-greenhouse" energy. Combustion of fossil fuels increases CO_2 content in the atmosphere and causes climate change. Use of biomass fuel as an energy source also has the potential to ameliorate CO_2 emissions. Use of biomass as fuel recycles atmospheric carbon unlike the conversion of fossilized carbon which only produces atmospheric carbon. Biomass fuels are CO_2 neutral and their use also reduces the emissions of NOx, SOx, and heavy metals.

Biomass has a higher volatile content than coal and it also contains oxygen. Biomass has lower carbon content and higher hydrogen to carbon ratio than coal. Wood-derived biomass consists of three principal components – cellulose, hemicellulose and lignin - along with minor amounts of extractives [1, 2].

Gasification is also called “staged combustion”, because the gas produced may be burnt later. Following are advantages of first gasifying and then burning over just burning of biomass [1].

- Ease of distribution in pipeline
- Continuous operation
- Easy control
- Efficient combustion since the correct amount of air can be mixed for optimum combustion
- Clean combustion since impurities are removed in the gasifier
- High temperature combustion for making glass or cement
- Intense combustion, increasing heat transfer an order of magnitude over coal and biomass
- Power generation
- Chemical synthesis

1.1 Biomass pyrolysis and gasification:

Gasification is a process in which carbon based fuel is converted into gases such as H_2, CO and CH_4 that have useable heating value. During the gasification process a number of exothermic and endothermic reactions take place. Heat needed for endothermic reactions is provided by combustion or partial combustion reactions. Air or oxygen can be used to produce combustible gas with medium calorific values ranging from 6 to 16 MJ/m^3 [3]. Gasification is an important process as it can be used to produce a consistent product that can generate electricity or can be used for manufacturing chemicals and transportation fuels. During gasification, physical,

chemical and thermal processes may take place sequentially or simultaneously, depending on the reactor design and the feedstock [4].

Drying:

When the feedstock is heated and its temperature increases the water evaporates first.

Devolatilization:

It is also called pyrolysis. When the temperature increases further, pyrolysis takes place and the feedstock is converted to char.

Dry feedstock + Heat → Char + Volatiles

The volatiles produced depend on the origin of the feedstock. They may include H_2O, H_2, N_2, O_2, CO_2, CO, CH_4, H_2S, NH_3, C_2H_6 and unsaturated hydrocarbons such as acetylenes, olefins, and aromatic materials.

Gasification:

Gasification occurs due to chemical reactions between the carbon in the char and steam, CO_2 and H_2 in the gasifier. There are reactions among the resulting gases as well [4].

$C + H_2O + Heat \rightarrow CO + H_2$

$C + 2H_2O + Heat \rightarrow CO_2 + 2H_2$

$C + CO_2 + Heat \rightarrow 2CO$

$C + 2H_2 \leftrightarrow CH_4 + Heat$

$CO + 3H_2 + Heat \leftrightarrow CH_4 + H_2O$

$CO + H_2O + Heat \leftrightarrow H_2 + CO_2$

Pyrolysis and gasification processes are shown in Figure 1. When an O_2-containing gasification agent (O_2, air, or a mixture of O_2 and steam) is used to partially oxidize the feedstock, direct gasification takes place. If gasification is done using an O_2-free gasification agent such as steam, an external energy source is needed, and the process is called indirect gasification. When indirect gasification is done in an inert gas atmosphere, the process is called pyrolysis. These processes produce three main products: combustible gas, tar, and char [5].

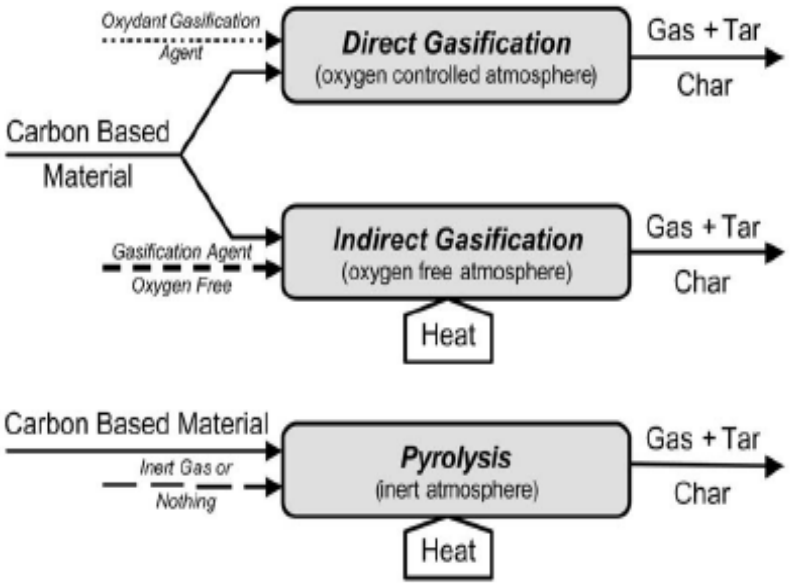

Figure 1: Gasification and pyrolysis processes [5]

Chemical composition, heating value and end use application of the product gas depend on a number of factors such as the nature of the gasification agent (air, oxygen, or steam),

temperature, and the pressure of reactor. Others factors influencing the products are feedstock composition, particle size, reactor heating rate, residence time, plant configurations etc [4].

Gasification differs from combustion in many respects. Combustion is an exothermic reaction which takes place under oxidative conditions in the presence of oxygen or air. Gasification is endothermic and heat has to be provided for the reaction to occur. With Integrated Gasification Combined Cycle (IGCC) it is possible to obtain more electrical output per unit of fuel by gasification than by combustion [6].

Currently coal or biomass is gasified to produce energy only in a limited number of plants. The fuel is fed into a gasifier and allowed to react with a carrier gas such as oxygen, air, water vapor or carbon dioxide, which produces a mixture of combustible gases consisting of CO, H_2 and CH_4 [6].

Integrated Gasification Combined Cycle (IGCC) is one of the emerging technologies to generate electricity using gasification. In this system, syngas produced during gasification drives a gas turbine and exhaust gases are heat exchanged to generate superheated steam which drives a steam turbine to produce additional electricity. This system produces very low pollution and runs at high efficiency. Figure 2 shows a schematic diagram of IGCC using a pressurized fluidized-bed coal gasification system. Biomass is also a potential fuel for IGCC. In addition to electricity production, the syngas can be used for synthesis of fuels or chemicals.

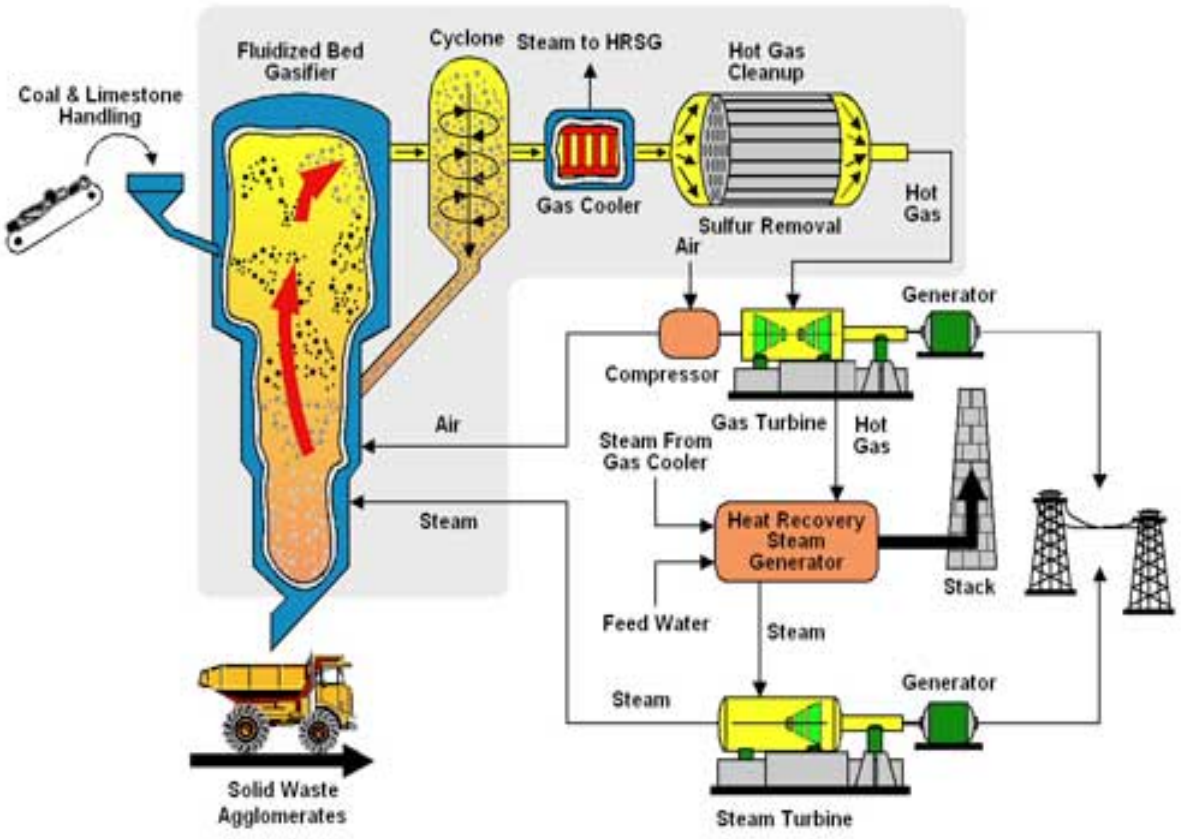

Figure 2: IGCC using pressurized fluidized-bed coal gasification system [7].

Cold gas efficiency is termed as the ratio of the energy of the produced gas to that of biomass. It is an important factor in determining the effectiveness of biomass used in gasification. Cold gas efficiency can be increased by decreasing oxygen use and increasing steam utilization. This results in a low reaction temperature, which is not desirable [8]. Previous studies[9-11] have demonstrated a cold gas efficiency of 35-70% during air gasification of biomass. Other studies [12-13] showed that fluidized bed steam-oxygen gasification without any catalyst resulted in a cold gas efficiency of 65-125%.

1.2 Lignin:

Lignin is the second most abundant naturally occurring biopolymer. Lignin is an important part of the cell wall. It is an amorphous, highly-polymerized substance. Lignin works as the cementing material for wood fibers and is present in the form of middle lamella. Figure 3 shows a SEM picture of the middle lamella which consists of lignin. It is very hard to isolate lignin from other wood components [14].

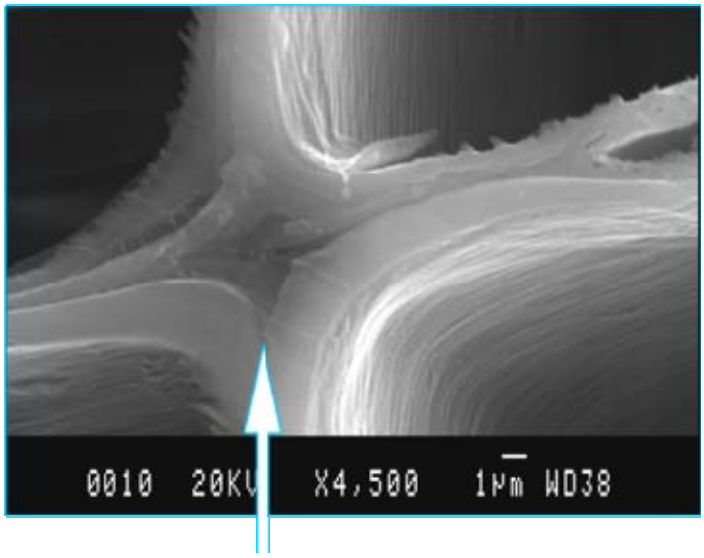

Figure 3: Lignin rich middle lamella holding the cell walls together [15].

Lignin has a very complex structure consisting primarily of phenyl propane units derived from three cinnamyl alcohols; p-coumaryl, coniferyl, and synapyl alcohols. Figure 4 and Figure 5 show the structural units and an example of structure of lignin.

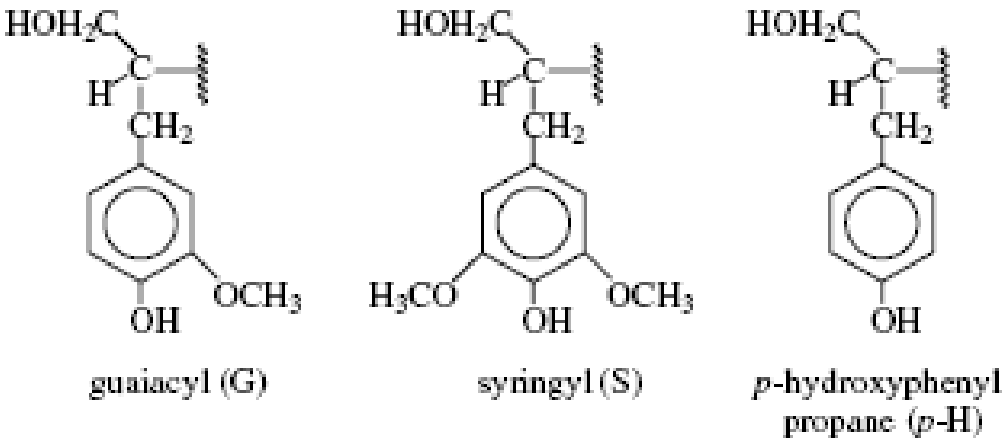

Figure 4: Structural units of lignin [16]

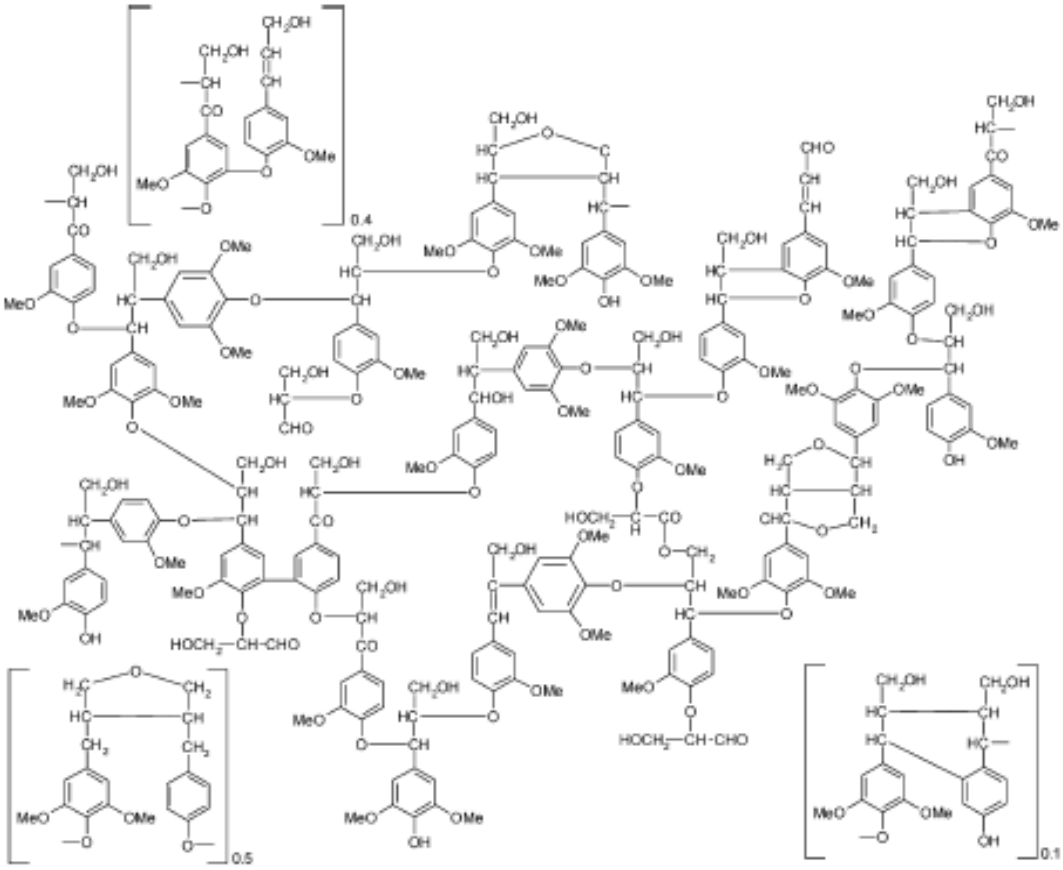

Figure 5: Lignin structure [17]

Lignin structure varies with the wood type and the species. Softwoods and hardwoods contain nearly 28% and 20% lignin, respectively. The typical carbon contents of softwood lignin and hardwood lignin are 64% and 60% respectively [2, 14].

Despite the present technological development and availability of different methods and methodologies to obtain lignin, its structure still needs to be accurately established. One of the most important problems in elucidating the structure of lignin has been the isolation of all of the lignin from wood in a chemically unaltered form [18-20].

The structure of lignin varies depending on the method used and the morphological regions from which it was obtained. Softwood only contains mainly guaiacyl units and hardwood contains both guaiacyl and syringyl units.

There are different methods to separate lignin from biomass. Hydrochloric acid, enzymatic treatment and steam explosion are well known methods for lignin separation. Currently the most used techniques to isolate lignin from wood without altering the structure are based on the extraction of ball-milled wood by neutral solvents. Milled wood lignin (MWL) is extracted from finely milled wood without any previous treatment while celluloytic enzyme lignin (CEL) utilizes celluloytic enzymes to remove most of the carbohydrate fractions before an aqueous dioxane extraction of ball-milled wood meal [18].

Different factors influence the properties and functionality of lignin preparations [21].

- Source of lignin
- Methods used to remove lignin from the plant
- Method(s) used for lignin purification
- The nature of the chemical modification of the lignin

1.2.1 Lignin from the pulping process:

Lignin is a major byproduct of the pulping process. The kraft process separates nearly 25 million tons of lignin per year in North America. In the kraft pulping process NaOH and Na_2S are used as cooking chemicals to dissolve lignin. Chemical breakage and solubilization of lignin take place during kraft pulping. During this process black liquor is produced. Black liquor contains almost all the cooking chemicals along with lignin and other organic matter separated from the wood. Lignin cannot be completely removed from the pulp and a certain amount of lignin remains in fibers causing the dark color of chemical pulps [22].

Lignin works as a low-grade fuel for the pulp and paper industry. It is burned in a recovery boiler to recover the inorganic cooking chemicals used in the pulping process as well as to produce steam for the mill. Figure 6 shows a schematic diagram of a recovery boiler.

There are other ways of processing black liquor which would allow for the production of lignin. Kraft lignin can be precipitated from black liquor and then converted to useful products such as activated carbon. There have been some studies in the past leading to the production of activated carbon by pyrolysis and gasification of Kraft lignin [23, 24]. Lignin can be gasified to produce

value-added products such as hydrogen, high Btu gas and aromatics that can improve the paper industry's global competitive position [24].

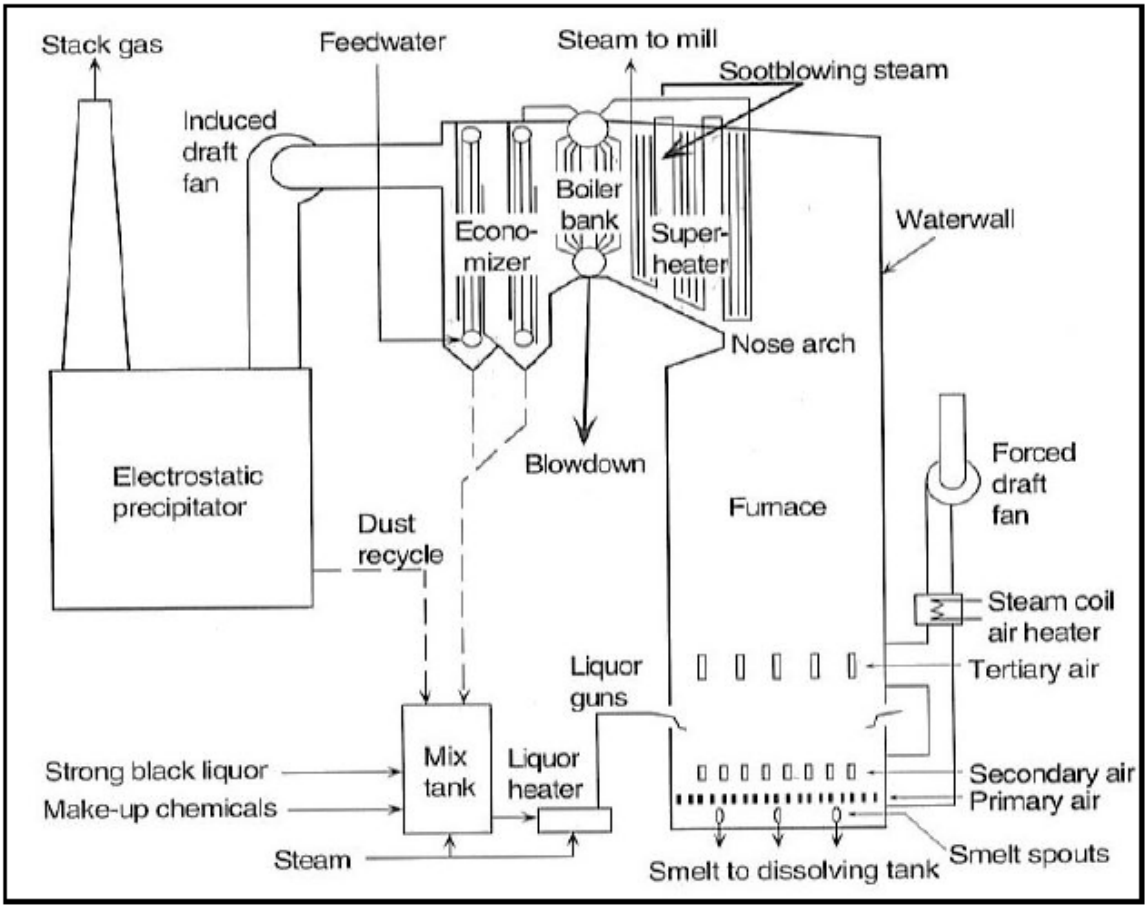

Figure 6: Kraft recovery boiler [22]

In a conventional paper mill powerhouse, black liquor is fired in a recovery boiler to produce high pressure steam which is then expanded in a steam turbine in a combined heat and power (CHP) unit. High power-to-heat ratio can be achieved if black liquor is gasified and combusted in a gas turbine CHP unit. This strategy should be very useful for future paper mills, for which available internal biomass fuels will be more than sufficient to satisfy the mill's heat demand. The excess biofuel could be used on-site to generate electricity for export or for use in other applications [25].

Figure 7 represents a schematic process layout of a black liquor gasification combined cycle powerhouse system. It includes the following operations.

- oxygen-blown, high temperature (ca 950 °C), pressurized (ca 25 bar) entrained flow gasifier
- rapid cooling of the product gas flow in a quench vessel
- further cooling of the gas in a waste heat boiler
- cryogenic air separation unit, partly integrated with the gas turbine
- acid gas removal system, with H_2S recycle to the gasifier
- combustion of the gas in an "F" class gas turbine, modified for air extraction,
- cooling of the gas turbine exhaust in a three-pressure heat recovery steam generator
- steam distribution system (including a back-pressure steam turbine)

If the black liquor gasification system is not able to generate enough process steam to meet the mill's demand, additional process steam can be produced using a lignin and black liquor co-gasifier. In this system, lignin may be imported and mixed with the available black liquor and gasified in the existing black liquor gasifier [25].

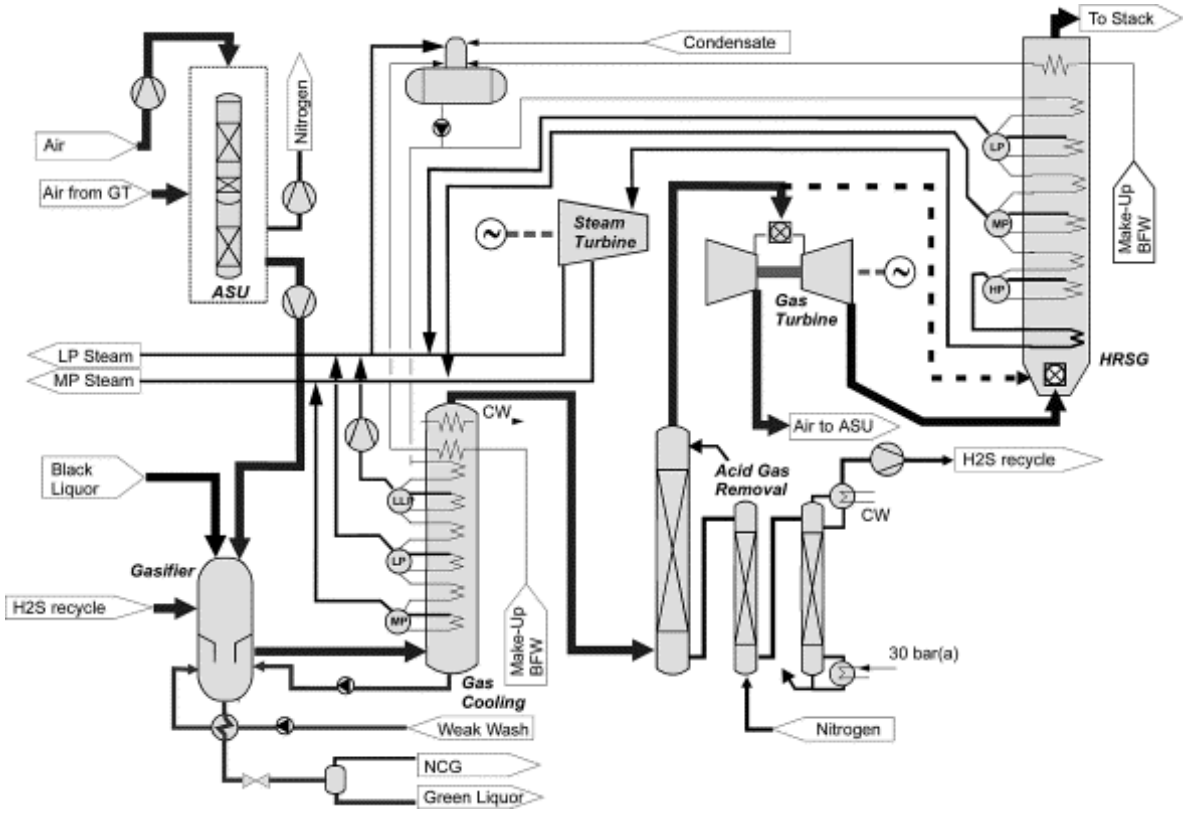

Figure 7: Flow sheet schematic of a black liquor gasification combined cycle powerhouse system [25]

In addition to the Kraft pulping process, lignin is also separated from other wood components by one of the following processes [21].

- Sulfate pulping
- Sulfite pulping
- Organosolv pulping
    - Ethanol/water pulping (Alcell)
    - Alkaline sulfite anthraquinone methanol pulping (ASAM)
    - Organocell pulping
    - Acetic acid/HCL pulping

1.2.2 Lignin from biochemical biorefineries:

Biorefineries that process lignocellulosic materials with the main purpose of producing ethanol from fermentable sugars from cellulose and hemicellulose are planned in the US and elsewhere in the world. They would produce lignin as a wet, solid residue that remains after the saccharification and/or fermentation stages, often in a form contaminated with residual cellulose. In the future, these biorefineries could produce lignin in very large quantities. Also, the lignin produced in this way will most probably have better performance quality and be of greater commercial value for its chemical properties than lignin from a chemical pulping process [26].

In a biorefinery different methods may be used to convert lignocelluloses into fuels, chemicals, polymers, and many other materials. Figure 8 shows the schematic diagram of a lignocellulosic biorefinery.

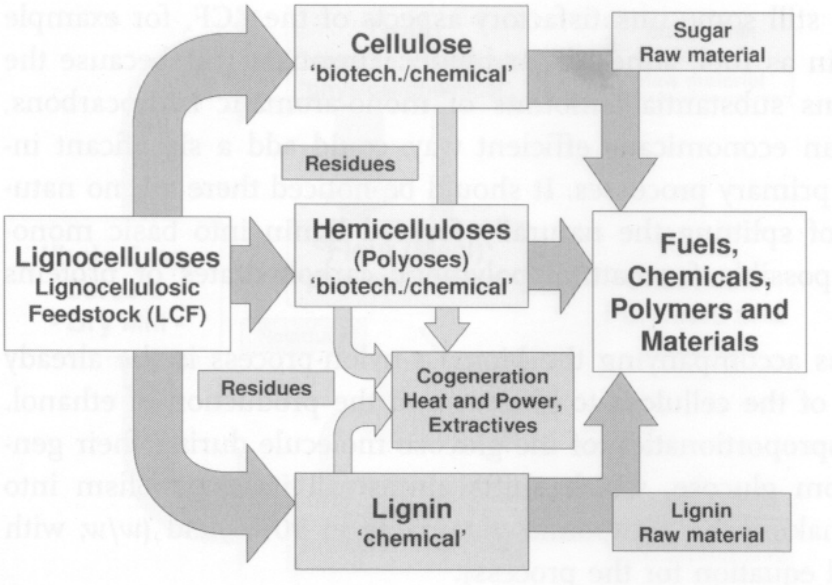

Figure 8: General scheme of a biochemical lignocellulosic feedstock biorefinery [26]

There are different physical and chemical methods used for pretreatment of lignocellulosic materials to separate cellulose from lignin [26].

1. Physical pre-treatment:

- Milling and grinding
- High-pressure steaming and steam explosion
- Extrusion and expansion
- High-energy radiation

2. Chemical methods:

- Alkali treatment
- Acid treatment
- Gas treatment
- Oxidizing agents
- Cellulose solvents
- Solvent extraction of lignin
- Swelling agents

3. Biological methods:

- Lignin-consuming microorganisms
- Cellulose-attacking microorganism
- Lignin and cellulose-attacking microorganism
- Lignin and/or cellulose attacking insects

In the last few years, enzymatic hydrolysis has gained importance as a method to convert cellulose to glucose for the production of ethanol from lignocellulose. Biorefoneries utilizing enzymatic hydrolysis typically consist of four main steps,

(i) Pretreatment

(ii) Enzyme production

(iii) Hydrolysis

(iv) Fermentation.

There are no side reactions or by-products from enzymatic hydrolysis. The hydrolysis process can potentially be performed with nearly 100% yields of glucose production from cellulose [26]. Enzymatic transformation of lignocelluloses into ethanol is shown in Figure 9.

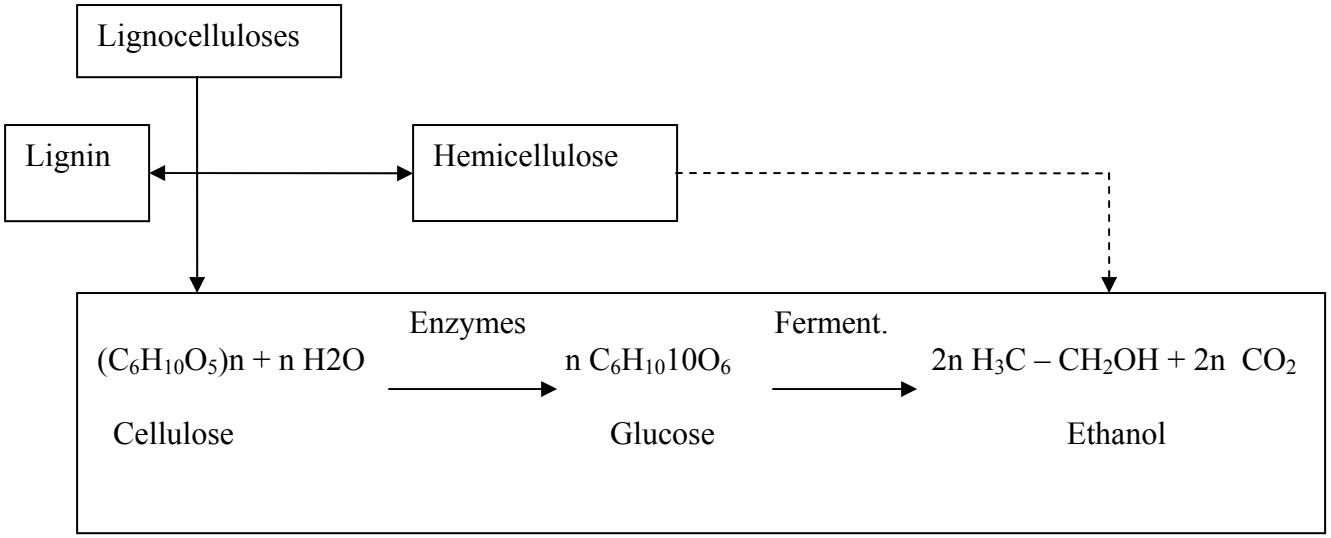

Figure 9: Enzymatic transformation of lignocelluloses into ethanol [26]

CHAPTER II

LITERATURE REVIEW

2.1 Biorefinery concept:

A biorefinery integrates biomass conversion processes and equipment to co-produce fuels, power, and chemicals from biomass. Figure 10 shows a detailed overview of an integrated biorefinery process. The biorefinery concept is analogous to today's petroleum refineries. A biorefinery can produce low volume but high value chemical products and low value but high volume platform chemicals and liquid transportation fuel. It can also be used for generating electric power and heat for its own use as well as for sale. High value products increase profitability and high volume chemicals and liquid transportation fuels fills energy needs [27].

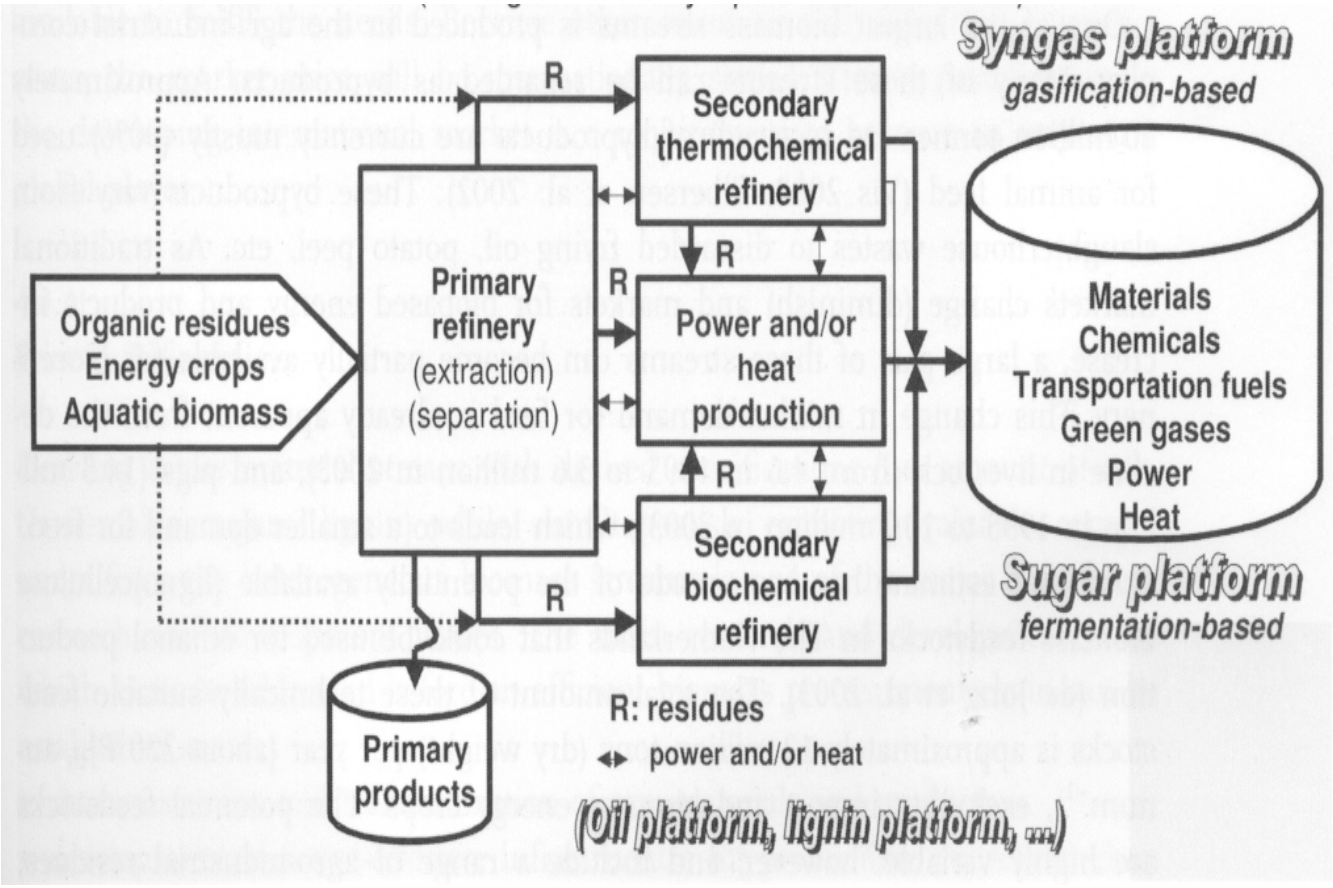

Figure 10: Detailed overview of integrated biorefinery process [27]

Some agricultural and forest product facilities such as pulp mills, corn wet milling, starch and sugar beet refining mills are very suitable for biorefineries, Some biorefineries are already in existence [27].

2.1.1 Integrated forest biorefinery

With the increasing global competition, pulp and paper industries need to change their business model. They can increase their revenue by producing bioenergy and biomaterials along with the existing pulp and paper products. This new concept, called Integrated Forest Biorefinery (IFBR)

is being evaluated by the existing pulp and paper mills. A chemical pulp mill can be transformed into an IFBR, which can produce higher value added commodity products such as ethanol, polymers and diesel fuel along with pulp [28].

Figure 11 represents an alkaline pulping based IFBR system. The round-cornered boxes with dotted line on the right hand side represent new products such as wood composites, liquid fuel, lignin-based chemicals, ethanol, and sugar-based chemicals and polymers. New processes, represented by dotted-line boxes inside the Figure need to be further developed before this concept can be successful [28].

Wood chips are cooked at temperatures higher than 100°C with caustic solution, and hemicelluloses are extracted. This produces dissolved polymeric hemicelluloses with some lignin. The extracted chips will go through alkaline pulping, where fibers are liberated and black liquor is produced. Pre-extraction generates a feed stream for new bioproducts. It also decreases alkali consumption during pulping, increases delignification rate and reduces black liquor load. IFPR may also involve black liquor gasification and/or lignin precipitation. Precipitated lignin and synthesis gas work as feed stocks for polyurethanes and liquid fuels respectively [28].

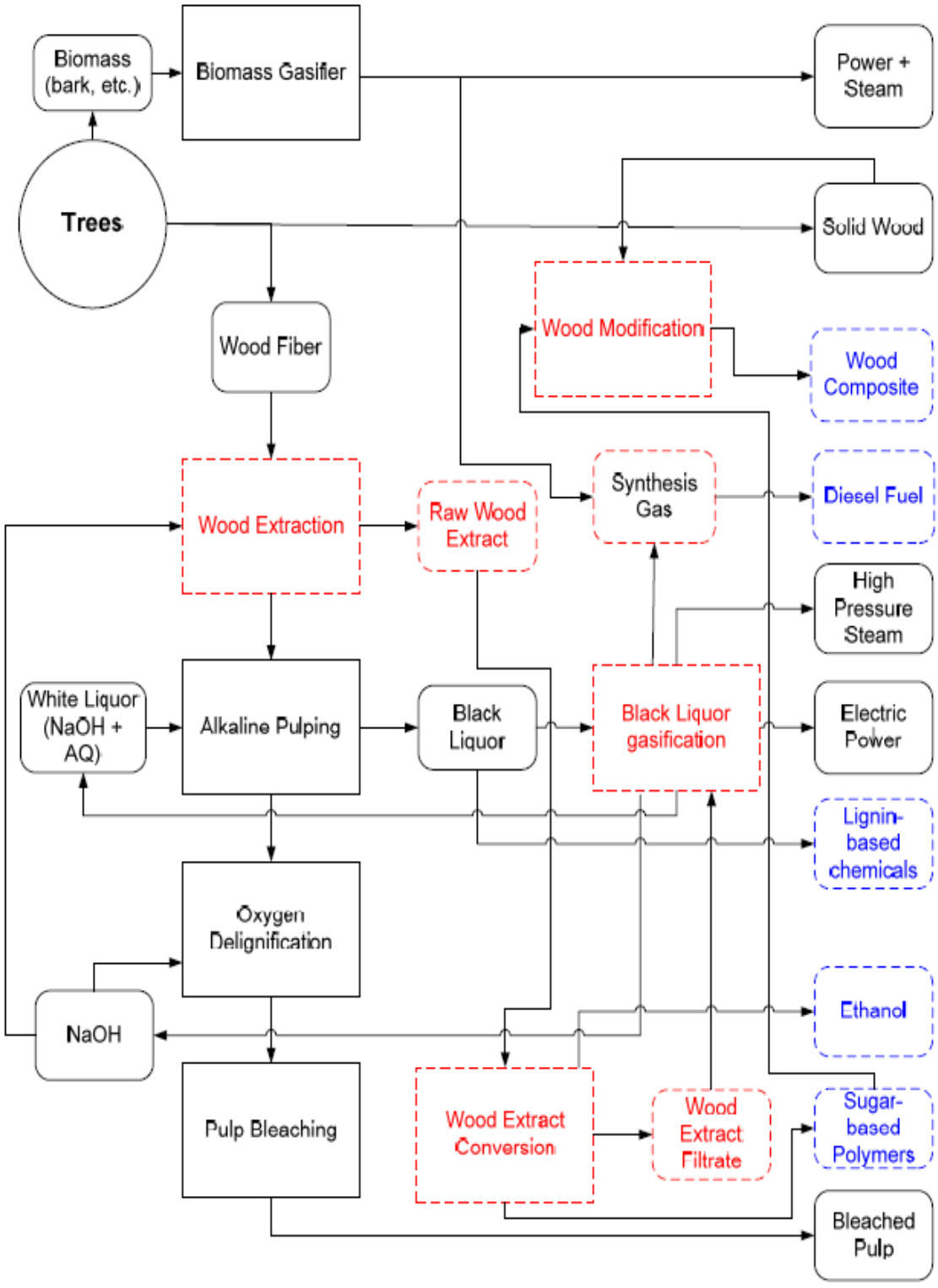

Figure 11: Integrated Forest Products Refinery [28]

2.2 Biomass properties affecting gasification:

A number of biomass properties affect gasification. These are important for the evaluation of the utility of a biomass material as feedstock for gasification.

Proximate analysis of the biomass is a very important factor in determining the usefulness of the feedstock as a fuel. Proximate analysis provides the moisture content, volatile matter, ash and fixed carbon contents in the biomass. The moisture content determined by proximate analysis only represents physical bound water. The water released in pyrolysis reactions is included in volatiles. Woody fuels, municipal solid waste and paper mill sludge are of varying moisture content. Moisture is important in determining the drying costs and the as-received heat content of the fuels. Ash content also represents an important factor for biomass behavior as feed stock for gasification. It represents the remaining fraction of mass after gasification of all the volatile and fixed carbon fractions originally present in the biomass. The wood ash consists primarily of CaO, K_2O, Na_2O, MgO, SiO_2, Fe_2O_3, P_2O_5, sulfates and Cl. Some trace elements such as aluminum, lead, zinc, copper, titanium, tin, nickel and thallium are also present [2, 29].

Ultimate analysis gives the amounts of C, H, N, S and O present in the fuel. The contents vary with the feedstock and have an effect on biomass pyrolysis and gasification. The carbon content of all biomass materials is considerably lower than that of coal. Due to ether, acid and alcohol groups in cellulose, hemicellulose or lignin, the bound oxygen content of biomass is very high. Typically the heating value of coal is much higher than that of biomass fuels because of the high carbon content of coal.

Biomass pyrolysis is a complex process and depends on several factors such as the composition of lignocellulosic material, heating rate and content of inorganic material etc. Alkali metals present in the biomass play a crucial role in thermal degradation of biomass [30]. The amounts of cellulose, hemicellulose and lignin present in the biomass affect the pyrolysis and gasification behavior.

During biomass pyrolysis a series of complex reactions takes place. At low heating rates (<100 °C/min) biomass decomposition takes place in well-described stages of moisture evolution, hemicellulose and cellulose decomposition along with slow decomposition of lignin [31, 32]. The amounts of volatiles, gases and char from pyrolysis are proportional to the three major components in the feedstock biomass [31-33]. Pyrolysis of cellulose gives tar as the major evolved product along with char and water. Cellulose tar mainly consists of levoglucosan along with aldehydes, ketones and organic acid. Pyrolysis of hemicelluose gives mainly tar along with water and char. Lignin decomposes very slowly and produces char as the major component with some water and tar [32-35].

Lignin contains hydroxyl groups which are useful as reactive chemical reaction sites. Depending on the extraction process and the genetic origin lignin also includes other major chemical functional groups such as methoxyl, carbonyl and carboxyl groups in various amounts [36, 37].

2.3 Lignin studies:

2.3.1 Pyrolysis of lignin - experimental studies:

The pyrolysis of lignin is a complex process. It is influenced by different factors such as the reaction temperature, the heating rate, the composition of lignin, and the carrier gas flow rate. Two types of reactions take place during pyrolysis: primary and secondary. During primary reactions direct decomposition of biomass takes place. During secondary reactions the volatiles generated in the primary reactions undergo coking, cracking and other complex reactions involving free radicals [38].

Ferdous et al. [38] did pyrolysis studies of Alcell and Kraft lignins in a fixed-bed reactor using helium and nitrogen. They varied the reaction temperature from 300 K to 1073 K and the heating rate from 5 to 15 K/min. They showed that at low temperatures the conversion to gases and tar at a given temperature was higher at the lowest heating rate (5 K/min) than at the higher heating rates (10-15 K/min). Beyond 850-900 K the conversion at the lowest heating rate leveled off but the conversion increased with temperature at the other two heating rates. Above 875 K for Kraft lignin and 1023 K for Alcell lignin, the conversion is higher at the high heating rates [Figure 12].

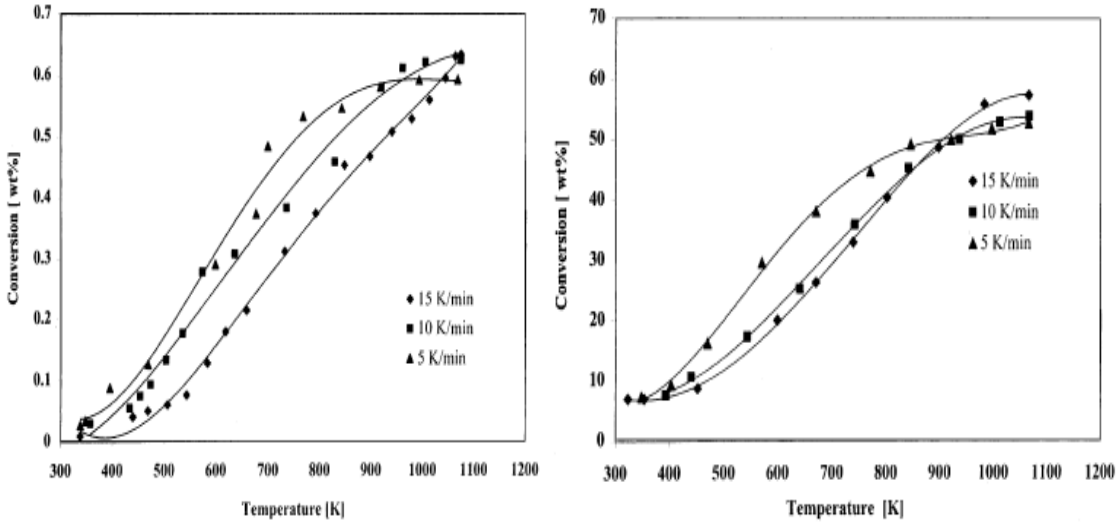

(a) (b)

Figure 12: Effect of temperature on conversion (a) Alcell Lignin (b) Kraft Lignin [38]

In a similar study of lignin pyrolysis, Ferdous et al. [39] reported the effect of temperature (350-800 °C) on the yield of char, tar and gas. The heating rate and the gas flow were kept constant. For Alcell lignin, the conversion to tar and gas increased linearly from 28 to 60% during a temperature change from 350 to 650 °C and then leveled off. The char yield decreased and the tar yield increased up to 650 °C. At higher temperatures the char yield became nearly constant and the tar yield decreased due to secondary decomposition. Kraft lignin conversion (25-57 %) was similar to that of Alcell lignin [Figure 13].

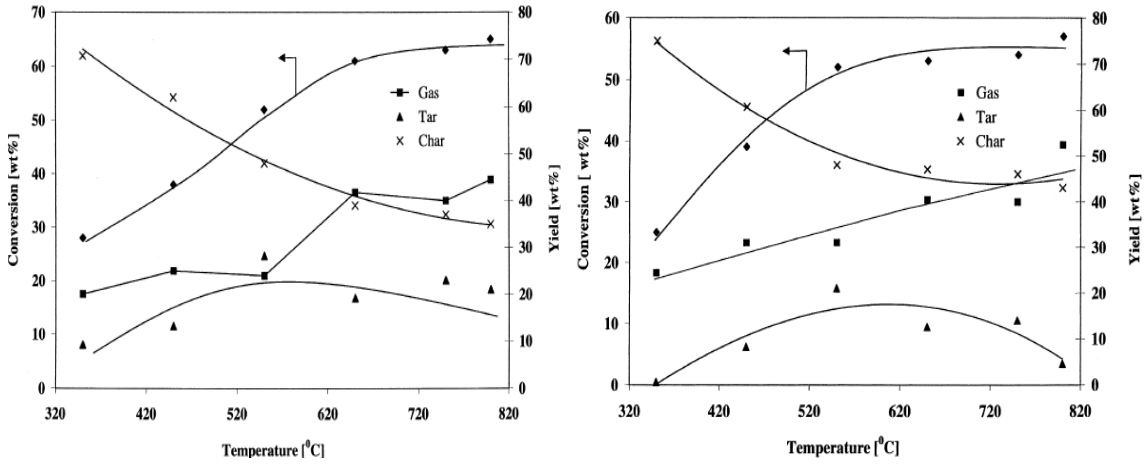

(a) (b)

Figure 13: Effect of temperature on lignin conversion and yield of gas, tar and char during pyrolysis of (a) Alcell lignin (b) Kraft lignin [39]

In another study, Caballero et al. [40] pyrolyzed Kraft lignin for 30 sec. at temperatures in the range of 450-900 °C at a nominal heating rate of 20,000 °C/s. They found that CO, CO_2 and water show increase in their yields over the whole temperature range. They observed a slow decrease in char and tar yields. The total gas yield increased over the whole temperature range.

In a study of flash pyrolysis of klason lignin, Caballero et al. [41] also found similar results. They did pyrolysis in a Pyroprobe 1000 in the temperature range of 500-900 °C with a residence time of 20 sec. They showed a decrease in the char and tar yield with increase in temperature. They also noticed an increase in gas yield over the whole temperature range. They reported noticeable increases in yields of hydrocarbons, CO, CO_2 and water as the pyrolysis temperature increased.

Sharma et al. [17] studied lignin under pyrolytic (100% helium) and oxidative (5% oxygen in helium) conditions at atmospheric pressure and temperature between 150 °C to 550 °C. This

study found that char yield decreased rapidly with increasing temperature to ca. 62% at 400°C. After that there was a gradual decrease to 40% at 750°C in pyrolytic conditions. Figure 14 shows the effect of temperature on char yield under pyrolytic and oxidative conditions.

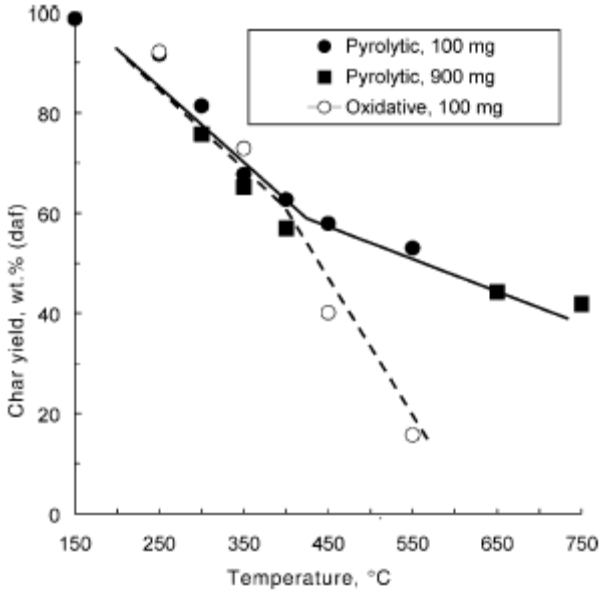

Figure 14: Effect of temperature on char yield from lignin pyrolytic and oxidative conditions [17]

Murugun et al. [42] studied the thermal behavior of hardwood lignin found in Eastern Canada by thermogravimetric analysis (TGA) and differential scanning calorimetry (DSC). Figure 15 show the weight-loss curves for lignin pyrolysis. The lignin was heated up to 300 °C at a heating rate of 15°C/min with a carrier gas of argon.

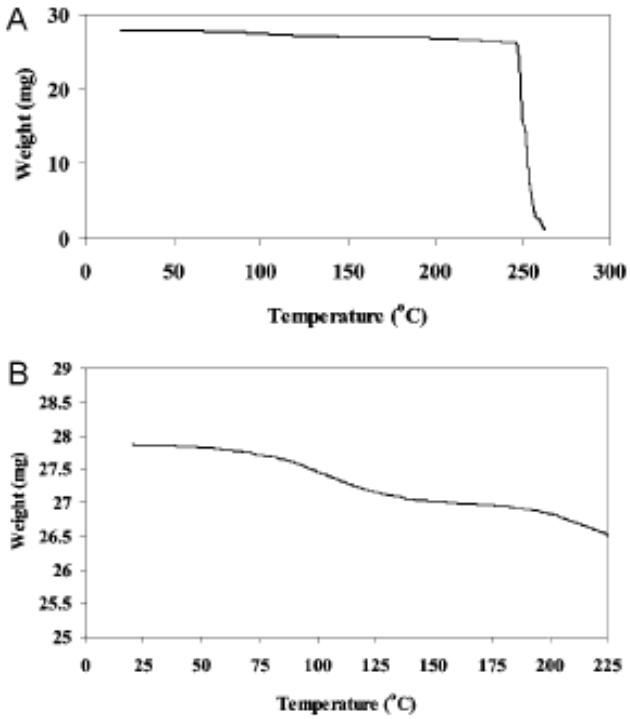

Figure 15: (A) TGA curve of lignin. (B) TGA curve of lignin to observe three different phases [42]

The results showed that the lignin was stable up to 71 °C and started losing weight after that. The initial weight loss was due to the loss of water contained in the polymeric film. Secondary and tertiary weight loss took place between 71- 162 °C and 162 – 246 ° C respectively. The reaction was complete in approximately 690 sec at 259 °C.

2.3.2 Effect of heating rate on lignin gasification:

It has been reported in studies that pyrolysis at high heating rate gave less char and higher volatile yield than pyrolysis at low heating rate. Fushimi et al. [43] carried out steam gasification and pyrolysis of char to see the effect of heating rate on steam gasification of biomass. They did their study on cellulose, bagasse and lignin with final temperatures of 973 K with a

thermobalance reactor at heating rates of 1, 10 and 100 K/s. They found that the pyrolysis of lignin yields 40-44 wt % of char. Figure 16 shows that at a slower rate of 1 K/s above 550 K, a rapid drop in the relative mass of lignin was observed. In the temperature range of 773-923 K, the rate of relative mass reduction was slow, and above 923 K it decreased gradually. As indicated in Figure 16a, with slow heating, the steam gasification reaction of lignin char produced by pyrolysis occurred above 923 K and finished approximately 900 seconds after the temperature reached 973 K. With rapid heating (Figure 16b), steam gasification started after a temperature of 973 K and was finished in close to 600 seconds. Rapid heating substantially increased the reactivity of lignin char during steam gasification. The study also showed the different time profiles of relative mass change for both pyrolysis and steam gasification.

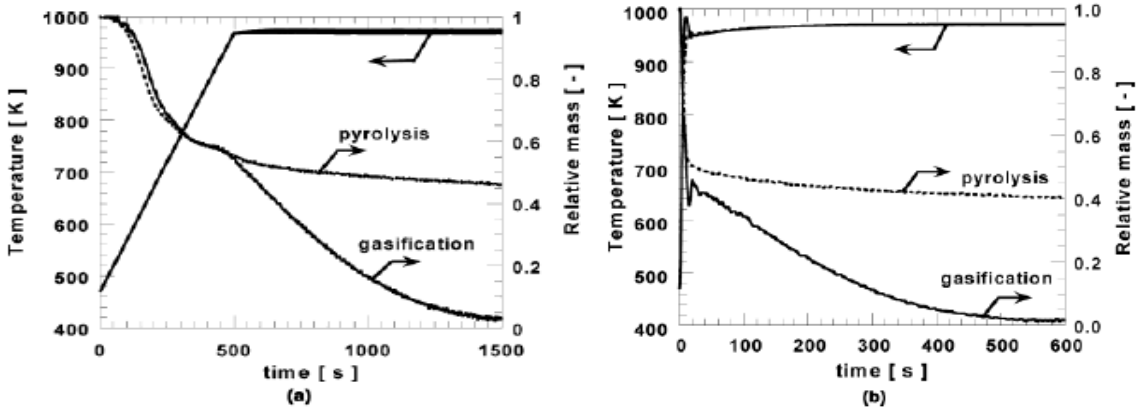

Figure 16: Profiles of temperature and relative mass of lignin: (a) 1 K/s (b) 100 K/s [43]

Fushimi et al. [44] also studied the evolution rate of low-molecular-weight gas products (H_2, CH_4, CO and CO_2) during pyrolysis and steam gasification of lignin. As seen in Figure 17, CO_2 evolved above 500 K followed by CO and CH_4. Lignin decomposed in the temperature range of 550 – 773 K. Up to 823 K, there is not much difference between pyrolysis and gasification. After that there is a drastic increase in H_2 evolution along with a steep rise in CO and CO_2 evolution.

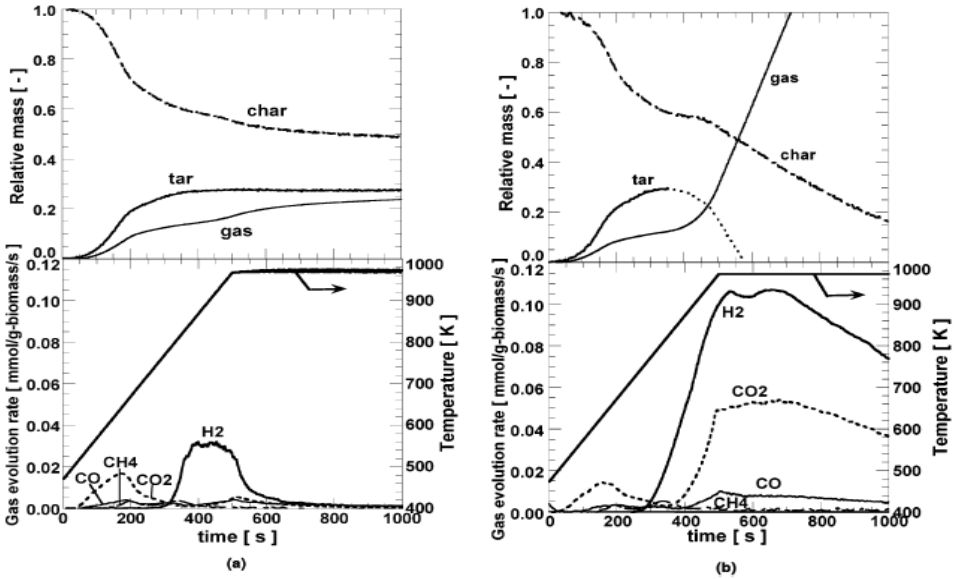

Figure 17: Gas evolution rate from lignin with a heating rate of 1 K/s during (a) pyrolysis (b) steam gasification [44]

The yields of CO, CO_2, H_2 and CH_4 during heating decreased with an increased heating rate. As shown in Figure 18, gas-yield curves during heating shifted to higher temperatures as the heating rate was increased.

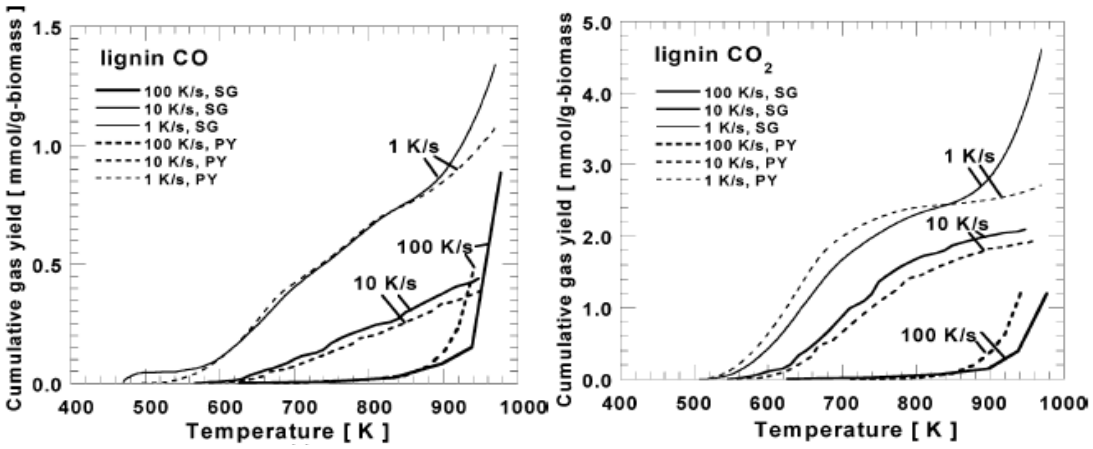

Figure 18: Cumulative gas yield vs. temperature for lignin: (a) CO (b) CO_2 [44]

2.3.3 Kinetics of lignin pyrolysis and gasification:

Caballero et al. [41] pyrolyzed Klason lignin in a Pyroprobe 1000 at temperatures between 500 and 900 °C. They introduced an empirical model for thermal decomposition. Equation (1) was developed for the pyrolysis of lignin for 20 sec where $X_{A\infty}$ is conversion at infinite time and T is the absolute temperature in K of the pyrolyzed sample. 20 s was deemed sufficiently long to attain complete decomposition of the lignin since a second pyrolysis of samples did not yield any significant amount of decomposition.

$$1- X_{A\infty} = 1.22757 – 0.00178395 * T + 7.3333 * 10^{-7} * T^2 \quad \textbf{(1)}$$

They also reported an activation energy of 8.2 kcal/mol along with a pre-exponential factor of 59 s^{-1} for weight loss during the pyrolysis of lignin.

Caballero et al. [40] further extended the knowledge of pyrolysis kinetics. This time they studied pyrolysis of Kraft lignin in a Pyrobrobe 1000 apparatus with a heating rate of 20000 °C/s over a temperature range of 450 to 900 °C. They modeled the thermal decomposition of lignin and derived equations for pre-exponential factors and activation energy as (2) and (3) respectively.

$$\ln (k_0) = 14.77 + 0.0208(T_R – 273)\ s^{-1} \quad \textbf{(2)}$$

$$E = 52.64 + 0.173(T_R – 273)\ kJ\ mol^{-1} \quad \textbf{(3)}$$

They used a C function model, which assumes that lignin is formed from a large number of fractions. A given fraction will decompose only if its temperature is equal to or greater than a characteristic temperature T_R (K) of this fraction.

Pasquali et al. [45] studied the kinetics of pyrolytic thermal degradation of lignins in an inert atmosphere using thermogravimetric techniques. Pyrolysis runs took place in the temperature range of 226 to 435 °C. They showed that the pyrolysis process obeys the Avrami – Erofeev equation (4).

$$[-\ln (1-\alpha)^{1/n}] = k.t \qquad \textbf{(4)}$$

where α is the conversion, n is the reaction order, k the rate constant and t the time. They also obtained activation energy values in the range of 12 to 43 kJ/mol for a reaction order of n = 0.5.

To study the pyrolysis kinetics of wood and wood components, Willner et al. [46] did a kinetic study of cellulose, hemi-cellulose and lignin in the temperature range of 300 – 500 °C at atmospheric pressure. They showed that lignin decomposes slowest and hemicellulose the fastest. They found in the modeling of reaction that cellulose and hemicelluose follow an autocatalytic reaction model but lignin pyrolysis does not show autocatalytic reaction effects. Rather, it follows the first order reaction model shown in Figure 19.

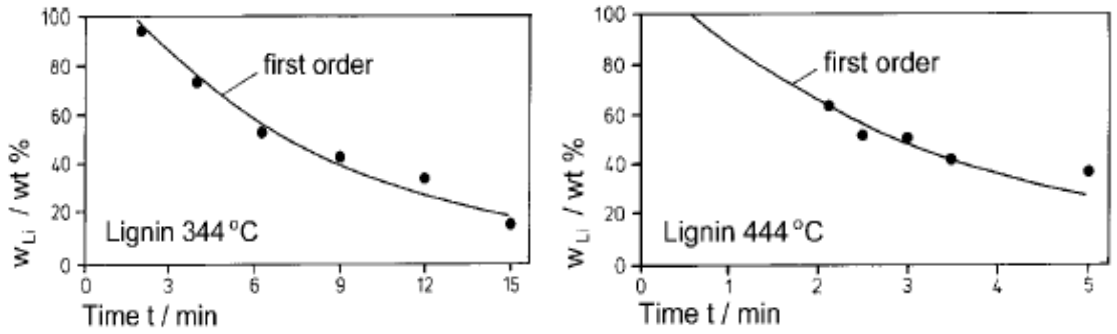

Figure 19: Decomposition of lignin at 344 °C and 444 °C [46]

Fushimi et al. [43] did a study to find the effect of heating rate on pyrolysis of lignin. Assuming pyrolysis to be a first order reaction they determined the effect of heating rate on Arrhenius parameters. They showed that the activation energy of lignin at the heating rate of 10 K/s was 56 kJ/mol, which is slightly higher than 53 kJ/mol, the activation energy at 1 K/s. But at a heating rate of 100 K/s the activation energy was 23 kJ/mol, which is smaller than that at 10 K/s. It was suggested that heat transfer limitations influences the temperature measurement of lignin at 100 K/s. Therefore the value at 100 K/s was believed to be inaccurate.

Pasquali et al. [45] also studied the kinetics of isothermal pyrolysis of lignins from hardwood found in north of Argentina using a TG/TGA. Isothermal runs were performed in a thermal scale Stanton Redcroft TG-750 in a nitrogen atmosphere. Lignin from Quebrancho Colorado (Q.C.) was obtained as residue from wood without extractives which gives Klason lignin after acid hydrolysis. Pyrolysis runs were done between 226 °C and 435 °C and a conversion value α was calculated as

$$\alpha = (m_i - m_t)/(m_i - m_f) \quad \textbf{(5)}$$

where m_t represents the mass at time t and m_i is the initial mass and m_f is the mass at infinite time. For lignin Q.C., the mass loss m_i-m_t as a function of time for each temperature was plotted and the kinetic parameters of the isothermal pyrolysis were calculated using Avrami-Erofeev equation (Eq 4) for a reaction in the solid state [Figure 20, 21].

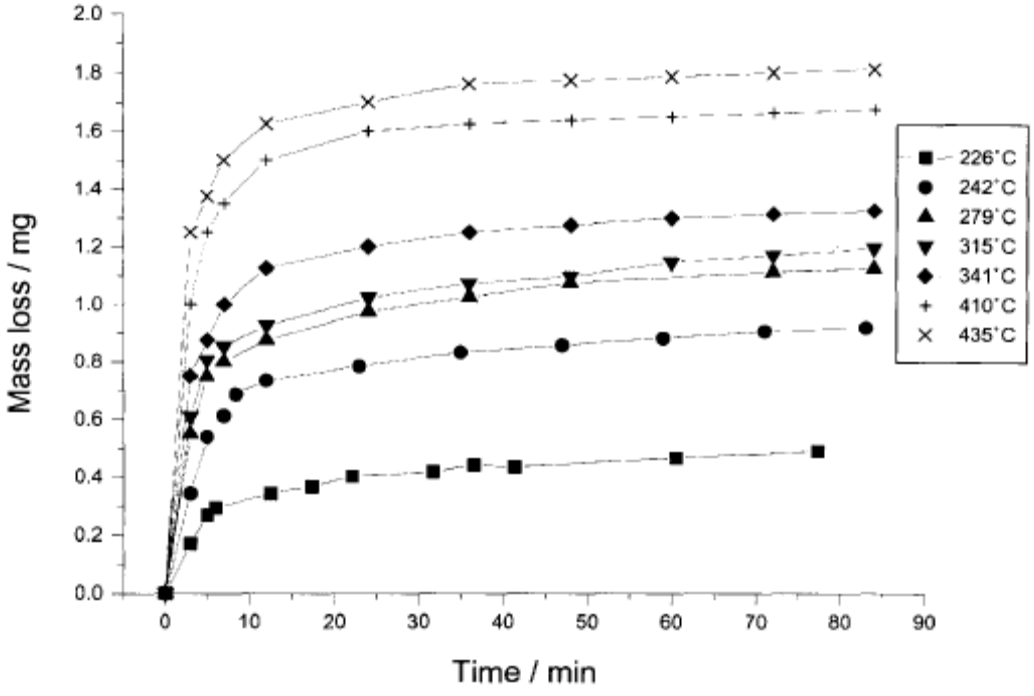

Figure 20: Mass loss vs. time for lignin of Quebrancho Colorado (Q.C.) [45]

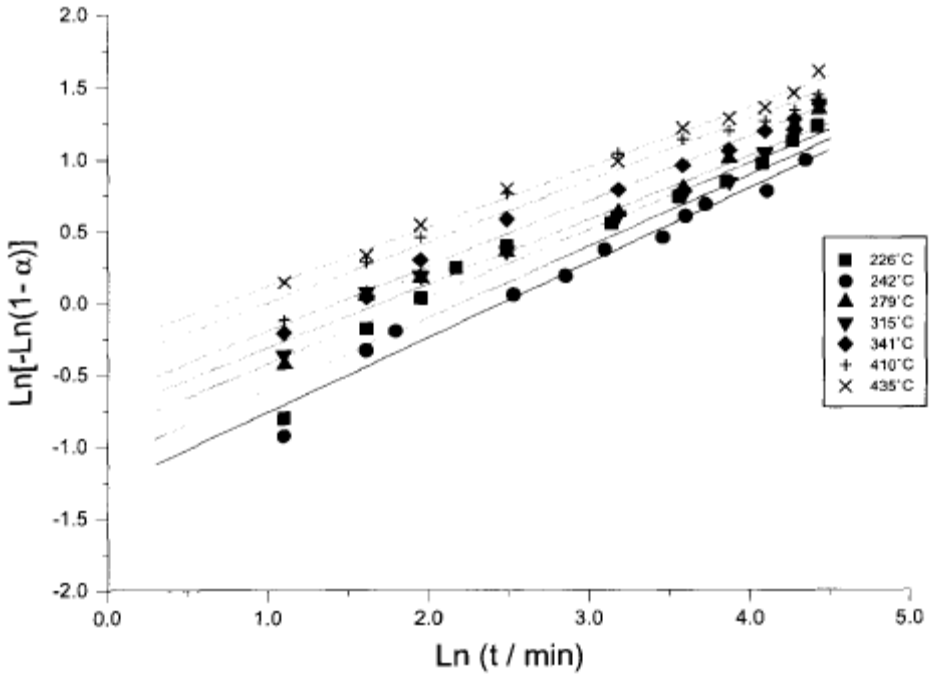

Figure 21: Ln[-Ln(1-α)] vs. ln t for Quebrancho Colorado (Q.C.) [45]

They found the activation energy of lignin pyrolysis in the range between 12.5 and 42.6 kJ/mol. The values were close to the values of 27.4 kJ/mol obtained by Guzman et al. [47] for isothermal pyrolysis of lignin obtained through acid precipitation from *Pinus radiata* black liquor.

Gustafsson and Tobias [48] studied pyrolysis kinetics of washed precipitated lignin using laminar entrained flow reactor [LEFR] at Chalmers University of Technology, Sweden. They found the activation energy to be 32.1 kJ/mol for first pyrolysis reaction, occurring from 0 to 1.04 sec residence time.

2.4 Effect of catalysts on pyrolysis and gasification:

There have been several studies on the effect of various catalysts on pyrolysis and gasification. Most of the metals, their oxides and salts are more or less catalytic in nature. There have been numerous researches on the catalysis of alkali and alkaline earth compounds, particularly the structure of active sites formed on carbon surfaces [49-52].

Mudge et al [53] studied the steam gasification of wood in the presence of alkali metal catalysts. Wood samples were prepared by dry mixing as well as impregnation with alkali metal catalyst. The catalyst concentrations of 3×10^{-3} and 3×10^{-4} mole of alkali per gram of wood were used in the study. Gasification experiments were conducted at atmospheric pressure and at three temperatures of 550, 650 and 750 °C. A steam flow rate of 1.2 g/min was established and the experiment was conducted for 1500 seconds. The product gas was passed through a calibrated wet test meter, which determined the gas volume. The study found that impregnating the wood particles with sodium carbonate catalyst is a better contacting method than dry mixing the equivalent amount of catalyst with the wood. Impregnation produces nearly 10% more gas than dry mixing and also increases the rate of gas production slightly. Both methods increase total gas production by 75-90 % and the rate of gasification also increases.

In a study by Nowakowski et al. [30], the effect of potassium catalysis on the pyrolysis behavior of a synthetic biomass - a mixture of the basic biomass components (cellulose, hemicellulose and lignin) - and short rotation willow coppice (SRC) was studied. The willow samples and synthetic biomass were pre-treated by hydrochloric acid to remove salts and metals and then were

impregnated with potassium. Figure 22 shows the influence of potassium on the pyrolysis of the willow SRC and synthetic biomass mixture. The first step in thermal degradation represents the decomposition of hemicelluose and the initial stage of degradation of cellulose. The second step represents lignin degradation and final degradation of cellulose.

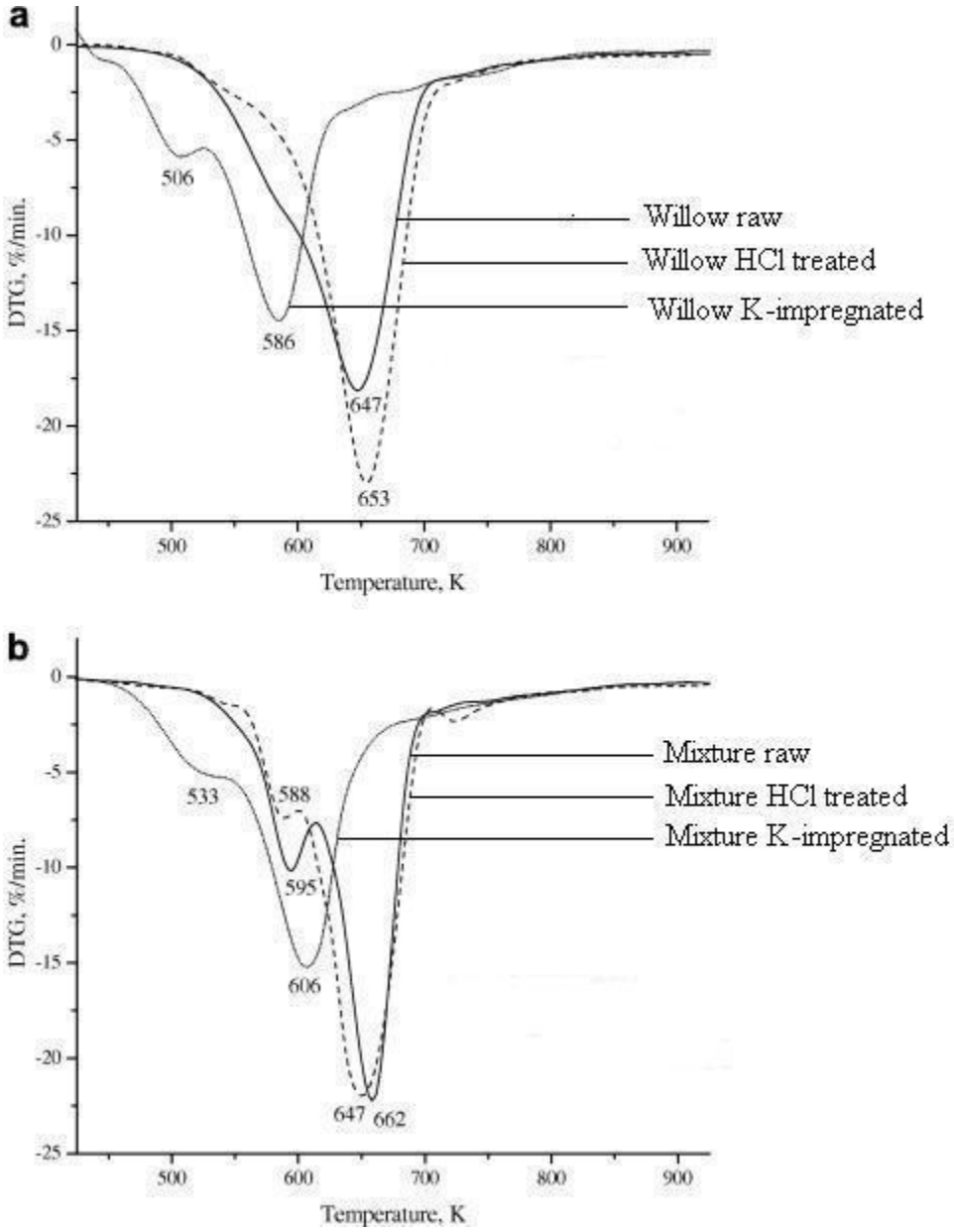

Figure 22: DTG profiles for (a) willow SRC and (b) synthetic biomass samples [30]

Results show that the cellulose decomposition position peak shifts from 662 K to 606 K for the synthetic biomass mixtures and from 647 K to 586 K for the willow SRC sample when the materials are impregnated with K. It suggests that potassium catalyzes pyrolysis. HCl treatment decreases char yield but potassium treatment increases char yield for both the cases. With the addition of potassium, the increase in char yield is more significant in the synthetic biomass than willow SRC. As seen by a larger decrease in the peak maximum temperature, potassium is more effective in catalyzing pyrolysis in the willow SRC than in the synthetic biomass but it is more effective in increasing the char yield from pyrolysis of the synthetic biomass [30]

2.5 Thermogravimetric study of biomass pyrolysis:

Thermogravimetric analysis (TGA) is a powerful technique for the analysis of the pyrolysis behavior under well defined reaction conditions. A number of TG analyses have been used to study the pyrolysis of biomass fuels. Several thermogravimetric studies of lignin were reported in the preceding sections.

Biagini et al. [54] studied the devolatilization of biomass fuels and biomass components by the TGA technique using lignocellulosic materials of different origin, properties and composition; namely pine wood, wood pellets, olive stones and hazelnut shells. A bituminous coal and paper sludge were also included in the study. Paper sludge was studied because of its large availability and the possibility of recovering energy. The high moisture and ash content of sludge reduces its

heating value. The lignin fraction present in it is significant and makes it interesting to study. The ultimate and proximate analysis is listed in Table 1.

Table 1: Ultimate and proximate analysis and heating value of fuels [54]

	ultimate analysis (% daf)				proximate analysis (% dry)			HV
fuel	C	H	N	S	VM	FC	ash	(MJ/kg)
pine wood	53	6.0	0.2	0.08	80.6	17.7	1.7	18.1
wood pellets	49.4	6.1	1.0	0.7	76.9	20.8	2.3	19
olive residue	51.2	6.7	0.8	0.05	78.4	20.4	1.2	20.1
hazelnut shells	51.0	5.4	1.3		78.5	20.2	1.3	nd
paper sludge	24.3	3.4	0.5	0.01	50.0	3.0	47.0	5.1
Kema coal	71.4	4.5	1.1	0.8	30.4	55.8	13.8	28.7

Figure 23 shows the weight loss and DTG curves of biomass fuels and biomass components. The results show that the devolatilization behavior of all the ligno-cellulosic materials is very similar. For all the biomass fuels, the main weight loss ends at 370-400 °C and a slow and continuous weight loss then takes place. The first step represents primary devolatilization and the later step represents secondary thermolysis, where degradation of heavier chemical structures in the solid matrix takes place. During the weight loss of paper sludge and Kema coal, a long tail of devolatilization is also observed. Xylan is the most reactive of all components and cellulose shows the maximum weight loss among all components. Lignin decomposes in a wider range of temperature than all other components and has the lowest final weight loss [54].

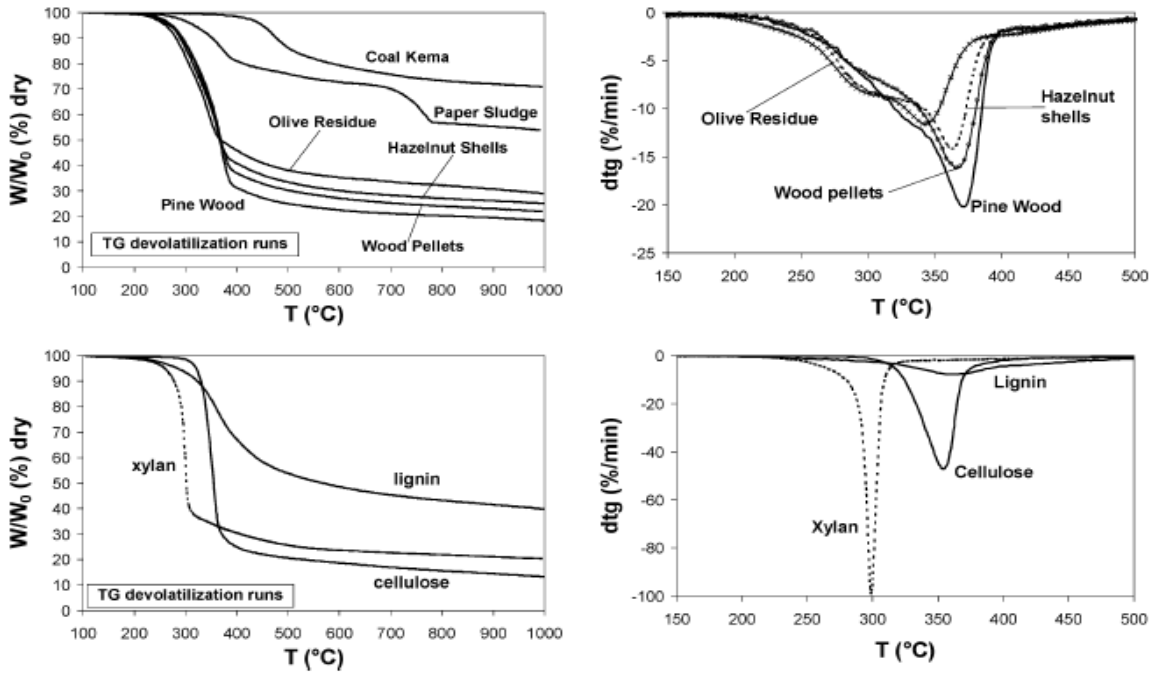

Figure 23: Weight loss and DTG curves of biomass fuels and biomass components [54]

2.6 Pyrolysis and gasification of black liquor in Laminar Entrained Flow Reactor:

Studies of black liquor pyrolysis and gasification had been conducted by Sricharoenchaikul et al. [55] in the laminar entrained flow reactor (LEFR) at IPST. The yields of char residue and fixed carbon were measured for black liquor char residue produced in the LEFR at heating rates of 4000-14000 °C/s. Their study found that after devolatilization the char yield decreases nearly linearly with temperature, from 75% at 700 °C to 58% at 1100 °C. Significant mass loss (30%-50%) is measured at the shortest residence time and additional mass loss occurs at a much slower rate. After an initial residence time of 0.3 s there is very little incremental decrease in char yield, it suggests that loss of volatile gases in pyrolysis of organic matter is complete in 0.3 s. Figure 24 shows the char residue collected at different temperature and residence time for black liquor particles in a LEFR.

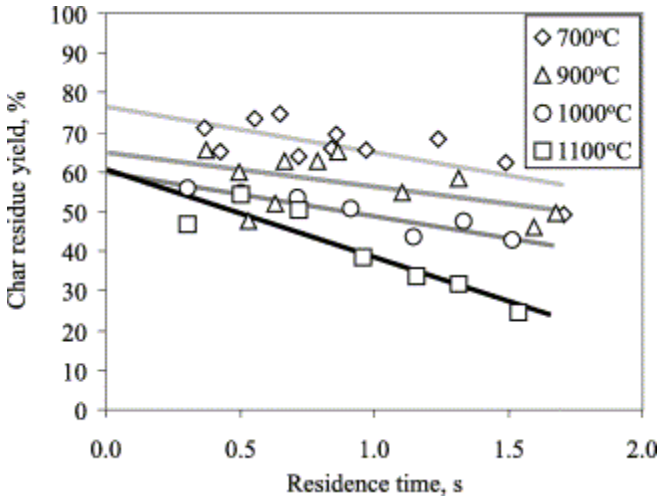

Figure 24: Char residue yield vs. furnace temperature and residence time for black liquor particles in a laminar entrained flow reactor [55]

In another study Sricharoenchaikul et al. [56] measured char yields and total carbon for black liquor solids after pyrolysis and gasification in an LEFR. They conducted the experiments between 700-1000 °C in N_2, CO_2/N_2 or water vapor/N_2 at 1 bar total pressure for residence times from 0.3 to 1.7 sec. Figures 25 and 26 show the char and char carbon yield from different gasification conditions at 800 °C and 900 °C, respectively.

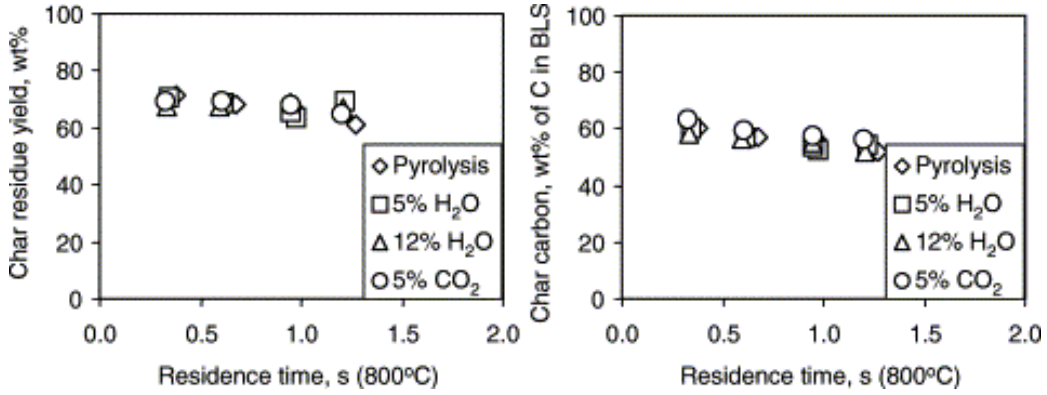

Figure 25: Char and char carbon yield from different gasification conditions at 800 °C [56]

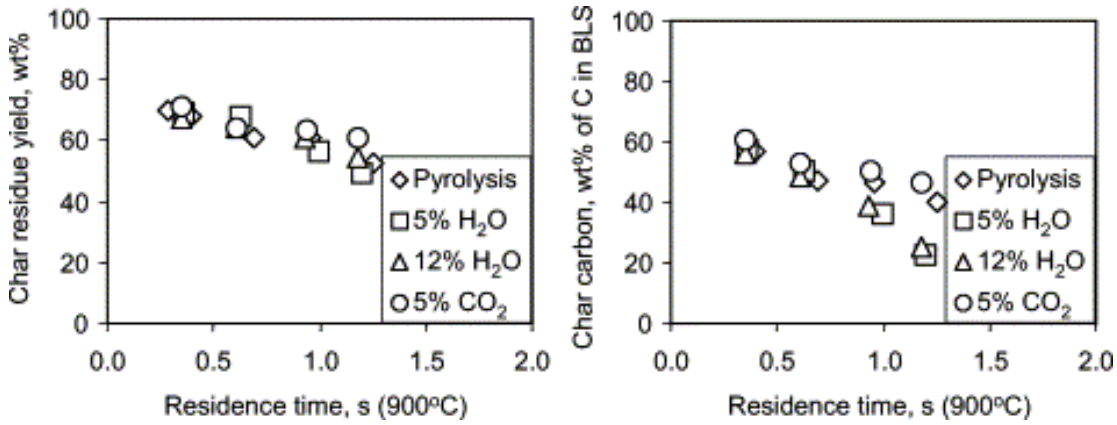

Figure 26: Char and char carbon yield from different gasification conditions at 900 °C [56]

Their results showed that at the same residence time the fixed carbon yield decreased with increasing reactor temperature. At 800 °C the effect of gas composition on char and char carbon yields was minimal. In comparison, at the reactor temperature of 900 °C with water vapor in gas phase, the char carbon decreased more rapidly than those for pyrolysis in N_2 and gasification with 5% CO_2 in N_2. No significant difference between char yields at this temperature was found.

CHAPTER III

OBJECTIVES

This work looks into the effect of different process variables as well as lignin type on pyrolysis and gasification. The objectives of this research were as follows:

1. Determine the effect of residence time, temperature and filler amount on fixed carbon conversion and char yield during sludge and pulp gasification using a Laminar Entrained Flow Reactor (LEFR).
2. Determine the effect of residence time and lignin type on fixed carbon conversion and char yield during pyrolysis and gasification using a Laminar Entrained Flow Reactor (LEFR).
3. Determine the effect of lignin type on pyrolysis and gasification using a Thermogravimetric Analyzer (TGA).
4. Determine the effect of alkali addition on lignin pyrolysis and gasification using a TGA.
5. Determine the effect of temperature and lignin type on lignin structure using Fourier Transform Infrared (FTIR) Spectroscopy.
6. Study of kinetic parameters during lignin pyrolysis and gasification using a TGA.

CHAPTER IV

EXPERIMENTAL PLAN

4.1 Lignin studied:

Two lignins were used for pyrolysis and gasification studies. Both were kraft lignin collected from different sources. The first lignin was a kraft lignin from MeadWestvaco Corporation (MWV). It is called INDULIN AT, and is a purified form of a kraft pine lignin. This lignin is free of all of hemicelluosic material and is generally used for polymeric applications where solid dispersants are required.

The second lignin studied was kraft lignin from Sigma Aldrich (SA). This lignin is used as a primary dispersing agent for dyestuffs and agricultural chemicals. It contained no reducing sugars and is compatible with anionic and nonionic surfactants and wetting agents.

Both MWV and SA lignins are brown in color. Both the lignins had comparable physical appearances with different chemical compositions, as shown in Table 2.

Table 2: Elemental analysis of lignins

Component	MeadWestvaco Lignin (MWV)	Sigma Aldrich Lignin (SA)
Carbon	61.6 %	51.4 %
Hydrogen	5.8 %	5.0 %
Oxygen*	29.7 %	33.4 %
Sodium	1.04 %	6.2 %
Sulfur	1.7 %	3.9 %
Potassium	0.10 %	0.11 %
Calcium	0.03 %	0.008 %
Ash	4.6 %	20.2 %

*obtained by difference

The MWV lignin has a higher carbon and hydrogen content than the SA lignin. The SA lignin contains nearly six times as much sodium and nearly twice as much sulfur than the MWV lignin. The SA lignin also has much higher ash than the MWV lignin.

4.2 Experimental methods:

The experimental plan was divided into three phases:

(1) Laminar Entrained Flow Reactor (FTIR) experiments

(2) Thermogravimetric Analyzer (TGA) experiments

(3) Fourier Transform Infrared (FTIR) spectroscopy experiments

Initially the Laminar Entrained Flow Reactor (LEFR) available at the Institute of Paper Science and Technology (IPST) was used for pyrolysis and gasification studies of lignins and primary sludge. Further studies of lignin pyrolysis and gasification were done with the Thermogravimetric Analyzer available at the School of Polymer and Textile Engineering at Georgia Institute of Technology. Lignin behavior at different temperatures was studied using Fourier Transform Infrared (FTIR) spectrometer present in the IPST analytical laboratory.

4.2.1 Laminar Entrained Flow Reactor (LEFR) studies:

The LEFR present at IPST has been used in the past for various types of research in the area of pyrolysis and gasification. In this study the LEFR was used to perform pyrolysis and gasification experiments of lignin and primary sludge. This reactor was selected because it provides a very high heating rate and negligible temperature gradients inside particles. It only allows very small particles to pass through the feeder and heating zone which is heated up to a uniform temperature. It also provides good control on temperature, residence time and gas flow rate. For

good results the particles need to be properly dried and sieved to pass through the feeding system and reactor zone. The reactor can be heated up to 1100 °C.

The LEFR reactor contains two ceramic tubes enclosed in a tubular three zone furnace. The inner ceramic tube has a 7 cm ID and a complete length of 1 meter. Out of this length 0.83 meter is inside the three-zone furnace. The reactor is shown in Figure 27.

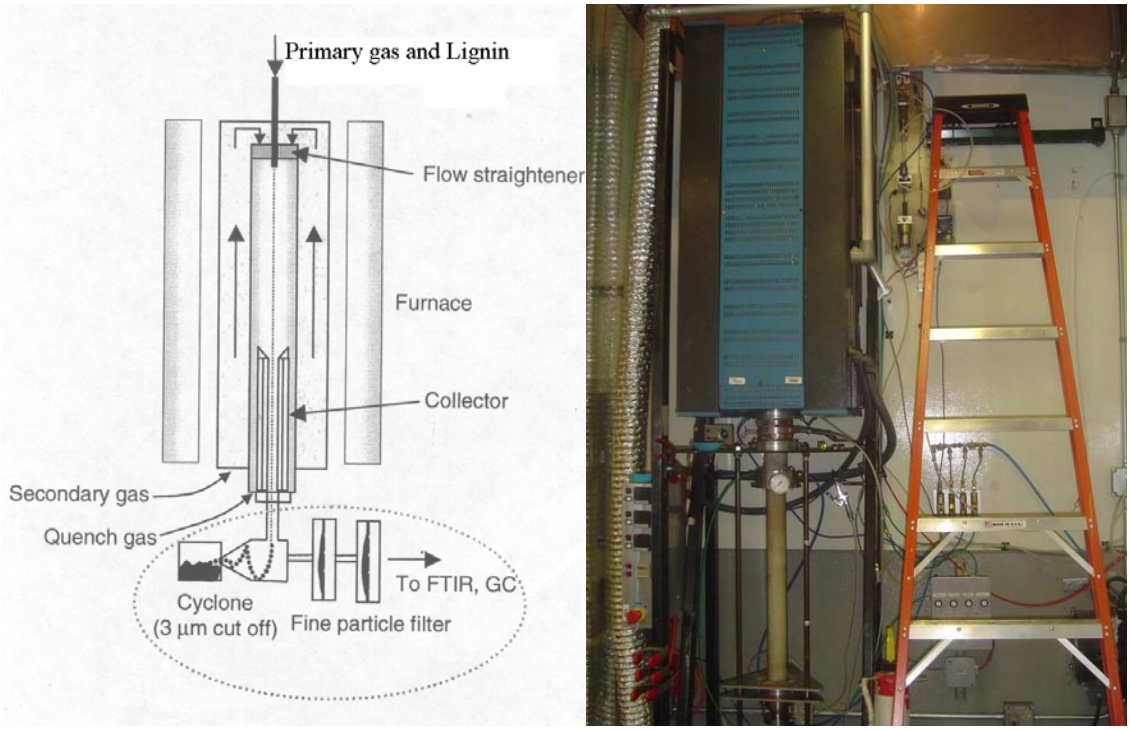

Figure 27: Laminar Entrained Flow Reactor (LEFR) system [3]

From the top of the reactor primary gas with a flow of 0.10 L/min enters with lignin particles into the inner tube of the reactor and the heating zone. A secondary gas at room temperature with a higher flow of 15-20 L/min enters between the two concentric tubes of the reactor and is preheated as it moves upwards. Nitrogen was used for the pyrolysis runs; a mixture of N_2, H_2O

and CO_2 was used for gasification. The secondary gas passes through the flow straightener and mixes with the primary gas. Particles flow downward and are heated at a very high rate and then move to the collector after the reactions. The reactor heats the particles at very high heating rate due to the radiation from the reactor wall as well as from the secondary gas convection. After reaction, the products pass through the collection zone where nitrogen and water-cooled walls are used for cooling. The porous wall of the collector through which additional quench gas is inserted does not allow particles to condense on the wall. The collector is adjusted up and down to vary the residence time of particles in the reactor. After reaction and cooling, a cyclone is used to collect the char particles at the bottom of the reactor [Figure 28]. The gases and char particles pass through a fine particle filter where char particles greater than 3 microns are blocked and collected in the cyclone. The gases pass out of the filter and then go to an FTIR or are collected in small bags to be analyzed later by GC.

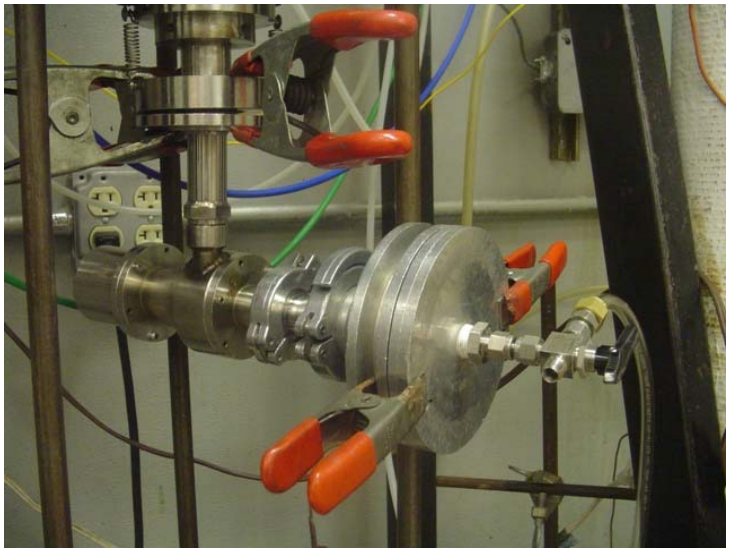

Figure 28: Char collector cyclone

4.2.1.1 Feeder:

Feeding the material to the reactor is very challenging. The opening of the mounted feeding tube on the top of the LEFR reactor is very small and only allows particles smaller than 125 micrometers to move easily into the reactor. The feeder system had been designed to feed black liquor. As shown in Figure 29, it has a motorized rotating plate which holds a test tube on top of it.

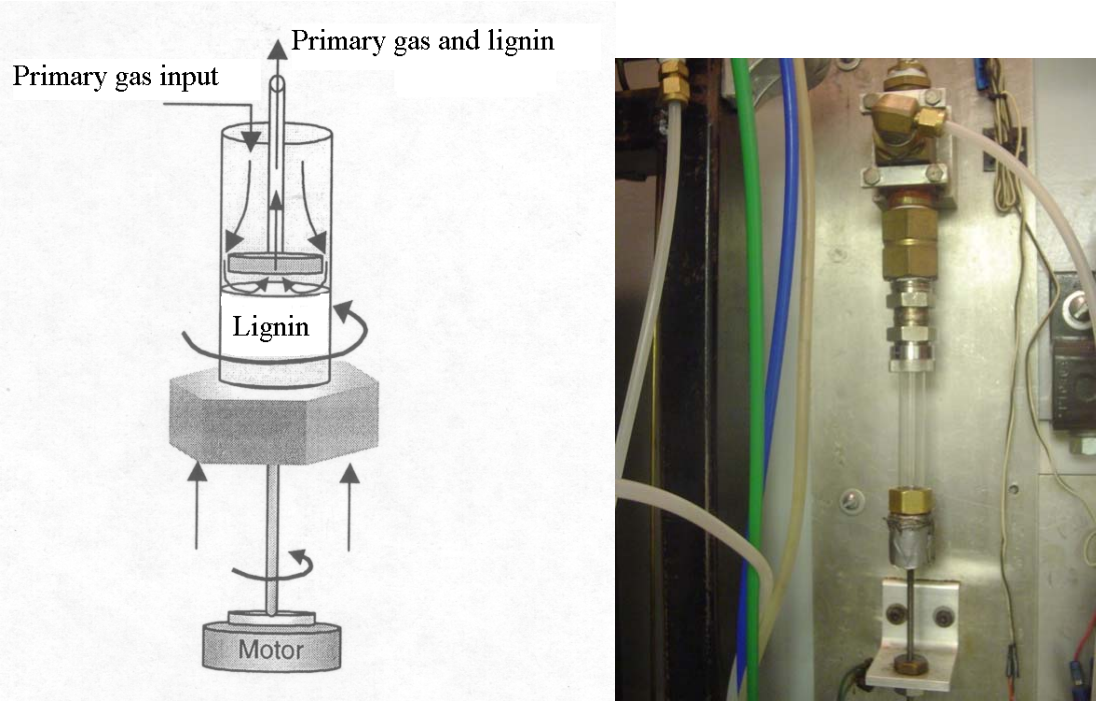

Figure 29: Feeder to feed lignin to LEFR [3]

A stainless steel tube with a diameter opening of 0.625 mm is fixed coaxially into the test tube with the other end attached to the top of LEFR. There is a prong attached to the feeding tube which acts as stirrer and helps lignin move up in the feeding tube. Lignin particles move into the

reactor with the help of primary flow from the top surface of the feeder. The feeding rate is controlled with a motor which changes the upward displacement rate of the test tube. The speed of the rotor is designed to be slow to avoid plugging of the feeding tube. Dried and sieved lignin was weighed in a test tube before feeding. The test tube was immediately attached to the feeder to avoid the effect of moisture and was also weighed after feeding. Mass flow controllers were used to control the flow of primary, secondary and quench gases. Water vapor was generated using a steam generator and temperature was controlled using a thermocouple.

4.2.1.2 Residence time:

Flaxman et al. [57] developed a software called the Laminar Entrained Flow Reactor Simulator for residence time calculations. The software works on the basis of computational fluid dynamics (CFD) and heat transfer calculations. It calculates the residence time in the LEFR using a simple CFD code. For this study, LEFR version 1.9 program available at IPST was used to calculate the particle residence times. Experimental conditions including primary gas flow rate, secondary gas flow rate, particle density and reactor temperature are entered in-to the program and the software gives the particle residence times and temperatures corresponding to the collector length.

4.2.1.3. LEFR experiments:

The pyrolysis and gasification of lignin and primary sludge were studied with the LEFR. The experimental plan for both the studies is discussed below.

4.2.1.3.1 Lignin pyrolysis and gasification experiments:

Two lignins were analyzed for their pyrolysis and gasification behavior using the LEFR with the conditions listed in Table 3.

Table 3: Experimental plan for lignin pyrolysis and gasification using the LEFR

Experiment	**Laminar Entrained Flow Reactor (LEFR)**
Residence Time	0.3 Sec – 1.5 Sec
Heating Rates	~ 10000 °C/s
Temperature	800 °C - 1000 °C
Pyrolysis	100% N_2
Gasification	70% N_2 , 15% CO_2 & 15% H_2O
Lignin	MWV lignin & SA lignin

The first lignin was kraft lignin received from Sigma-Aldrich. The second was from MeadWestvaco. Both were received in powdered form. The lignin was oven dried in a vacuum oven for 24 hours. It was then sieved for 20 minutes using sieves of sizes 63 and 90 micrometer [Figure 30]. All the sieves were properly cleaned and dried before and after each sieving. After sieving, the lignin was brushed into a Teflon pan and stored in jars until the runs. Lignin particles with size fractions in the size range of 63-90 micrometer were selected for this study.

Figure 30: Sieves

Figure 31 shows the initial lignin and the char after a LEFR run.

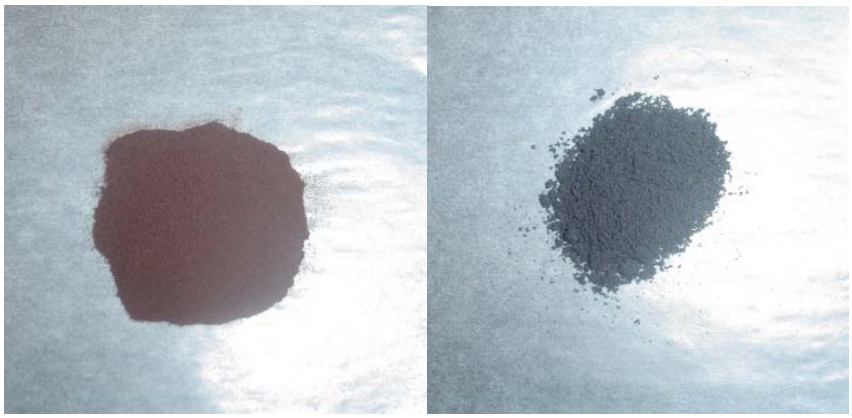

Figure 31: (a) lignin (before run) (b) char (after run)

4.2.1.3.2 Sludge studies:

4.2.1.3.2.1 Primary sludge studies:

Paper mills produce large amounts of sludge which become a waste stream and is generally landfilled. Over the last few decades landfilling costs have increased. Sludge can be gasified to produce low grade fuel gas. For this study primary sludge from Weyerhaeuser, Oglethorpe, GA was collected from a screw press. Table 4, shows the elemental analysis of primary sludge.

Table 4: Elemental analysis of primary sludge

Component	**Primary Sludge (Wayerhaeuser)**
Carbon	30.0%
Hydrogen	4.0%
Oxygen*	58.6%
Aluminum	1.1%
Calcium	4.4%
Silicon	1.0%
Iron	0.9%

*obtained by difference

The moisture content in the sludge was found to be 40%. The laminar entrained flow reactor (LEFR) works with a feeding system that can only feed materials of less than 125 micrometer in diameter. The small particle size is necessary to eliminate intraparticle temperature gradients.

The received sludge was dried in the oven at temperature of 105 °C for 72 hours. After drying the sludge turned into a fluff-like material, which was further ground in a Wiley mill to smaller size particles. The ground sludge was sieved and the fraction with diameter between 63 and 90 micrometer was selected for the LEFR runs.

4.2.1.3.2.2 Bleached pulp and unbleached liner studies:

The purpose of this study was to see the effect of filler content on the gasification behavior of sludge. Two artificial sludges were selected for this study, (S1) bleached pulp and (S2) unbleached liner pulp. Precipitated calcium carbonate (PCC) from Imerys was selected as filler. Both pulps were at 15 – 30 % consistency, and were diluted to 12% consistency. Filler (in an amount to produce a pulp-filler mix with 40% filler by weight) was then added as a powder to the sludge. After the addition, the slurries were mixed using a Hobart mixer available at IPST. The mixture was oven-dried at 105 °C for 72 hours. The dried sludge was ground in a Wiley mill and sieved to the 63 – 90 micrometer particle size. Figure 32 shows the bleached pulp after addition of PCC filler.

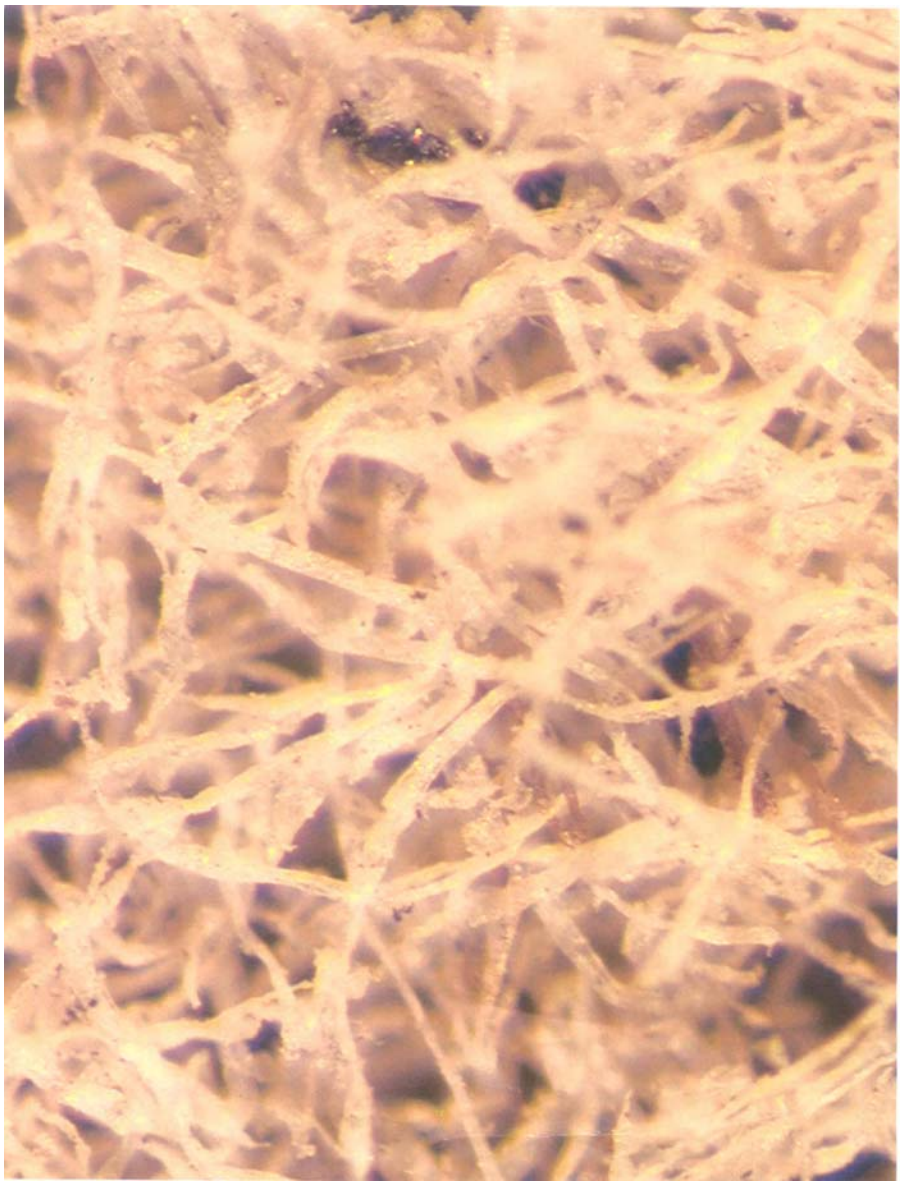

Figure 32: Bleached pulp with PCC filler

The 63 – 90 micrometer size fraction was selected and gasified in the LEFR. The input gas used was a combination of 15%CO_2, 15%H_2O and 70%N_2, and the reactor temperature was between run at 800 and 1000 °C. The residence times used for these studies were 1.25 and 1.85 seconds. Table 5, shows the experimental plan for the sludge runs.

Table 5: Experimental plan for sludge/pulp runs

Experiment	**Gasification**
Primary Sludge	70% N_2, 15%CO_2 & 15% H_2O
Bleached Pulp + 40% PCC Filler	70% N_2, 15%CO_2 & 15% H_2O
Unbleached liner + 40% PCC Filler	70% N_2, 15%CO_2 & 15% H_2O

4.2.1.3.3 Analytical methods:

After each run the char was collected in a small bottle and sent for elemental analysis, carbonate carbon analysis and total carbon analysis to the IPST analytical laboratory. The following methods and techniques were used for these studies.

Inductively coupled plasma atomic emission spectrometry (ICP-AES) was used to determine metals after digestion with nitric acid and peroxide. The char contained mainly sodium, sulfur, potassium and calcium along with other elements with minute quantities.

Carbonate carbon in the char was analyzed coulometrically. The total carbon present in the char sample was determined with a Total Carbon Analyzer. H elemental analysis was performed by Huffman Laboratories, Golden, CO.

4.2.2 Thermogravimetric Analyzer (TGA) studies:

A Thermogravimetric Analyzer (TGA) measures the weight of a sample with respect to the change in temperature. It represents a quantitative weight change associated with a thermally induced transition. A TG directly records the loss in weight as a function of temperature or time. TG curves represent the characteristic of a material due to a sequence of physical transitions and chemical reactions occurring over definite temperature ranges. Volatile products are produced at elevated temperature resulting in a weight change. Thermogravimetric studies are appropriate for material characterization as well as for investigating the thermodynamics and reaction kinetics resulting from the heating of the material. TG studies are affected by the experimental conditions and material characteristics. Some of the factors affecting the results include furnace atmosphere, the size and shape of the furnace and the sample holder material. Other factors are layer thickness, particle size, packing density, amount of sample, heat capacity and the atmosphere surrounding the sample [58]. Careful preliminary experimentation is required to ascertain that the results are not affected by external mass or heat transfer rates and that true kinetic information is obtained.

In this study a Thermogravimetric / Differential Thermal Analyzer (model TG/DTA - 320 U, from Seiko Instruments Inc.) available at the School of Polymer, Textile and Fiber Engineering at Georgia Institute of Technology, was used for the pyrolysis and gasification runs. This TGA equipment operates at atmospheric pressure.

Figure 33 shows a schematic diagram of the TGA system. The TGA consists of a high precision balance with two pans. One pan is used for weight calibration and the second is loaded with the sample before each run. The pans are held in a furnace which can be heated to the desired temperature. A thermocouple is attached to accurately read the temperature. Nitrogen is used as the carrier gas. The TGA also provides a derivative weight loss curve and provides data useful for reaction rate analysis during the heating of the sample.

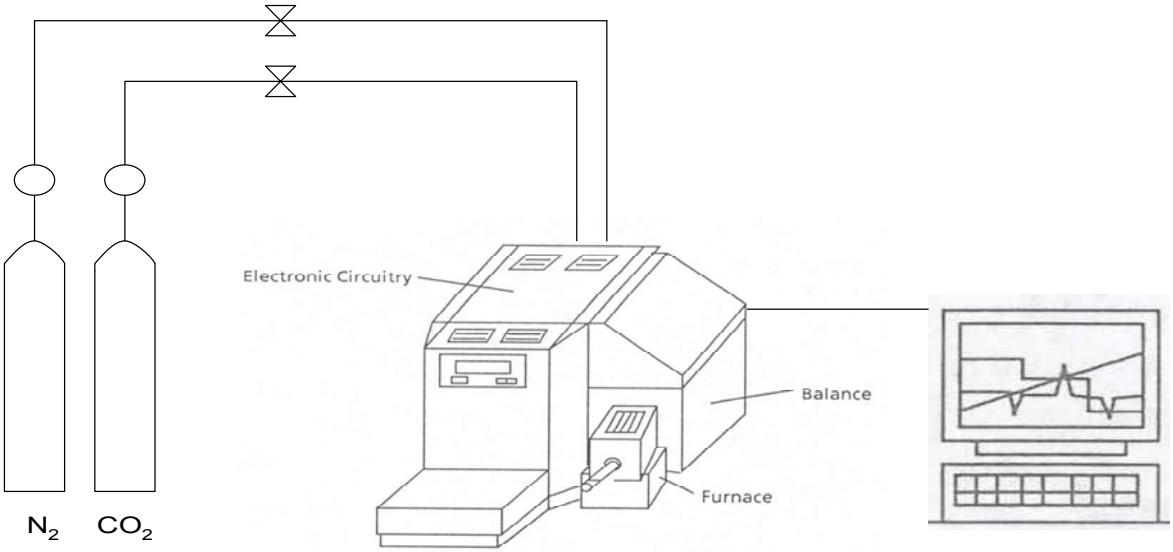

Figure 33: Schematic of the TGA testing system

Figure 34 shows the details of the TGA system.

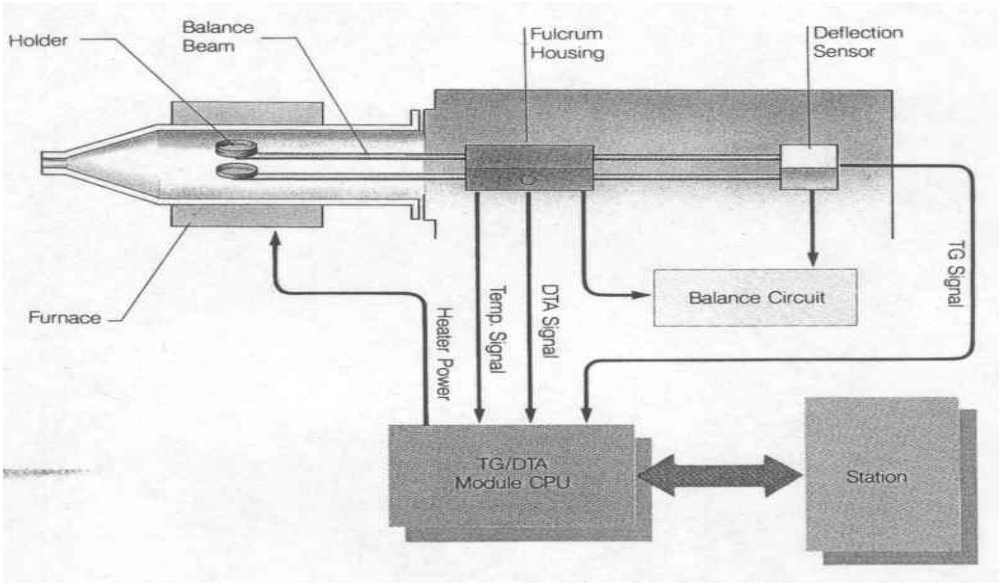

Figure 34: Details of the TGA system [59]

For these studies an initial sample mass of 10 mg was used. The sample was placed in a tared platinum pan and heated to 800 °C at constant heating rates of 20 °C/min. The sample was kept for 30 minutes at 800 °C. For the pyrolysis runs, pure N_2 at a constant flow rate of 110 mL/min was used as the carrier gas to provide an inert atmosphere. For gasification runs a 75% N_2 and 25% CO_2 mixture was used with a total constant flow rate of 110 mL/min. Different tests were made to determine that at 800 °C pyrolysis and gasification rate was not affected by sample size, gas flow rate or particle size.

The experimental conditions used for the thermogravimetric study are shown in Table 6.

Table 6: Experimental conditions for lignin pyrolysis and gasification using Thermo Gravimetric Analyzer (TGA)

Experiment	**TGA (Thermo Gravimetric Analyzer)**
Hold Time at final temperature	0.5 hr
Heating Rates	20°C/min
Temperature	800 °C
Pyrolysis	100% N_2
Gasification	75% N_2 & 25% CO_2
Lignin	MWV lignin & SA lignin

4.2.2.1 Alkali addition:

Elemental analysis of the lignins shows that the SA lignin had a much higher amount of sodium and ash as compared to the MWV Lignin. The effect of alkali metal addition on lignin pyrolysis and gasification was studied. The difference between the amount of sodium between MWV and SA lignin was calculated and a corresponding equivalent amount of Na_2CO_3 was added to the MWV lignin. First, a weighed amount of Na_2CO_3 was dissolved in deionized water to prepare a solution of the desired concentration. A weighed amount of lignin was added to the Na_2CO_3 solution. The resulting solution was allowed to stand overnight and freeze-dried for four days to completely remove moisture. After freeze-drying, the dry mixture was well mixed using a mortar and pestle and kept dry for TGA analysis.

4.2.3 Fourier Transform Infrared (FTIR) Spectroscopy studies:

A Nicolet Manga-IR 550 - FTIR available at IPST was used in this study. This spectrometer can collect data with a rate of 20 scans/second. The data were collected and analyzed by using Nicolet's Omnic software. The temperature and humidity of the room was controlled and N_2 was continuously purged into the system.

4.2.3.1 Pellet preparation:

The lignin used in this study was in powder form. The pellet technique for sample preparation is good for the study of powder like materials. In this technique finely ground sample is mixed with potassium bromide powder and pressed at a high pressure of 60,000-100,000 psi to form a transparent disk. Potassium bromide turns into plastic at high pressures and flows to form a pellet.

For this study, a 0.5 gm KBr powder packet (FTIR Grade – 99 +%) from Thermo Spectra-Tech was used. KBr was properly mixed with lignin grains and initially KBr wafers were formed without evacuation in a Mini-Press. Two highly polished bolts, turned against each other in a stainless steel cylinder, produced a clear wafer of KBr and lignin placed between the bolts. After that, high pressure was applied for one minute and pellets were formed [58].

Both the lignins were studied for structural changes with increase in temperature. Lignin samples were heated to temperatures between 155 °C and 800 °C using Thermogravimetric analyzer and

the char was collected. These char were analyzed using FTIR for both lignin pyrolysis and gasification reactions. Table 7 shows the experimental conditions used for the FTIR study.

Table 7: Experimental conditions for lignin pyrolysis and gasification using Fourier Transform Infrared (FTIR) Spectroscopy

Experiment	**Char collected for FTIR study**
Heating Rate	20 °C/min
Temperature	155 °C – 800 °C
Pyrolysis	100% N_2
Gasification	75% N_2 & 25% CO_2
Lignin Studied	MWV lignin & SA lignin

CHAPTER V

RESULTS AND DISCUSSION

This section includes all the results and findings. The results have been divided into following sections.

(1) Laminar Entrained Flow Reactor (LEFR) results

(2) Thermogravimetric Analyzer (TGA) results

(3) Fourier Transform Infrared (FTIR) spectroscopy results

(4) Study of kinetic parameters

5.1 Laminar Entrained Flow Reactor (LEFR) results:

5.1.1 Sludge results:

The pulp and paper industry produces large amounts of sludge such as primary sludge from clarifiers and secondary sludge from biological treatment. This sludge is a waste and can not be reused in the process. Typically sludge is disposed off in landfills. Due to the limited availability of sites the costs of landfill disposal are increasing. Due to higher costs and stringent environmental laws there is a need to find alternate disposal means for the sludge. Recovery of energy, conversion to useful materials or both could provide an economical alternative to landfill disposal [60]. Sludge has some heating value and it could be utilized as an energy source. It can be gasified to produce a low grade fuel gas which can also be used to produce steam onsite. Data is required for proper gasifier designing to use sludge as a fuel.

Two types of sludge pyrolysis and gasification studies were made: (a) with primary sludge from a mill and (b) with artificial sludges produced by mixing pulp fibers with filler.

5.1.1.1 Primary sludge studies:

For this study primary sludge from Weyerhaeuser, Oglethorpe, GA was selected. This sludge had a HHV of 9.66 kJ/kg. The sludge was collected and experiments were done using the LEFR available at the Institute of Paper Science and Technology. This section discusses the results of gasification of primary sludge.

The solid residue after pyrolysis or partial gasification process is called "char". It contains carbon and other remaining materials from the organic and inorganic matter originally present in the sample. Organic carbon in the char is referred to as "fixed carbon" and carbon present in carbonate form is called "carbonate carbon". The char yield varies with fuel characteristics as well as with process conditions.

Primary sludge from Weyerhaeuser, Oglethorpe, GA was dried and sieved. This sieved sludge was gasified using the LEFR at two residence times of 1.1 and 2.2 seconds at 900 ºC and 1000 ºC. A combination of 15% CO_2, 15% H_2O and 70 % N_2 was used for the gasification experiments. The char yield remaining after gasification is shown in Figure 35.

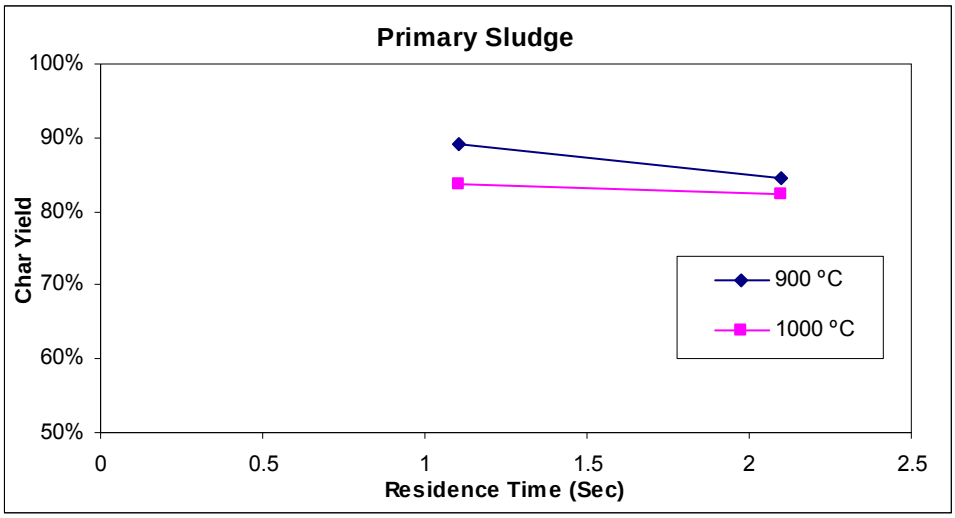

Figure 35: Char yield in primary sludge after gasification at 900 ºC and 1000 ºC.

At longer residence times, the sludge has more time to react with the reaction gases. When residence time increases, the char yield decreases. Also seen in Figure 35 is the difference in the char yield at different temperatures. At the same residence time the char yield is lower when sludge is exposed to the higher temperature of 1000 ºC than to 900 ºC. The increase in temperature increases C conversion and results in lower char yield. Char yield was found to be 89% at 900 ºC (1.1 sec residence time) and changed to 82 % at 1000 ºC (2.2 sec residence time).

Frederick et al. [60] did a pyrolysis study of sludge from a recycled fiber plant using the same LEFR and obtained 70 % and 59% char yield at 700 ºC (1.4 sec residence time) and 900 ºC (0.9 sec residence time) respectively. Results from the current study show that the char yields were higher than those from the previous study which likely reflects the higher inorganic content of the sludge in the present study.

Several more experiments were made but the results in general showed very poor reproducibility. As mentioned earlier feeding to the LEFR is very challenging and uniform particles of less than

125 micrometer are needed. The fluffy fibrous nature of primary sludge makes it hard to feed it to the LEFR through a small opening. With the current LEFR there are limitations to doing sludge studies and the reproducibility of the experiments is not very good.

5.1.1.2 Bleached pulp and unbleached liner results:

This study was conducted to see the effect of filler on sludge gasification rate. Filler is added to paper to obtain different required end properties. The filler is not completely retained on paper and becomes part of sludge. Different sludges contain of varying amounts of filler depending on the grade of paper produced and the type of filler used. Recycle mills also use coated paper, which contains significant amounts of clay, $CaCO_3$ and TiO_2 as filler. The fillers become part of the sludge and affect sludge quality. This study was aimed at seeing the effect of precipitated calcium carbonate (PCC) filler on sludge gasification. PCC is a widely used filler in the paper industry and was received from Imerys for this study. Artificial sludge was prepared by mixing pulp and the filler, and the gasification of the pulps with and without the sludge was compared. Gasification results for bleached pulp are shown in Figure 36. The fixed C remaining in the char was expected to decrease with increasing the residence time, but there was not much change in the fixed C remaining for bleached pulp with filler addition. When compared to pure bleached pulp, the fixed C remaining is higher and the gasification rate is slower. This decrease in rate is not very significant.

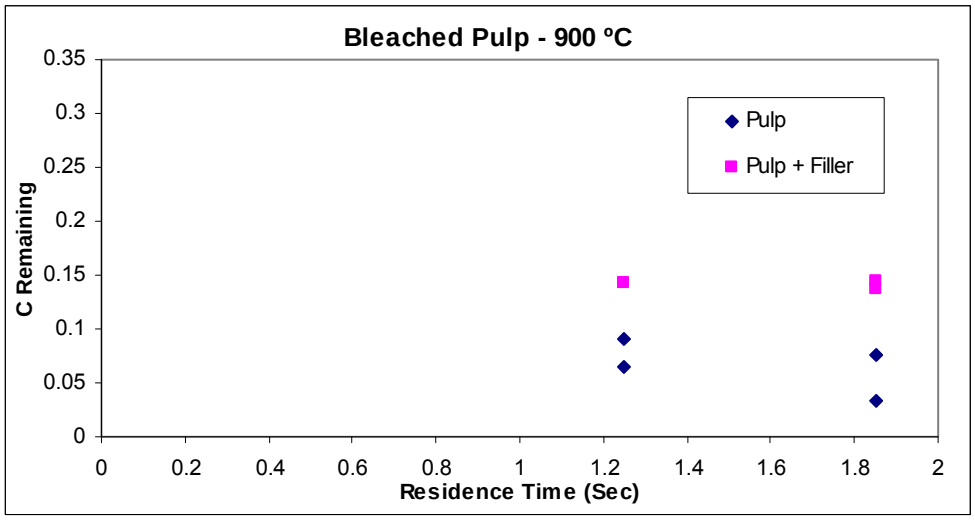

Figure 36: Fixed C remaining at 900 °C for bleached pulp gasification

The effect of filler on unbleached liner is shown in Figure 37. With filler addition, a slight increase in fixed C remaining is observed at the same residence time compared to pure unbleached liner. The gasification rate is nearly the same for both cases, i.e. with and without filler addition.

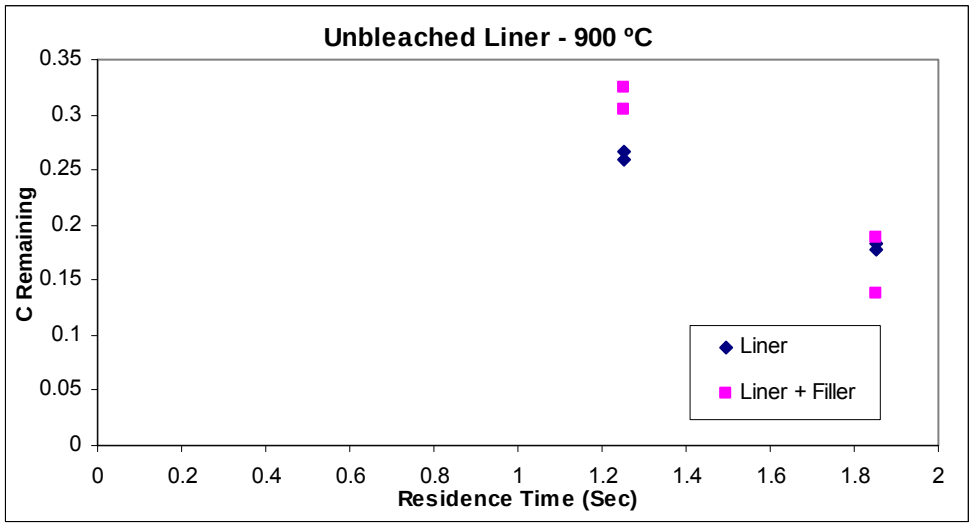

Figure 37: Fixed C remaining at 900 °C for unbleached liner gasification

Both bleached and unbleached pulps were also compared in terms of their gasification behavior. As seen in Figure 38, there is some difference between the gasification rates of the two pulps.

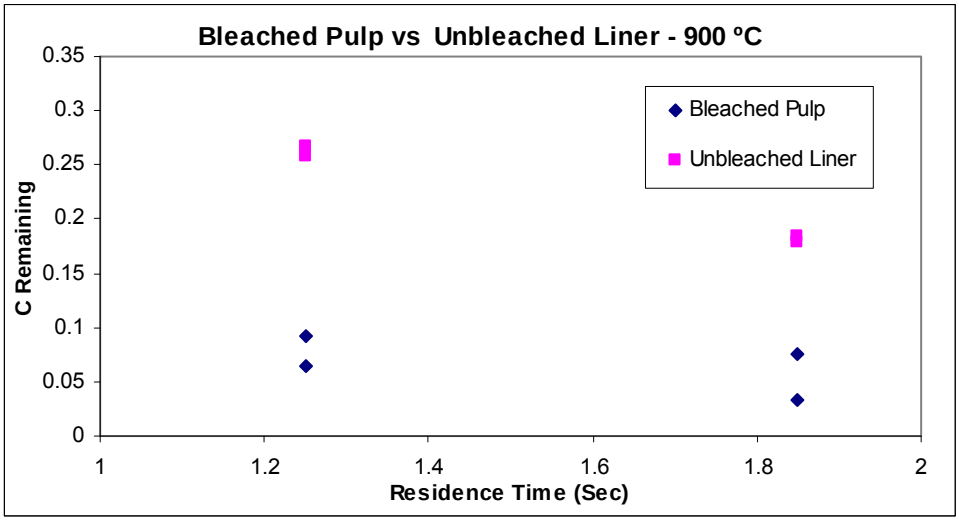

Figure 38: Fixed C remaining at 900 °C in bleached pulp and unbleached liner gasification

Much more fixed C remains in the unbleached liner than in the bleached pulp. The kappa number of the unbleached pulp was nearly 105, which indicates that the unbleached pulp had very high lignin content. The presence of lignin in the liner must be responsible for the higher fixed carbon yield.

The data suggests that filler addition decreased the gasification rate of bleached pulp. A large difference was seen in the gasification rates of bleached and unbleached pulp. The difference was attributed to the higher lignin content of the unbleached pulp. All the remaining experiments were done on pyrolysis and gasification of lignin.

The pulp gasification experiments had a lot of operational problems. A better feeding system with a wider feeder opening is needed to get consistent results for materials such as sludge and pulp.

5.1.2 Lignin pyrolysis and gasification results:

The data on carbon conversion and char yield are important for maximizing the use of lignin as an alternative fuel for generating electricity. In a good gasifier, the carbon must be converted to a fuel gas within certain operational conditions and time limits. This section discusses the char yield and carbon conversion results during the pyrolysis and gasification of MWV lignin and SA lignin at different residence times.

5.1.2.1 Lignin gasification results:

5.1.2.1.1 Mead Westvaco (MWV) lignin results:

Results for the char yield and residual C for MWV lignin during gasification experiments in the LEFR are shown in Figure 39. The results show the char yield and C remaining at 800 °C after MWV lignin gasification (70% N_2, 15% H_2O and15% CO_2). Overall, the char yield and C remaining decreased with the increase in residence time from 0.3 sec to 1.0 sec. The most pronounced effect on char yield and C remaining was seen before the residence time of 0.3 sec. They both decreased very rapidly in the very beginning of the reaction.

When lignin is heated beyond 200 °C, devolatilization takes place [Figure 39]. The results indicate that initial devolatilization takes place very rapidly in the LEFR when particles are heated at very high heating rates of the order of 10000 °C/sec. At 800 °C and at the shortest residence time of 0.3 second, the char yield is 40 – 52 %. It shows that the maximum mass loss takes place in the initial stage and at longer residence times there is a smaller decrease in the char yield.

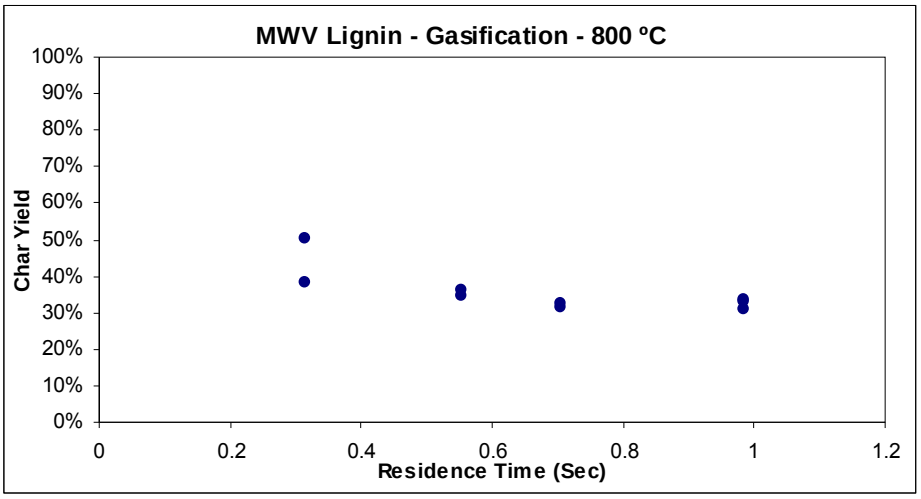

(a)

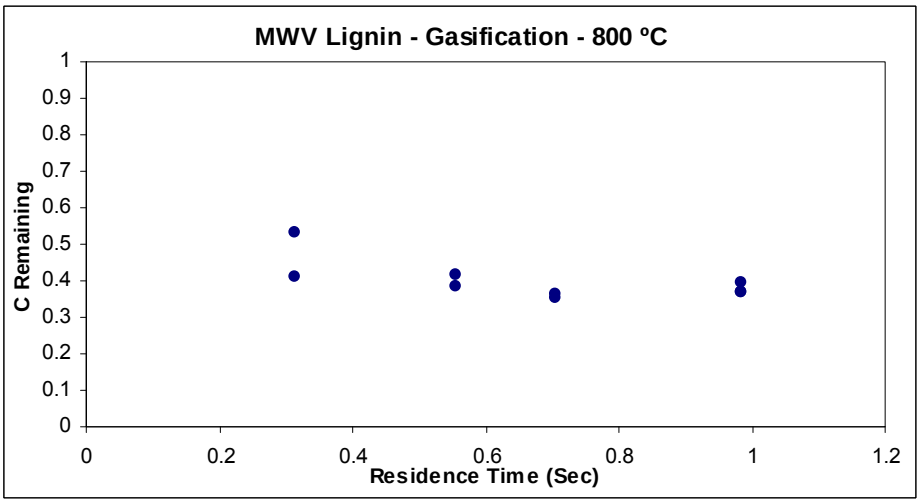

(b)

Figure 39: (a) Char yield and (b) C Remaining at 800 °C after MWV lignin gasification (70% N_2, 15% H_2O and15% CO_2) using LEFR

At this temperature, the initial mass loss may have continued at 0.3 seconds but is finished by 0.5 seconds, after which there is little decrease in the char yield. Most of the organic decomposition of lignin takes place before 0.3 seconds, after which mostly carbonate and sulfate reduction occurs (Eq 6-9).

$$Na_2SO_4 + 2C \rightarrow Na_2S + 2CO_2 \quad \textbf{(6)}$$

$$Na_2SO_4 + 4C \rightarrow Na_2S + 4CO \quad \textbf{(7)}$$

$$Na_2CO_3 + C \rightarrow 2Na + CO + CO_2 \quad \textbf{(8)}$$

$$Na_2CO_3 + 2C \rightarrow 2Na + 3CO \quad \textbf{(9)}$$

Sricharoenchaikul et al. [3] did a study of black liquor gasification using the LEFR and found that char yield rapidly dropped to 76% within the first 0.3 seconds of reaction.

Figure 40 shows the char yield and C remaining for MWV lignin at 1000 °C. The data show similar trends with respect to change in residence time for both temperatures. The results at 1000 °C also suggest that most of the devolatilization takes place very early. Some of the results are not very consistent [Figure 40] and may have been caused by experimental uncertainties.

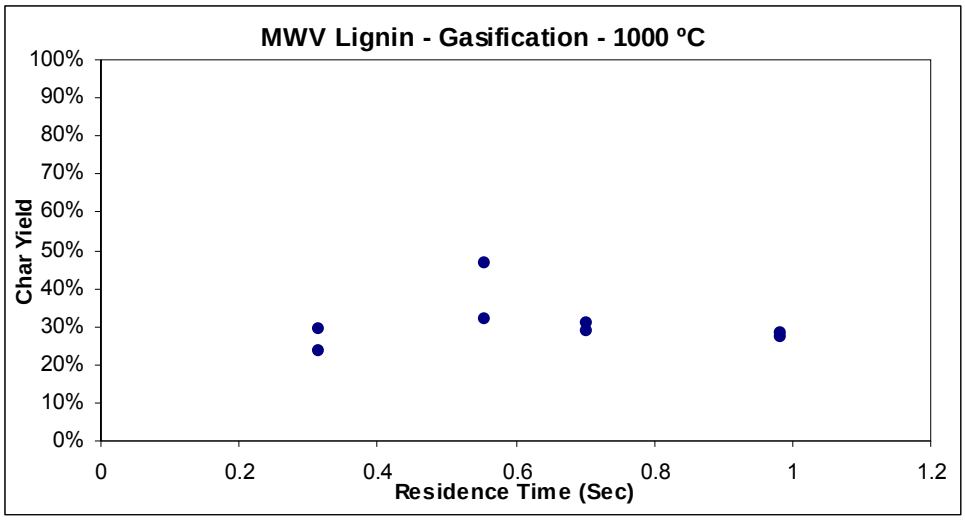

(a)

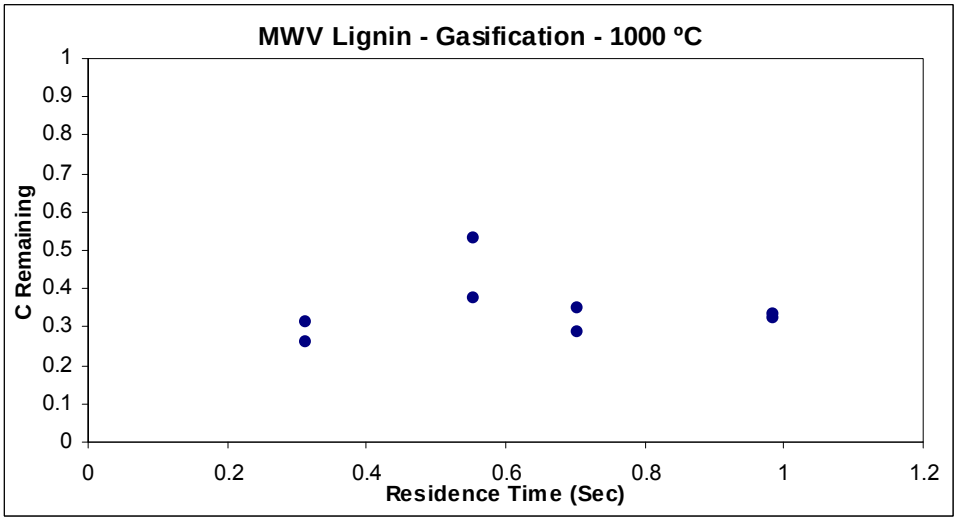

(b)

Figure 40: (a) Char yield and (b) Fixed C Remaining at 1000 °C after MWV lignin gasification (70% N_2, 15% H_2O and15% CO_2) using LEFR

Under the harshest experimental condition of 1.0 sec and 1000 °C, the char yield was 27% and 32% of the fixed C remained. At the current gasification conditions used this is the minimum char yield and C remaining possible. It suggests that the LEFR can not completely gasify MWV lignin under these conditions.

Figure 41 shows SEM pictures of MWV lignin and gasification char generated at 0.7 seconds residence time. The pictures show that before the reaction there are no uniform spheres present. After gasification hollow spheres of 25 - 200 micrometer diameters are present in the char. Both individual spheres and clusters of spheres are visible. The morphology of these char particles is quite different from that of lignin and shows particle swelling during the reaction. Char shows continuous, unbroken appearance with higher porosity and roughness than did the initial particles. The roughness on the surface is likely due to carbon removal by CO_2 from the sphere surface during gasification [61].

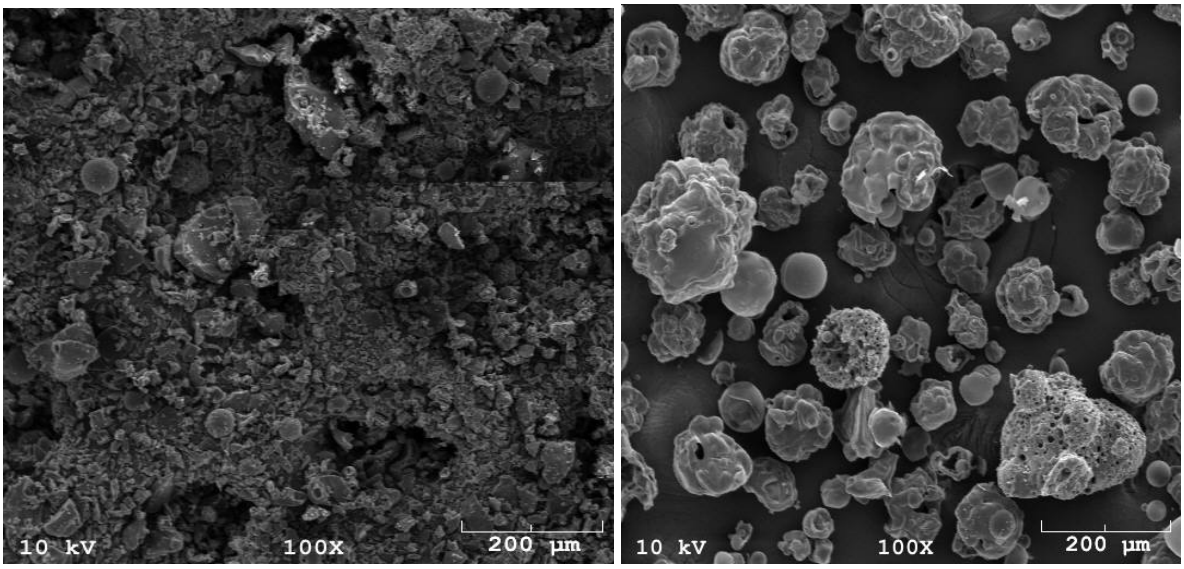

(a) (b)

Figure 41: SEM images of (a) MWV Lignin (b) Char residue after LEFR run at 0.7 sec residence time

5.1.2.1.2 Sigma Aldrich (SA) lignin results:

The change in char yield and C remaining after SA lignin gasification at 800 °C is shown in Figure 42. As for the MWV results, the char yield and C remaining decrease with increase in

residence time but there is some difference in the behavior. The SA lignin shows a much higher char yield and fraction of C remaining as compared to the MWV lignin. After initial devolatilization the mass loss continues up to 0.5 seconds. After that there is little if any change in the char yield and C remaining.

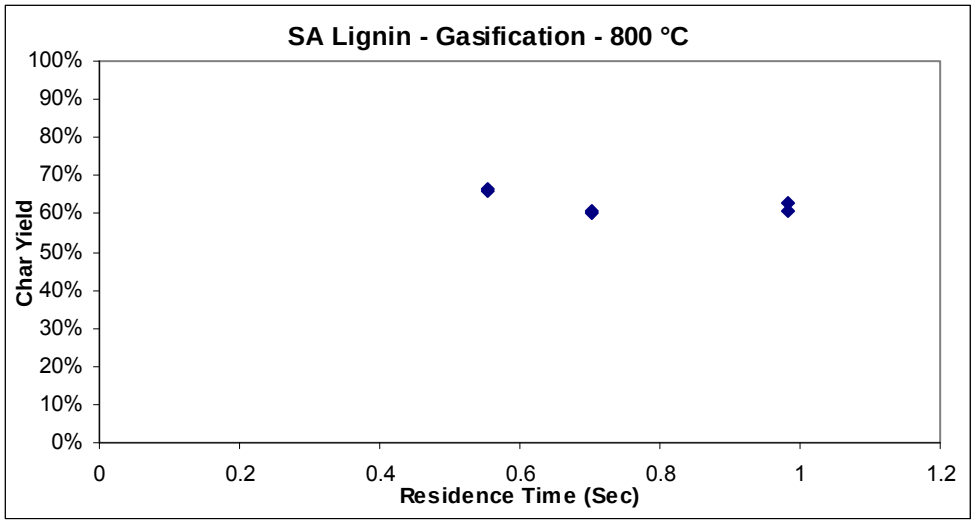

(a)

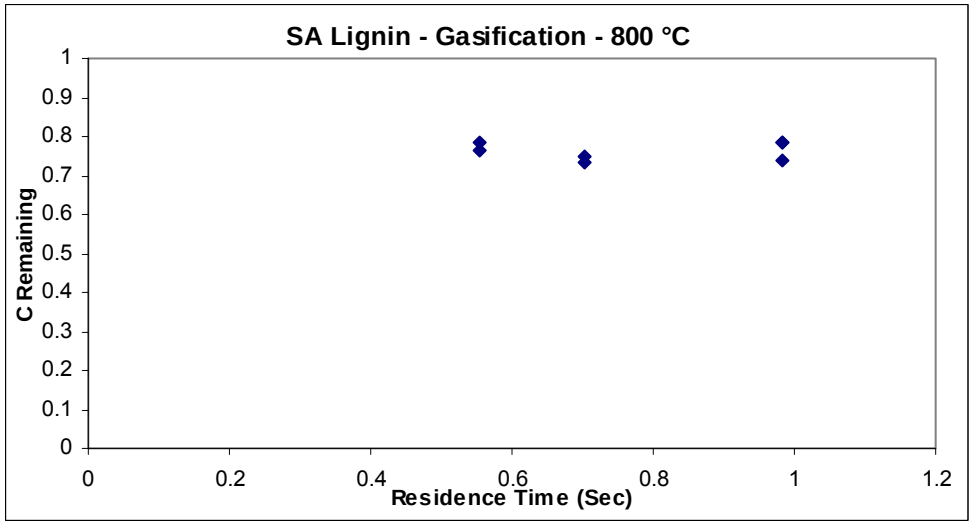

(b)

Figure 42: (a) Char yield and (b) Fixed C Remaining at 800 °C after SA lignin gasification (70% N_2, 15% H_2O and15% CO_2) using LEFR

Figure 43 shows the char yield and C remaining during SA lignin gasification at 1000 °C. At this temperature the mass loss continues until the final residence time of 1.0 seconds.

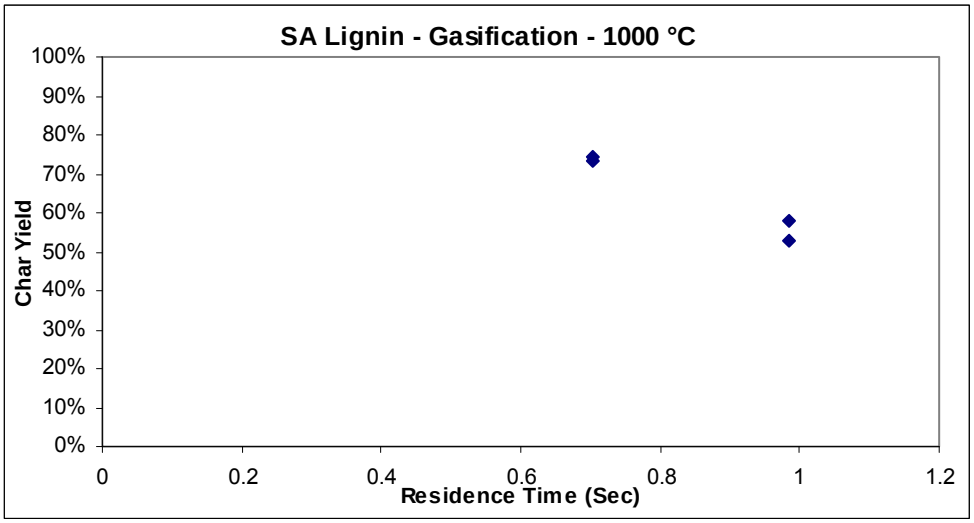

(a)

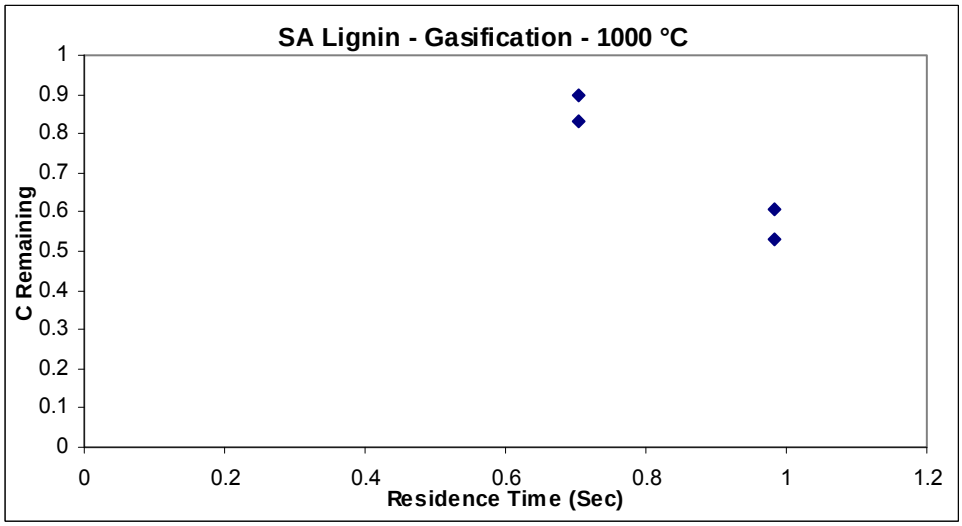

(b)

Figure 43: (a) Char yield and (b) Fixed C Remaining at 1000 °C after SA lignin gasification (70% N_2, 15% H_2O and15% CO_2) using LEFR

The results suggest that at 1000 °C for SA lignin, sulfate and carbonate reduction continue and hence mass change takes place even at a long residence time of 1.0 second.

Figure 44 shows SEM pictures of SA lignin and gasification char generated at 0.7 seconds residence time. As seen during the gasification of MWV lignin [Figure 41], particle swelling also takes place during SA lignin gasification.

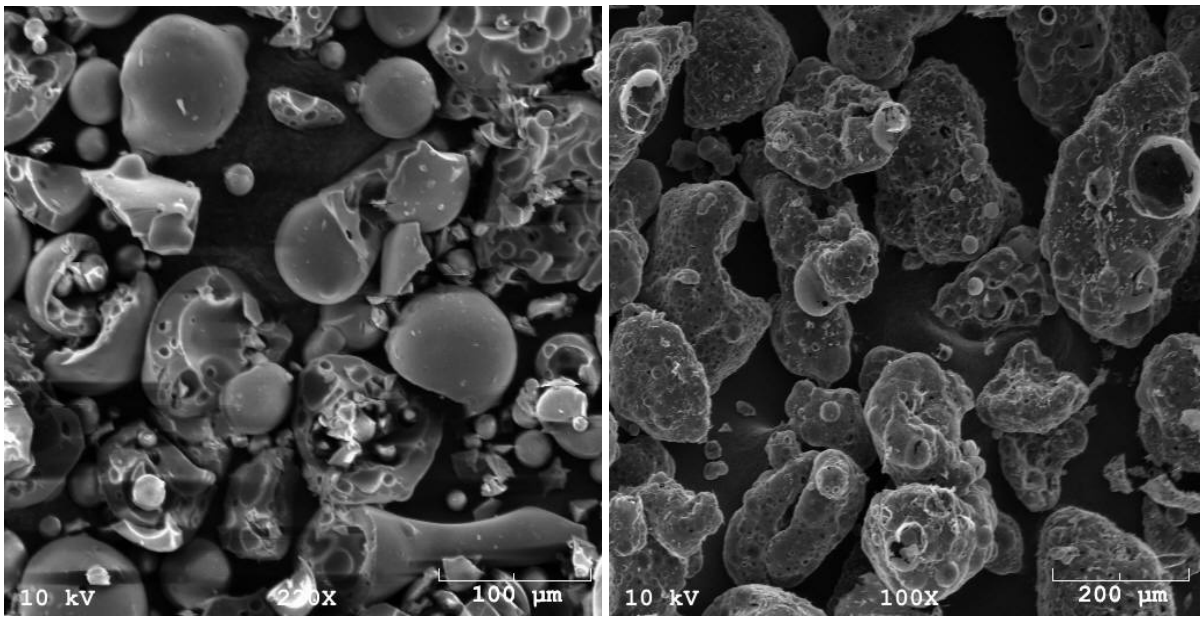

(a) (b)

Figure 44: SEM images of (a) SA lignin (b) char residue after LEFR run at 0.7 sec residence time

Char particle morphology is different than that of lignin particles and indicates swelling during the reaction. Lignin particles before reaction are relatively smooth and have very little porosity. After the reaction particles turn into porous spherical structure. Pure SA lignin did not contain uniform spheres but after gasification spheres with 100 - 200 micrometer diameters were present in the char.

Chars from both the lignins have some similarity as well as differences. For both the lignins, the char morphology is different than that of the original lignin. Both chars have a continuous,

unbroken appearance with a different morphology than those of the initial particles. It suggests that these chars are plastic during their initial devolatilization and swelling. If the chars were not conformable they would appear broken [61].

It is hard to compare the swelling behavior of both the lignins [Figure 41 & Figure 44]. MWV lignin particles were not present as uniform spheres before the reaction but after gasification, they turned into hollow spheres of 25 – 200 micrometer diameter. SA lignin initially consisted of individual particles of varying sizes, they swelled into porous spheres of ~ 200 micrometer diameter.

The surface of SA lignin char particles is rougher than that of MWV lignin char. SA lignin has higher amount of ash and Na compared to MWV lignin. The higher amount of Na_2CO_3 in SA lignin would form crystals and result in higher roughness [61].

Figure 45 compares char yields during MWV lignin and SA lignin gasification at 800 °C and 1000 °C using the LEFR. Temperature does have an effect on the char yield during lignin gasification.

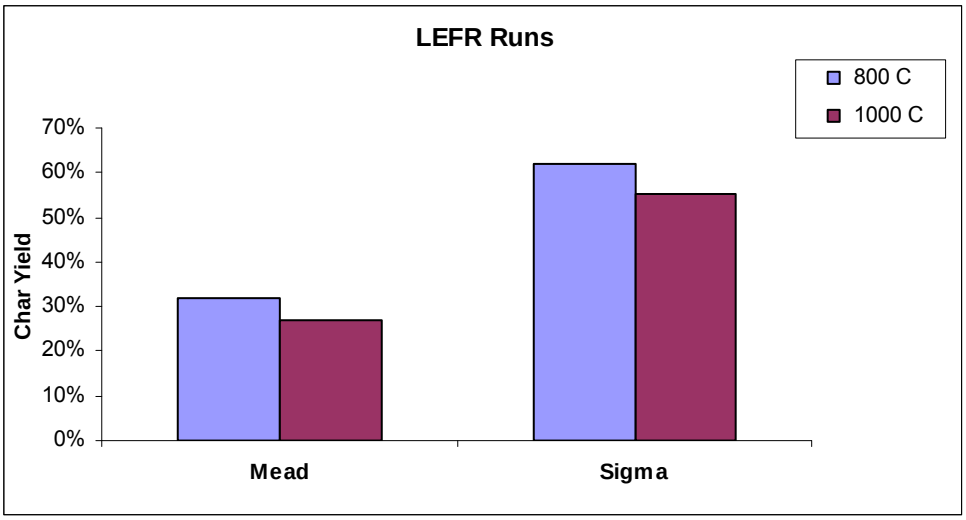

Figure 45: Char yield at 1.0 second residence time after MWV lignin and SA lignin gasification (70% N_2, 15% H_2O and15% CO_2) using LEFR

The results clearly indicate that SA lignin has much higher char yield at both temperatures than MWV lignin. The effect of raising temperature from 800 °C to 1000 °C is significant for both lignins. During gasification of MWV lignin, the char yield decreases from 32% to 27% as the temperature is increased from 800 °C to 1000 °C. The SA lignin shows a decrease in char yield from 62% to 57% with the same temperature increase.

5.1.2.2 Lignin pyrolysis results:

Char yields after pyrolysis and gasification of MWV lignin in the LEFR are compared in Figure 46. The results show the char yield at 800 °C and 1000 °C after pyrolysis (100% N_2) and gasification (70% N_2, 15% H_2O and15% CO_2).

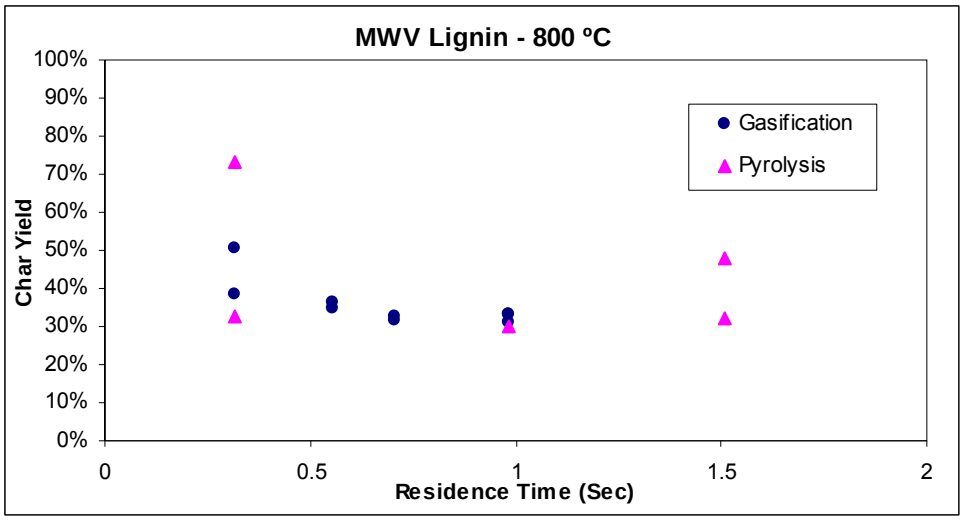

(a)

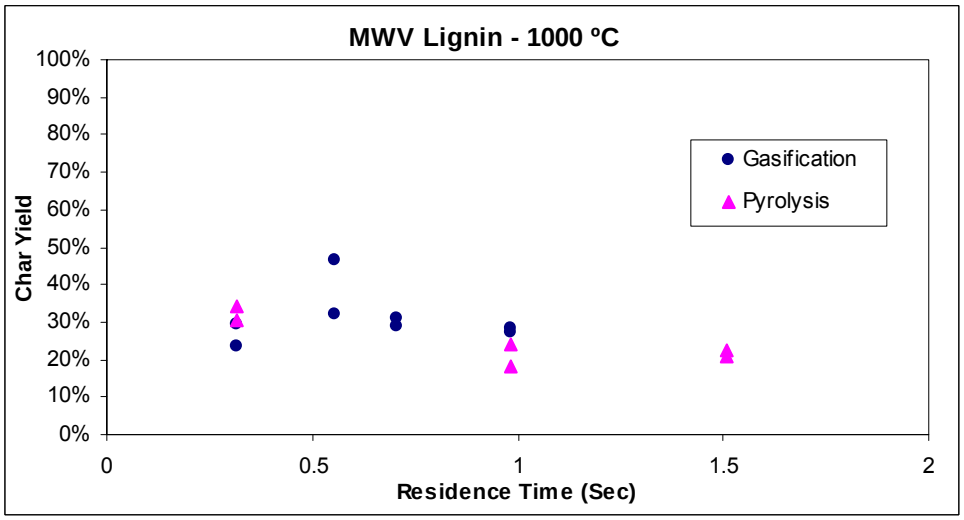

(b)

Figure 46: Char yield at (a) 800 °C and (b) 1000 °C after MWV lignin pyrolysis (100% N_2) and gasification (70% N_2, 15% H_2O and15% CO_2) using LEFR

Initial devolatilization takes place very rapidly in the reactor during both pyrolysis and gasification. Primary devolatilization is completed as soon as heat is supplied to the lignin. At 1000 °C and the shortest residence time of 0.3 second, the char yield is 25 – 35 %. It shows that during both pyrolysis and gasification, the maximum decrease in char yield takes place in the initial stage of the reaction and at longer residence times there is little change. At 800 °C at the shortest residence time of 0.3 seconds, the char yield is between 30 and 70%. The char yield of

70% at 0.3 second is an outlier and probably derives from experimental error. At 800 °C temperature, the initial mass loss continues at 0.3 seconds and finishes by 0.5 seconds. After that there is little decrease in the char yield in either gas atmosphere. Hence, most of the organic decomposition of lignin takes place during initial devolatilization. Further decrease in char yield takes place mostly due to reactions of inorganics present in lignin, specially carbonate and sulfate reduction as per (Eq 6-9). The above char yield results show that there is not much difference between pyrolysis and gasification experiments at either temperature.

Sricharoenchaikul et al. [56] did pyrolysis and gasification studies of black liquor solids using the LEFR at IPST [Figure 47]. They did experiments with four different gas compositions, 100% N_2, 5% H_2O in N_2, 12% H_2O in N_2 and 5% CO_2 in N_2 at residence times from 0.3 sec to 1.7 sec. They also found that at 800 °C the effect of gas composition was minimal. Their results at 800 °C are consistent with our data in that there is very little difference in char yield during lignin pyrolysis and gasification.

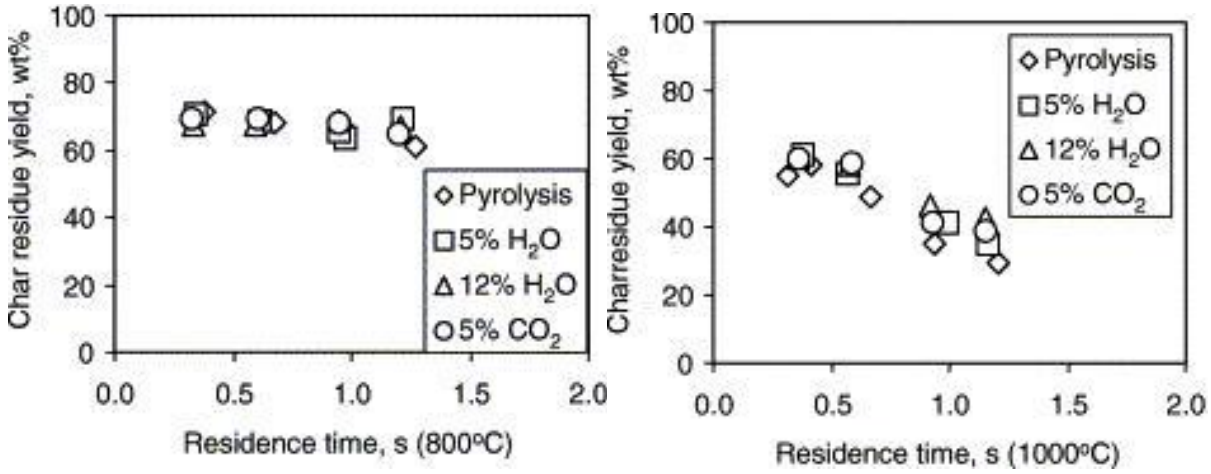

(a) (b)

Figure 47: Char yield for black liquor pyrolysis and gasification at (a) 800 °C (b) 1000 °C using LEFR at IPST [56]

At the higher temperature of 1000 °C the char yield decrease rate became faster for both pyrolysis and gasification. The gasification in a H_2O atmosphere was slightly faster than pyrolysis in N_2 and gasification with CO_2 in N_2. They also found that during pyrolysis the char yield decreased gradually with increase in temperature. The char yield changed from 75% at 700 °C to 60% at 1100 °C [3].

In another study, Gustafsson and Richards [48] studied lignin pyrolysis using a LEFR at Chalmers University of Technology in Sweden. They did pyrolysis experiments between 700 °C and 1000 °C between 0.7 sec and 4.2 sec [Figure 48]. Their results showed that char yield decreased with longer residence time and higher temperatures. After initial devolatilization the char yield was not much affected by residence time.

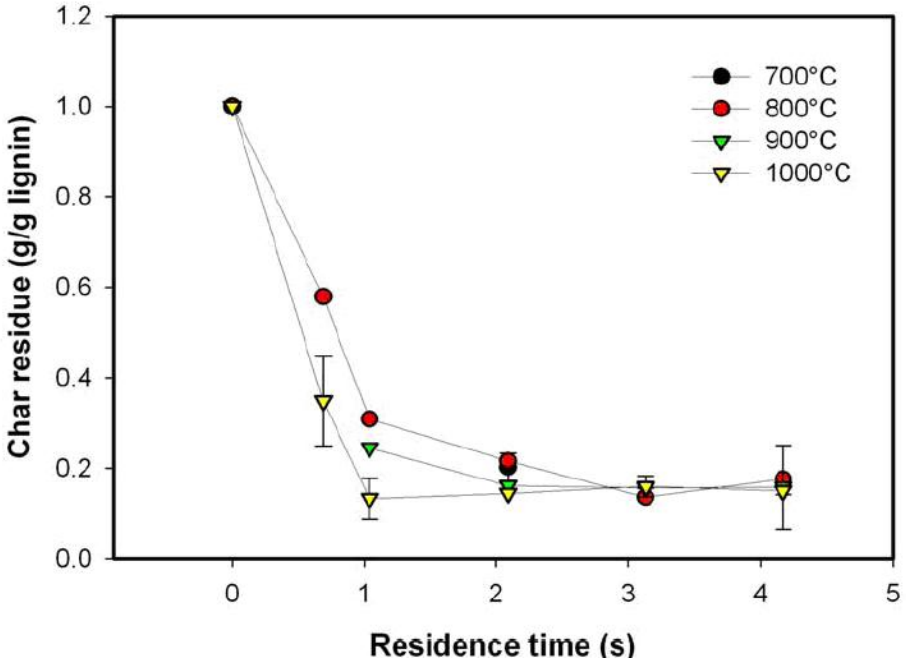

Figure 48: Char residue at different temperatures and residence times using Chalmers LEFR [48]

The results from the current study show that there is not much difference between pyrolysis and gasification experiments in the LEFR [Figure 46]. Rapid devolatilization is complete at 0.3 – 0.5 seconds, and the maximum possible residence time of 1.5 second is too short for appreciable gasification. As a longer residence time is required for substantial gasification to take place, the LEFR is unsuitable for lignin gasification studies beyond the initial devolatilization at these temperatures.

5.2. Thermogravimetric Analyzer (TGA) results:

5.2.1 Pyrolysis results:

The TG curve reflects the weight loss (char yield) of the sample due to thermal degradation with increasing temperature. Figure 49 shows the char yield curves for pyrolysis of SA lignin at 800 °C and 1000 °C. All the calculations were done on an ash free basis. SA lignin samples were pyrolyzed at a heating rate of 20 °C/min under nitrogen atmosphere and were kept for 30 minutes at the final temperature.

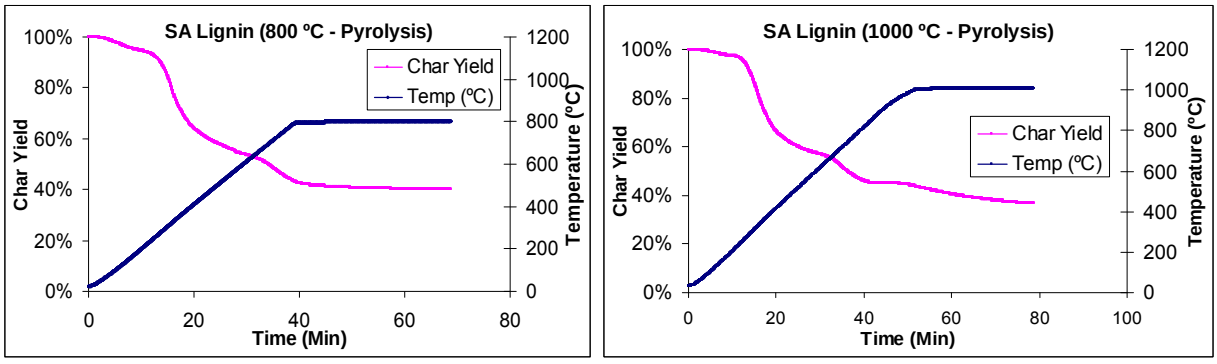

(a) (b)

Figure 49: Char yield -TG curve for pyrolysis of SA lignin at (a) 800 °C and (b) 1000 °C using TGA

The SA lignin shows a gradual decrease in mass at both pyrolysis temperatures but there are some differences in the mass loss behavior. After reaching the temperature of 800 °C, the mass loss rate decreases for 800 °C pyrolysis. Upon extended holding of the lignin sample at 800 °C, the reaction slows down and the mass becomes nearly constant. Upon extended holding at 1000 °C mass loss continues until the end of the experiment.

The pyrolysis of MWV lignin was also studied at 800 °C and 1000 °C with a heating rate of 20 °C/min using N_2 as a carrier gas. Figure 50 shows the change in char yield with respect to temperature change for both pyrolysis temperatures.

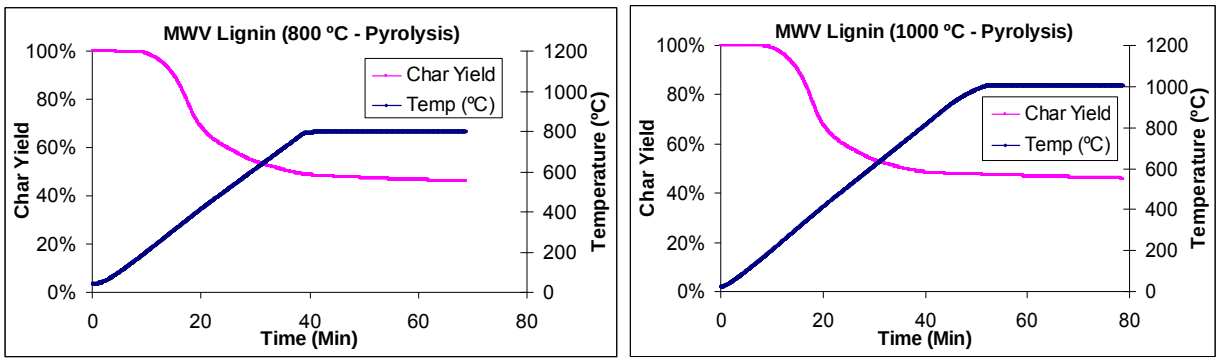

(a) (b)

Figure 50: Char yield -TG curve for pyrolysis of MWV lignin at (a) 800 °C and (b) 1000 °C using TGA

The mass loss behavior is very similar for both temperatures. The mass loss takes place gradually up to 780 °C, beyond which the mass loss is minimal. Even after extended holding at respective temperatures of 800 °C and 1000 °C there is little or no mass change taking place. The MWV lignin shows nearly the same char yield after pyrolysis at 800 °C and 1000 °C.

The MWV lignin behaves differently than SA lignin during pyrolysis. The char yield after pyrolysis at 800 °C and 1000 °C for both MWV and SA lignins are shown in Figure 51. The SA lignin shows lower char yield than the MWV lignin. The SA lignin has much higher ash and Na content than MWV lignin. It is believed that the ash present in the form of Na salts catalyzes the pyrolysis reaction which results in lower char yield for SA lignin. Hallen et al. [62] studied the

effect of Na_2CO_3 on biomass steam gasification and found that it increases char yield during the devolatilization stage and decreases char yield during the second gasification stage.

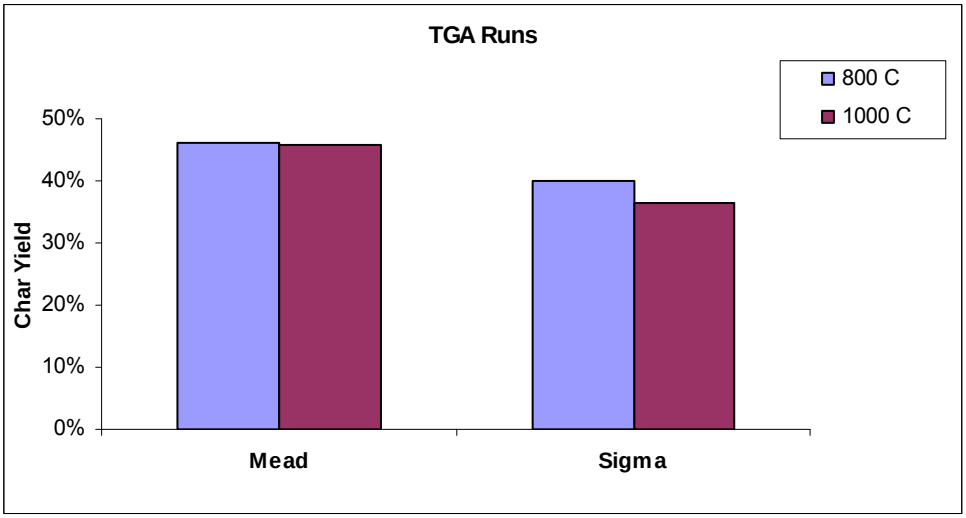

Figure 51: Char yield after pyrolysis at 800 °C and 1000 °C for MWV and SA lignins using TGA.

The char yield for the MWV lignin is nearly 46 % at both the pyrolysis temperatures while the SA lignin shows a change in char yield from 40% to 36%.

Tejado et al. studied the thermal degradation of three different lignins extracted from black liquor [16]. They did thermogravimetric analysis of, kraft pine lignin (L1), soda-anthraquinone flax lignin (L2) and Organosolv wild tamarind lignin (L3) at 10 °C/min heating rate in helium atmosphere. Figure [52] shows the DTG and TG curves for all three lignins.

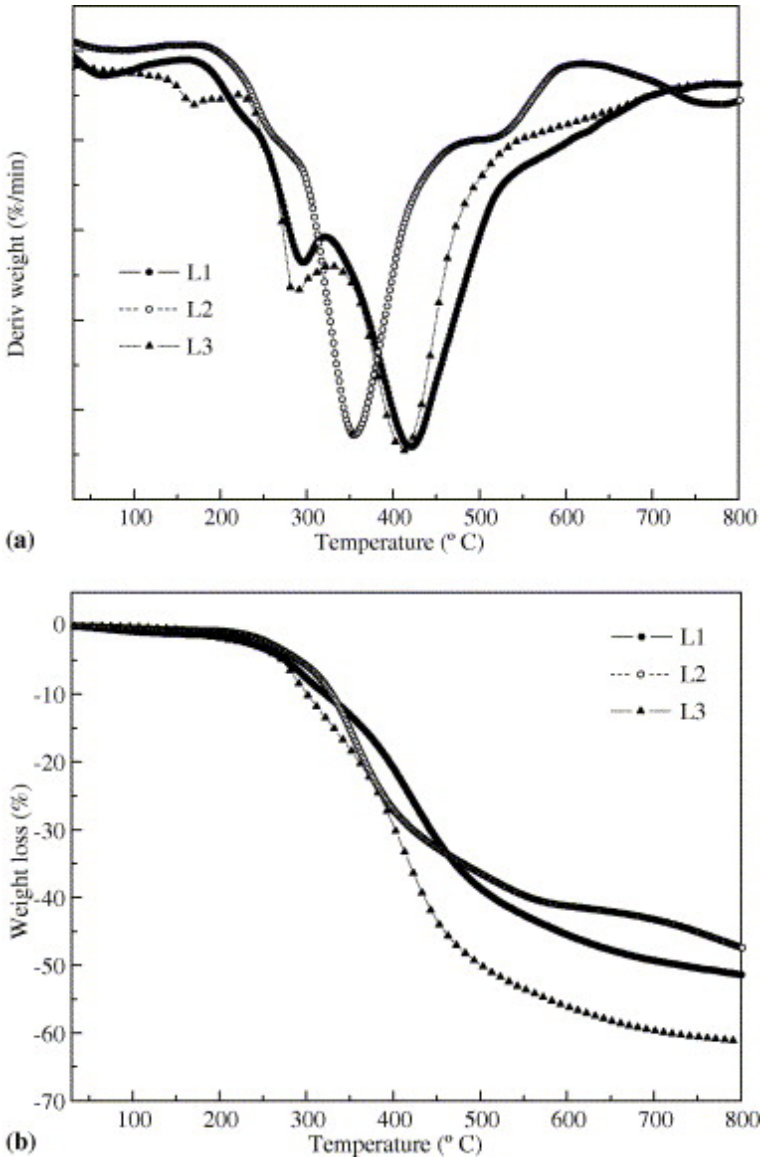

Figure 52: (a) DTG and (b) TG curves of L1 Kraft pine lignin (- ● -), L2 Alkali flax lignin(- ○ -) and L3 Organosolv lignin(- ▲ -) [16]

They found char yields of 48%, 53% and 38% for lignin L1, L2 and L3 respectively. These char yield values are in the range of the char yields obtained in the current study.

5.2.1.1 MWV lignin vs. SA lignin during pyrolysis:

Figure 53 shows the ash-free char yield and reaction rate curves for MWV and SA lignin pyrolysis at a heating rate of 20 °C/min under a nitrogen atmosphere. Both lignins show sharp DTG profiles, but there are some differences in the behavior. In both cases pyrolysis starts at about 200 °C and the reaction rate progressively increases with temperature and reaches a maximum between 300 and 380 °C. Tejado et al. also reported DTG_{max} value between 350 and 425 °C for kraft lignin and anthraquinone flax lignins [16]. In this region, fragmentation of inter-unit linkages takes places and monomeric phenols are released. Above 500 °C the decomposition of some aromatic rings also occurs [16, 63, 64].

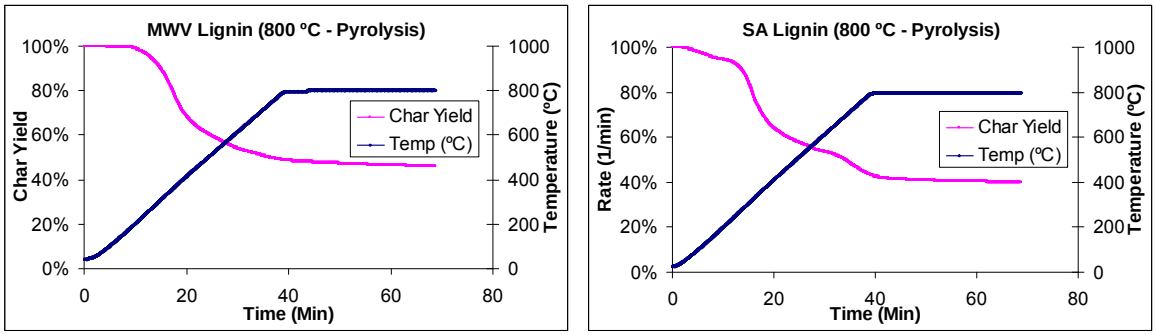

(a)

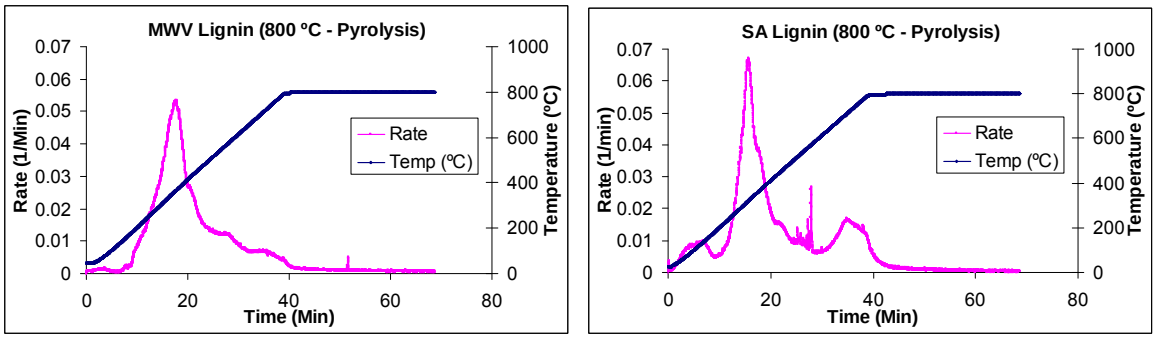

(b)

Figure 53: (a) Char yield -TG and (b) reaction rate - DTG curves for pyrolysis of MWV and SA lignins.

For both lignins, the pyrolysis reaction rate decreases up to 600 °C above which the SA lignin undergoes a secondary mass loss, which causes an increase in the reaction rate at about 800 °C. The SA lignin has a higher ash and sodium content than the MWV lignin, which suggests that the SA lignin has more Na_2CO_3 than the MWV lignin. The Na_2CO_3 is probably responsible for the secondary reactions according to reactions (Eq 8) and (Eq 9). Upon extended holding of the sample at 800 °C, the reaction slows down and the mass becomes nearly constant. The MWV lignin gives approximately 46% final char yield while 40% char yield is obtained from SA lignin. Tejado et al. also found a high char yield of 40-50% after heating up to 600 °C [16]. Highly condensed polymeric structures formed during the reaction contribute to the high char yield because of their high thermal stability [38, 16].

5.2.2 Gasification results:

5.2.2.1 MWV lignin vs. SA lignin during gasification:

Figure 54 shows TG and DTG curves for gasification of SA lignin and MWV lignin under a 75% N_2 and 25% CO_2 atmosphere and at a heating rate of 20 °C/min. Between 190 and 400 °C both lignins show similar pyrolysis characteristics and experience similar mass loss behavior. Both show DTG_{max} values between 340 and 380 °C. During gasification both the lignins show a secondary mass loss region while this is only shown by the SA lignin during pyrolysis. CO is produced during gasification as per the Boudouard reaction (Eq 10).

$$C + CO_2 \rightarrow 2CO \qquad \textbf{(10)}$$

The Na_2CO_3 decomposition reaction (Eq 8) is suppressed by the presence of CO_2 in the atmosphere. During gasification a higher amount of ash and sodium in the SA lignin does not lead to a higher reaction rate for this lignin.

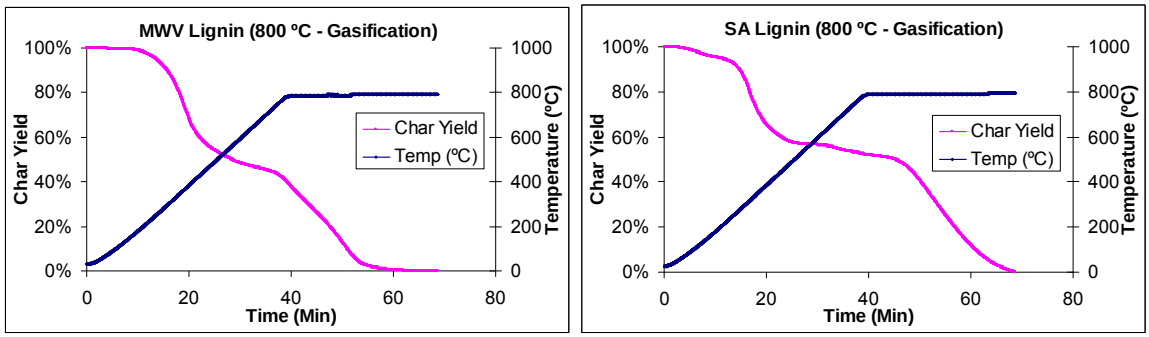

(a)

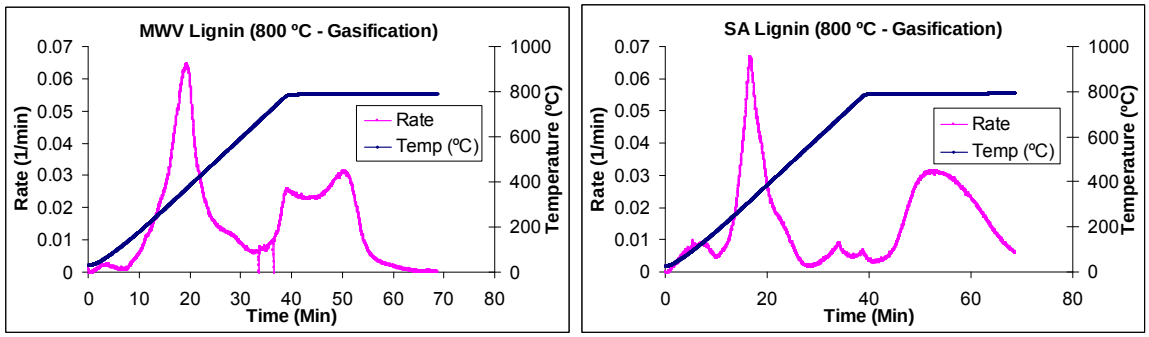

(b)

Figure 54: (a) Char yield -TG and (b) reaction rate - DTG curves for gasification of MWV and SA lignins

Secondary reactions, which are gasification reactions (represented by the Boudouard reaction, Eq 10), during MWV lignin gasification start at 650 °C and continue through 800 °C. After plateauing at 800 °C, the mass loss finally slows down and the char yield becomes nearly zero. The SA lignin shows initially slower secondary reaction compared to that of the MWV lignin. Significant gasification of the SA lignin does not begin until the sample has been held at 800 °C for some time.

MWV lignin and SA lignin were compared for their behavior during pyrolysis and gasification. Figure 55 shows the reaction rate curves for pyrolysis and gasification of both the lignins.

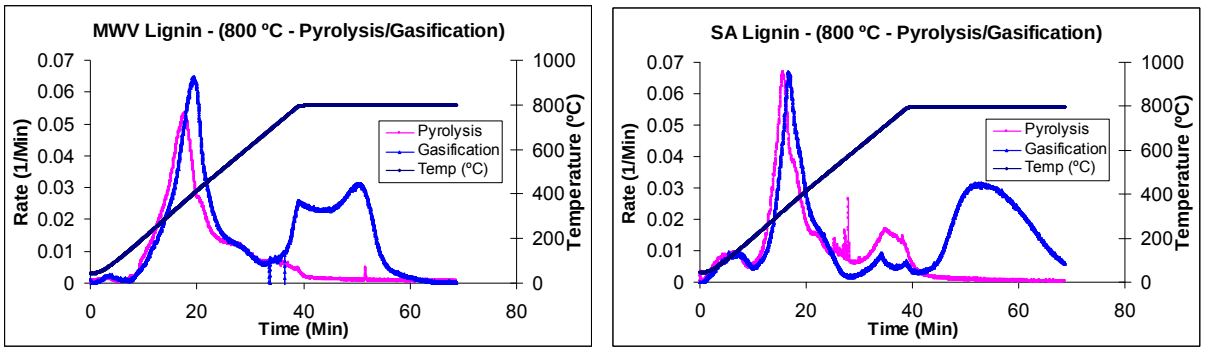

(a) (b)

Figure 55: Reaction rate - DTG curves for pyrolysis and gasification of (a) MWV lignin and (b) SA lignins

As seen above, the behavior during pyrolysis in an inert atmosphere and gasification in an atmosphere containing CO_2 was distinctly different. During pyrolysis, secondary reactions believed to be due to reactions with Na_2CO_3 were observed for SA lignin but not significantly for MVW lignin at 600-800°C. These reactions for SA lignin are suppressed when CO_2 was added to the gas atmosphere. Consequently, the mass loss for SA lignin was higher during pyrolysis than during CO_2 gasification at 600-800°C.

5.2.3 Effect of Alkali Addition:

The SA lignin contains much more ash and Na than does MWV lignin. Na is one of the main components of the ash. It is known to catalyze carbon gasification. Reactions with Na salts are

expected to be responsible for the secondary pyrolysis reactions above 600 °C for the high-ash SA lignin.

To verify our assumption that the secondary reaction during SA lignin pyrolysis is caused by the ash component, a study was done to determine the effect of Na_2CO_3 addition to the lignin. A quantity of Na_2CO_3 corresponding to the difference in sodium between the two lignins was added to the MWV lignin. TGA experiments were done at 800 °C with the same heating rate of 20 °C/min, and the results compared with earlier experiments.

Figure 56 shows the reaction rate curves of MWV lignin after Na_2CO_3 addition during pyrolysis. Primary devolatilization reaction starts at ~ 200 °C and continues up to ~ 400 °C. This behavior is very similar to that of the initial SA lignin and MWV lignin.

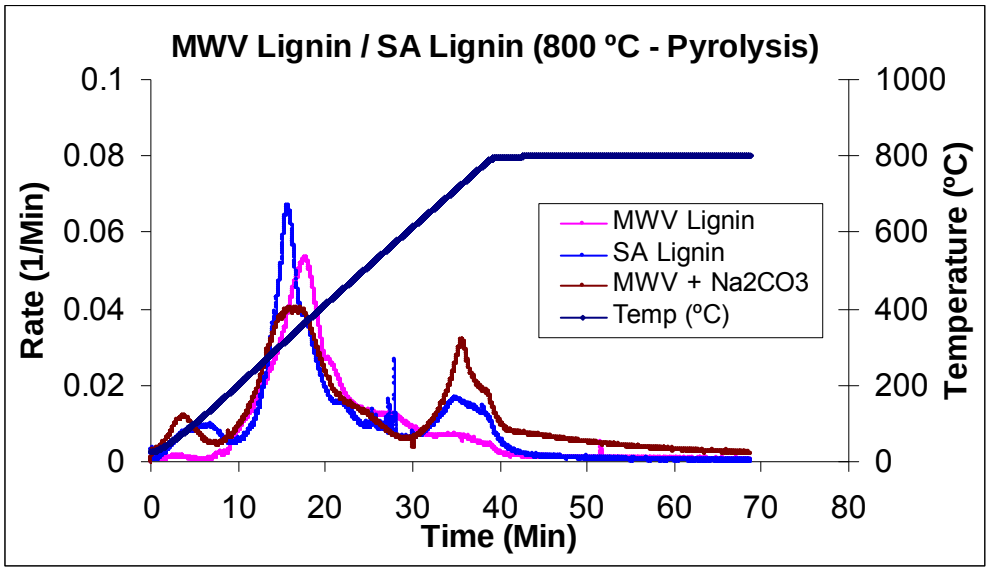

Figure 56: Reaction rate curves during pyrolysis of MWV lignin after Na_2CO_3 addition.

The results showed that Na_2CO_3 addition had both positive and negative effect on reaction rate. Comparison of the results for SA and MWV lignins with and without Na_2CO_3 addition shows that the addition of Na_2CO_3 made the primary pyrolysis reaction occur at lower rate and enhanced the rate for secondary reaction.

With the addition of Na_2CO_3, MWV lignin also shows secondary reaction as expected. It shows that reactions with Na salts according to Eq 8-9 are likely responsible for the secondary reactions. It is also noteworthy that MWV lignin with Na_2CO_3 addition experienced a higher reaction rate at 600 – 800 °C than did either the MWV or the SA lignin. It suggests that all Na is not present as Na_2CO_3 and is not available for reactions Eq 8-9.

Figure 57 shows the reaction rate curves during gasification of MWV lignin with Na_2CO_3 addition.

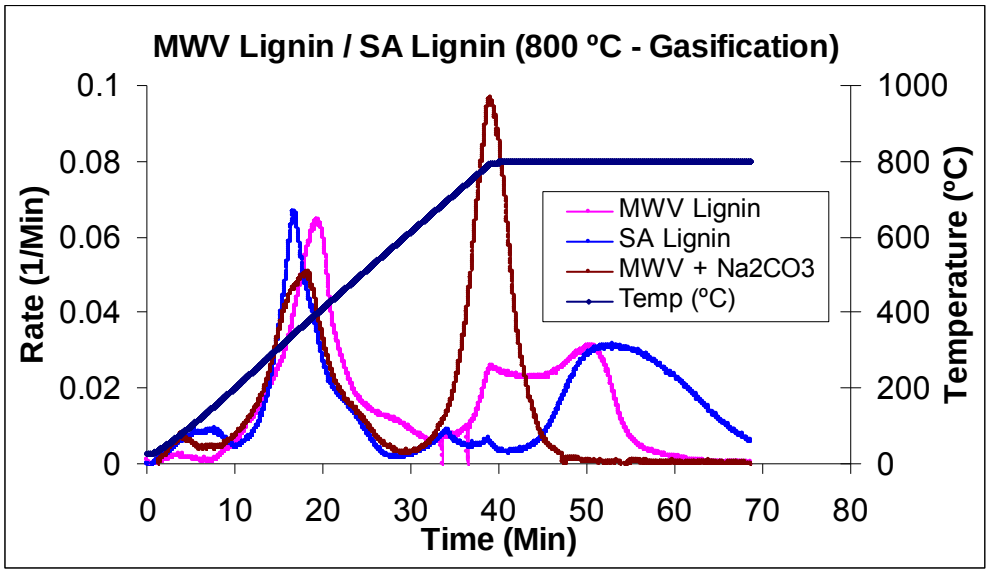

Figure 57: Reaction rate curves during gasification of MWV lignin after Na_2CO_3 addition.

The reactions at 200 – 500 °C are due to thermal decomposition of the organic matrix as explained earlier. Na_2CO_3 addition made devolatilization occur at a lower rate. In the devolatilization range there is a similar decrease to lower rate due to suppression as in the case of pyrolysis.

Some of the reactions at 600 – 800 °C may be due to reactions of the inorganic salts (e.g.Na_2CO_3 or Na_2SO_4) with carbon (Eq 6-9). However, these reactions are suppressed by CO_2 and not as important in CO_2 containing atmospheres as in inert atmospheres

Differences in behavior are seen at 800 °C between the gasification of SA lignin and MWV lignin with and without Na_2CO_3. The original high-ash SA lignin had a delay in gasification whereas the original low-ash MWV lignin had two gasification rate peaks, one as temperature reached 800°C and one at a time corresponding to the rate peak of the original high-ash lignin.

Addition of Na_2CO_3 to MWV lignin increases the gasification rate immediately with no delay in the gasification as was experienced with the high-ash lignin. It shows that Na catalyzes the gasification rate. The mechanism of alkali-metal-catalyzed gasification is explained by the following reaction sequence (Eq 11 – 14) [65, 66].

$*+CO_2 \Leftrightarrow *CO_2$ **(11)** [CO_2 absorbs on an unoxidized catalyst site]

$*CO_2 \Leftrightarrow *O + CO$ **(12)** [CO_2 decomposes and gives CO and oxidized catalyst site]

$*O + C \Rightarrow * + C(O)$ **(13)** [Oxygen is transferred from oxidized catalyst site to free carbon]

$C(O) \Rightarrow CO$ **(14)** [CO gas is released]

As seen in Figures 56 and 57 the pyrolysis and gasification profiles of lignin are different. For MWV lignin with or without Na_2CO_3, gasification begins earlier than it does for SA lignin. During pyrolysis, only the SA lignin, which has higher ash content than MWV lignin, experienced secondary reaction. The original MWV lignin had two gasification rate peaks: one at the time at which Na_2CO_3 enhanced the gasification and one at the time corresponding to the peak for the high-ash SA lignin.

During pyrolysis, the presence of Na_2CO_3 in the high-ash lignin could explain the difference in the secondary reactions at 600-800°C. However, the difference during gasification between the low-ash MWV lignin and the high-ash SA lignin can not be explained by the presence of additional Na_2CO_3 in the high-ash lignin. Na_2CO_3 increased the gasification rate already at temperatures below 800°C whereas gasification was suppressed in the high-ash lignin.

Na corresponding to the difference in MWV lignin and SA lignin was also added to SA lignin in the form of Na_2CO_3. Figure 58 shows the curves for pyrolysis and gasification after Na_2CO_3 addition.

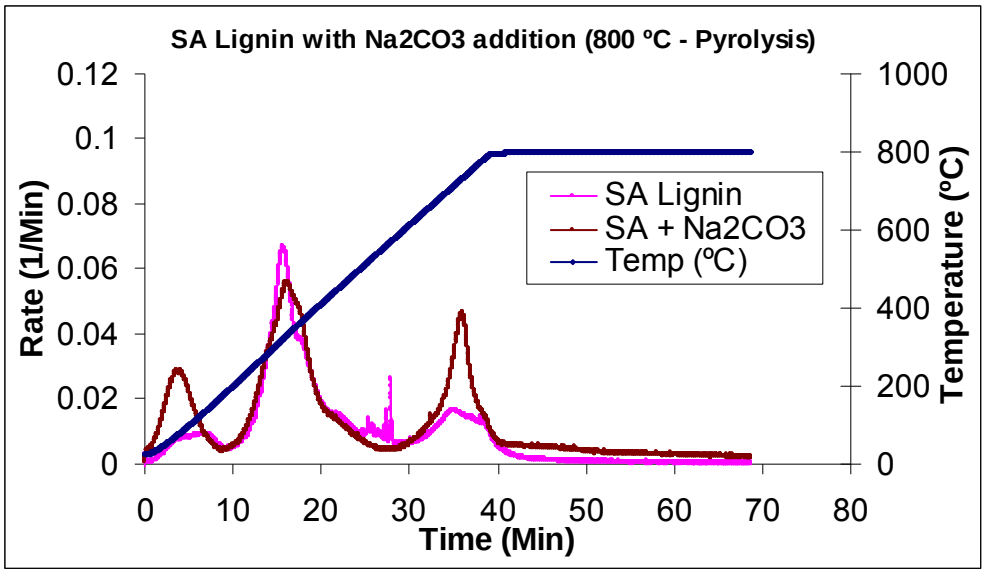

(a)

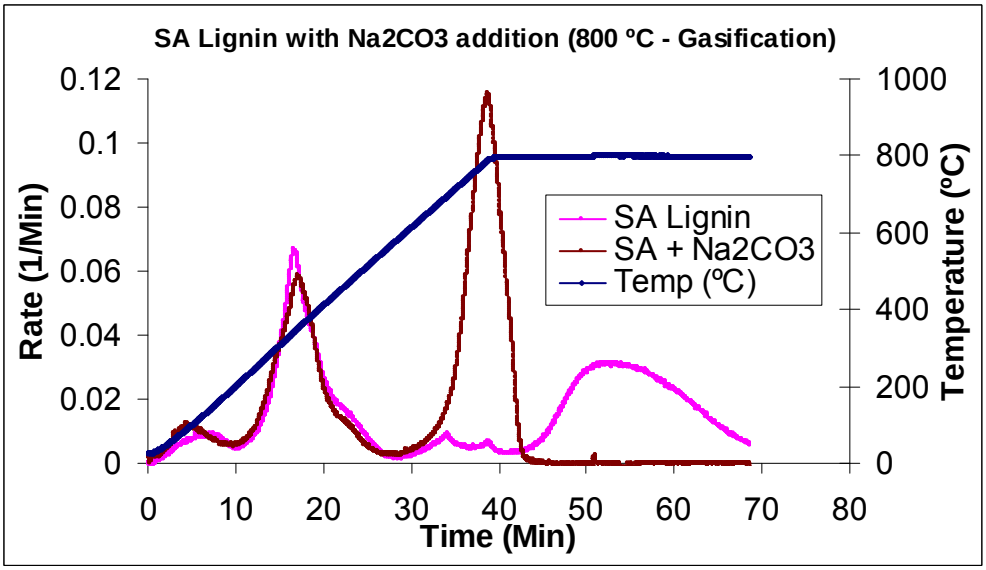

(b)

Figure 58: Reaction rate curves during (a) pyrolysis (b) gasification of SA lignin after Na_2CO_3 addition

The Na_2CO_3 addition shows both a suppressing and enhancing effect for SA lignin pyrolysis [Figure 58 a]. The primary reaction is suppressed and the secondary pyrolysis reaction shows a higher rate. The rate increase for secondary reaction takes place at the same time corresponding

to the original SA lignin. It suggests that ash originally present in the form of Na_2CO_3 causes the secondary reactions which are further increased by addition of Na_2CO_3.

During gasification the initial devolatilization occurred at a lower rate in the presence of Na_2CO_3 addition than in the original SA lignin. There is a big increase in the gasification reaction rate immediately at a time corresponding to the rate peak of the original SA lignin [Figure 58 b]. The addition of Na_2CO_3 does not show any peak during extended holding at 800 °C as seen in the original SA lignin. By that time all carbon has been gasified.

Three different amounts of Na_2CO_3 (100%, 60% and 20%) were added to MWV lignin to determine the effect of sodium addition on gasification. One hundred percent Na_2CO_3 addition represents the amount of Na_2CO_3 corresponding to the difference in the quantity of sodium between the MWV and SA lignins. Figure 59 shows the reaction rate behavior of MWV lignin with and without Na_2CO_3 addition.

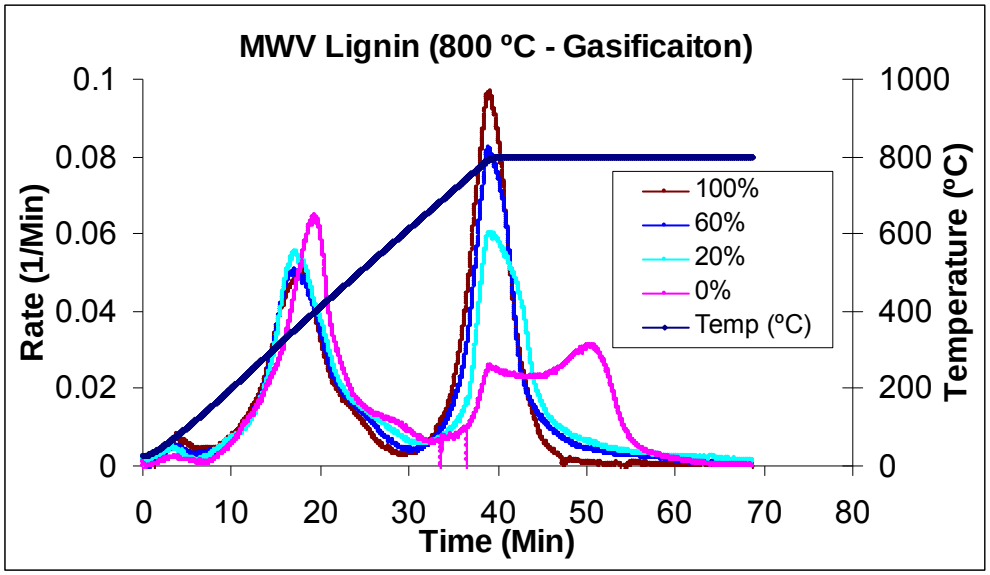

Figure 59: Reaction rate curves during gasification of MWV lignin after different amounts of sodium addition

The results show that the gasification rate increases proportionally to the amount of added Na. These results also confirm that the addition of Na_2CO_3 shifted the primary devolatilization to lower temperatures and decreased the peak devolatilization rate. The amount of Na_2CO_3 addition does not seem to have a large impact on the peak volatilization rate.

The decrease in the peak volatilization rate is consistent with the findings of Baker and Mudge [67]. They studied the steam gasification of biomass and found that addition of alkali carbonates increased the char yield during devolatilization.

To further see the effect of Na on lignin pyrolysis and gasification, Na_2SO_4 was added to the MWV lignin. The amount of Na_2SO_4 corresponded to the difference in the quantity of Na between the MWV and SA lignins. Equal moles of Na_2CO_3 and Na_2SO_4 were added. Figure 60 (a) and (b) show the reaction rate with addition of Na_2CO_3 and Na_2SO_4 for pyrolysis and gasification respectively. The rates have been normalized to an ash free basis with all of Na_2CO_3 and Na_2SO_4 assumed to remain in the ash.

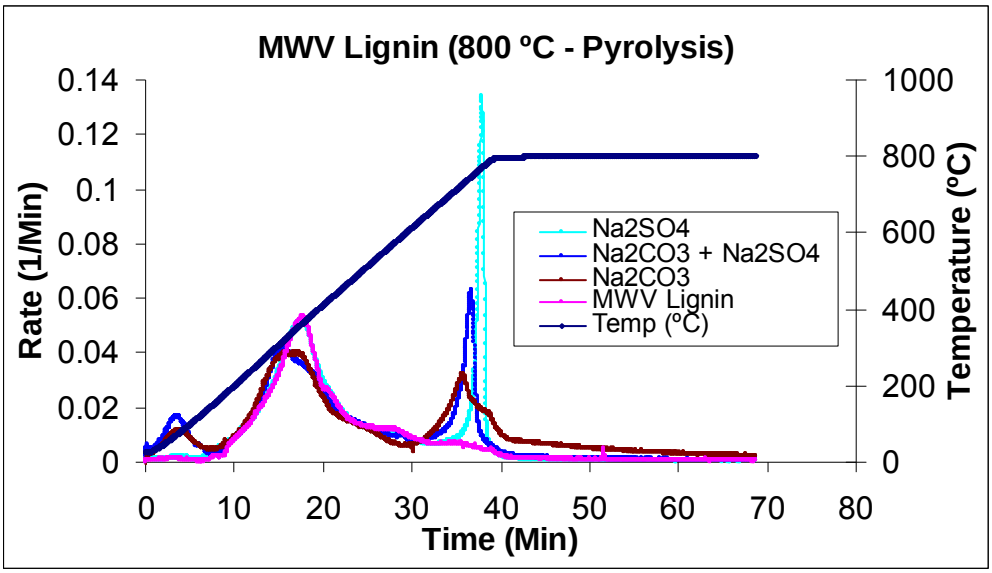

(a)

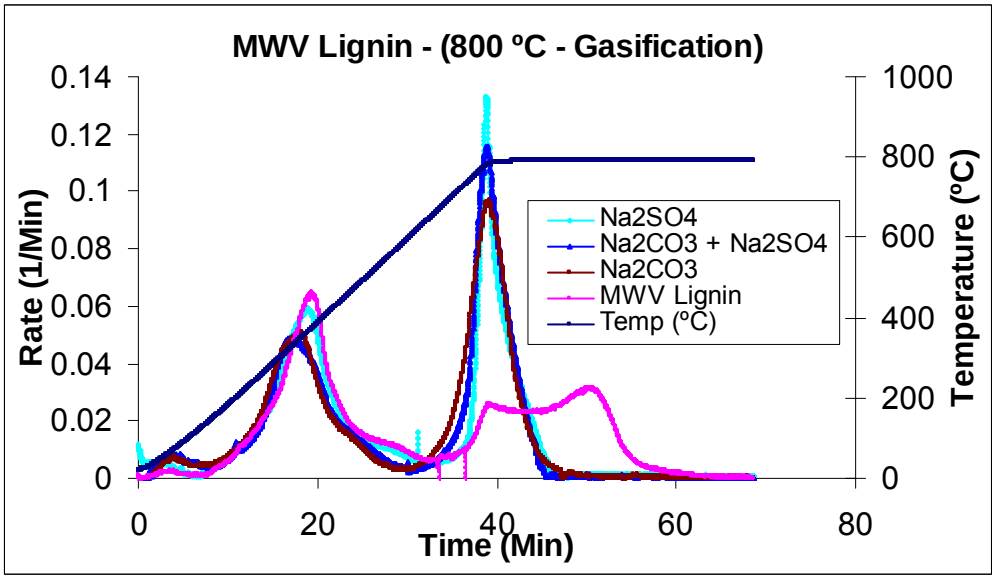

(b)

Figure 60: Effect of different Na salts on MWV lignin pyrolysis and gasification

In both the cases with the addition of Na_2SO_4 to MWV lignin increases the rate as compared to Na_2CO_3 addition. This suggests that Na_2SO_4 is a more efficient catalyst for carbon pyrolysis and gasification than is Na_2CO_3.

To see the effect of alkali metals on gasification three different salts, Li_2CO_3, Na_2CO_3 and K_2CO_3 were added to MWV lignin. Li, Na and K were added in the form of Li_2CO_3, Na_2CO_3 and K_2CO_3 in amounts corresponding to the difference in moles of Na between the original MWV and SA lignins. Figure 61 show the effect of different salts on MWV lignin gasification.

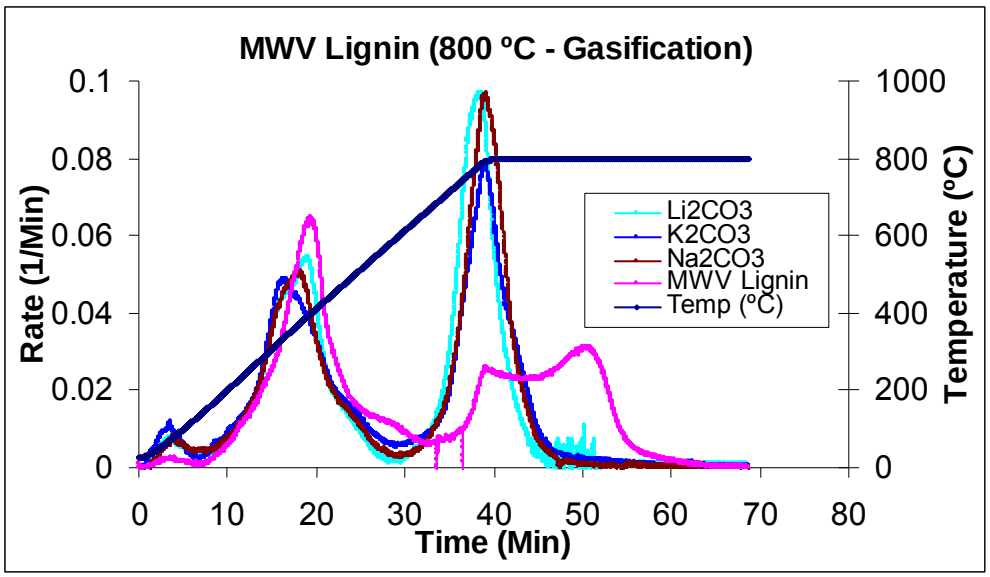

Figure 61: Effect of different salts on MWV lignin gasification

As seen in the results, all three salts suppress the primary devolatilization reaction and enhance the secondary reaction (carbon gasification) rate. Li_2CO_3 and Na_2CO_3 gave very similar but better results than K_2CO_3. Both Li_2CO_3 and K_2CO_3 caused peaks at the time corresponding to the peak for the Na_2CO_3. None of these catalysts resulted in an extended peak during extended holding time at 800 °C. All carbon had been gasified by that time.

These results are consistent with the findings of Mudge et al. [68]. They studied the catalytic steam gasification of wood using alkali carbonates and naturally occurring minerals and found

the order of the activity of the catalysts as K_2CO_3 > Na_2CO_3 > trona ($Na_3H(CO_3)_2C.2H_2O$)> borax $Na_2B_4O_7$ .10 H_2O.

5.2.3.1 Effect of CO_2 concentration:

Most of the lignin gasification experiments were done using 25 % CO_2 along with 75% N_2. To see the effect of CO_2 partial pressure on lignin gasification, a few experiments were conducted with variable amounts of CO_2. MWV lignin with Na_2CO_3 addition was gasified using 15%, 25% and 35% CO_2 along with remaining N_2. Figure 62 shows the DTG curves of lignin gasification with variable partial pressures of CO_2.

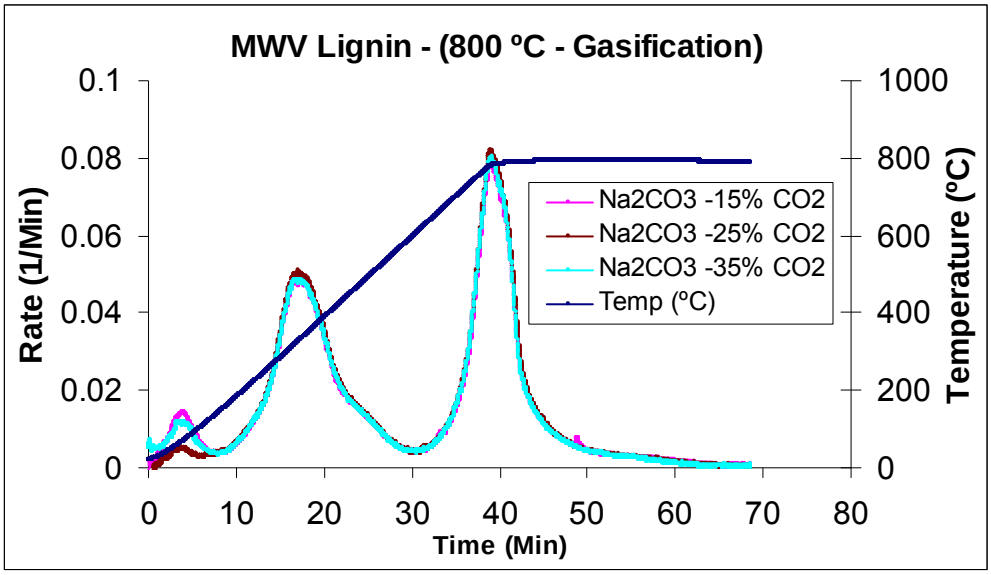

Figure 62: Effect of CO_2 partial pressure on MWV lignin gasification

As seen in the above figure, all three rate curves are very similar in their behavior. It means that above a certain value, gasification rate is not affected by CO_2 concentration.

As explained above, the reaction rate is catalyzed by alkali metals as per equations (11-14). If equation 11 and equation 12 are at equilibrium and equation 13 is rate limiting, using Langmuir-Hinshelwood method, the reaction rate can be expressed as,

$$-r = kpCO_2/(ApCO_2 + BpCO) \quad \textbf{(15)}$$

(where A and B are constants)

It can be further simplified as,

$$-r = k/(A + BpCO/pCO_2) \quad \textbf{(16)}$$

As per equation (15), the reaction rate depends only on the ratio of partial pressures of CO and CO_2. Initially, CO was not present and only CO_2 was present. As time progresses, CO is produced by reactions (11-14). Reactions represented by equation 11 and equation 12 come to equilibrium and CO and CO_2 also reach equilibrium. It makes the ratio of the concentration of CO and CO_2 constant; hence the gasification reaction rate does not change with change in CO_2 partial pressure.

5.3 Fourier Transform Infrared (FTIR) Spectroscopy results:

5.3.1 Lignin analysis:

Lignin is a very complex material. There is a necessity to understand the structure of lignin and the changes in structure from various treatments. Infrared spectroscopy is a very useful method for obtaining information about the structure of lignin constituents and the chemical changes taking place in lignin due to different treatments. The FTIR technique has been used in the past to characterize biomass and estimate the lignin and carbohydrate content of materials. The thermal degradation behavior of lignin is affected by the method through which the lignin is isolated.

Table 8 shows the important IR bands of lignin.

Tale 8: Important FTIR bands [16, 45, 69]

Band (cm^{-1})	Band Origin
3450-3400	OH Stretching
2960-2925	CH Stretching in CH_3, CH_2
2850-2840	CH Stretching in OCH_3
1715-1705	C=O Stretching nonconjugated to the aromatic ring
1675-1660	C=O Stretching in conjugated to the aromatic ring
1605-1600	Aromatic ring vibrations
1515-1505	Aromatic ring vibrations
1470-1460	Asymmetric C-H deformations
1430-1425	Aromatic ring vibrations
1370-1365	Symmetric C-H deformations
1330-1325	Syringyl (S) ring breaking
1275-1270	Guaiacyl (G) ring breaking
1125	Guaiacyl (G) In plane deformation of Ar C-H
1115	Syringyl (S) In plane deformation of Ar C-H
1085-1030	C-H C-O deformations

The chemical characteristics of MWV and SA lignins were determined in the 4000 – 400 cm^{-1} region [Figure 63]. The spectra of both lignins are very similar, but they also show some differences.

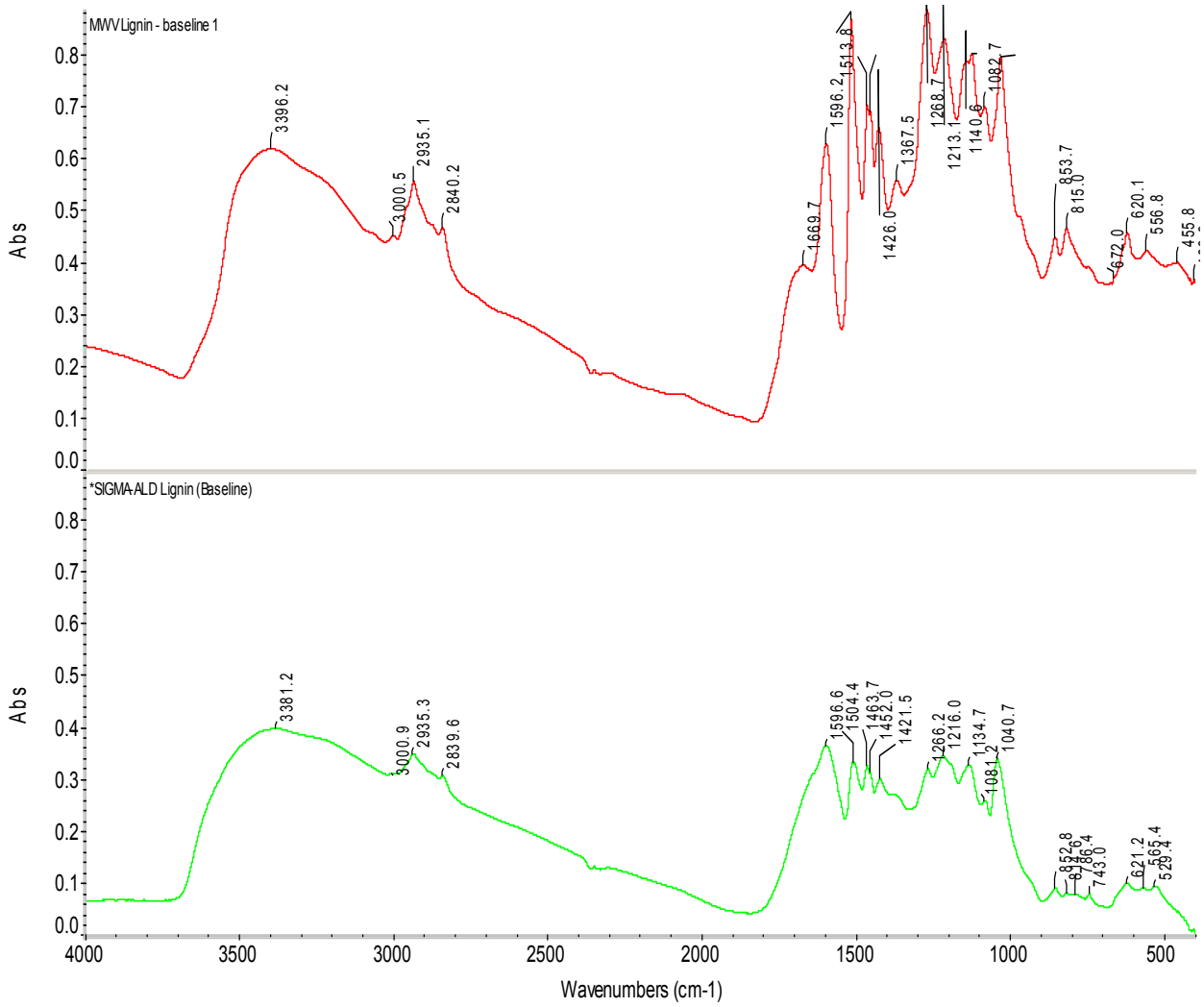

Figure 63: FTIR peaks of MWV lignin and SA lignin at room temperature

Na_2CO_3 and Na_2SO_4 were added to MWV lignin to see the effect of alkali salts on the pyrolysis and gasification of lignin. The spectra of MWV lignin was compared before and after addition of alkali salts [Figure 64]. The spectrum of pure Na_2CO_3 shows two big peaks at 1440 cm^{-1} and 879

cm^{-1}. Na_2CO_3 addition did not significantly affect the spectrum of MWV lignin. The spectrum of Na_2SO_4 consists of a broad peak at 1124 cm^{-1} and a sharp peak at 615 cm^{-1}. The addition of Na_2SO_4 to the lignin clearly shows changes at 1124 cm^{-1} and 615 cm^{-1}. Peaks changes were visible with the addition of only Na_2SO_4 as well as a mixture of Na_2CO_3 and Na_2SO_4 but not for the addition of only Na_2CO_3.

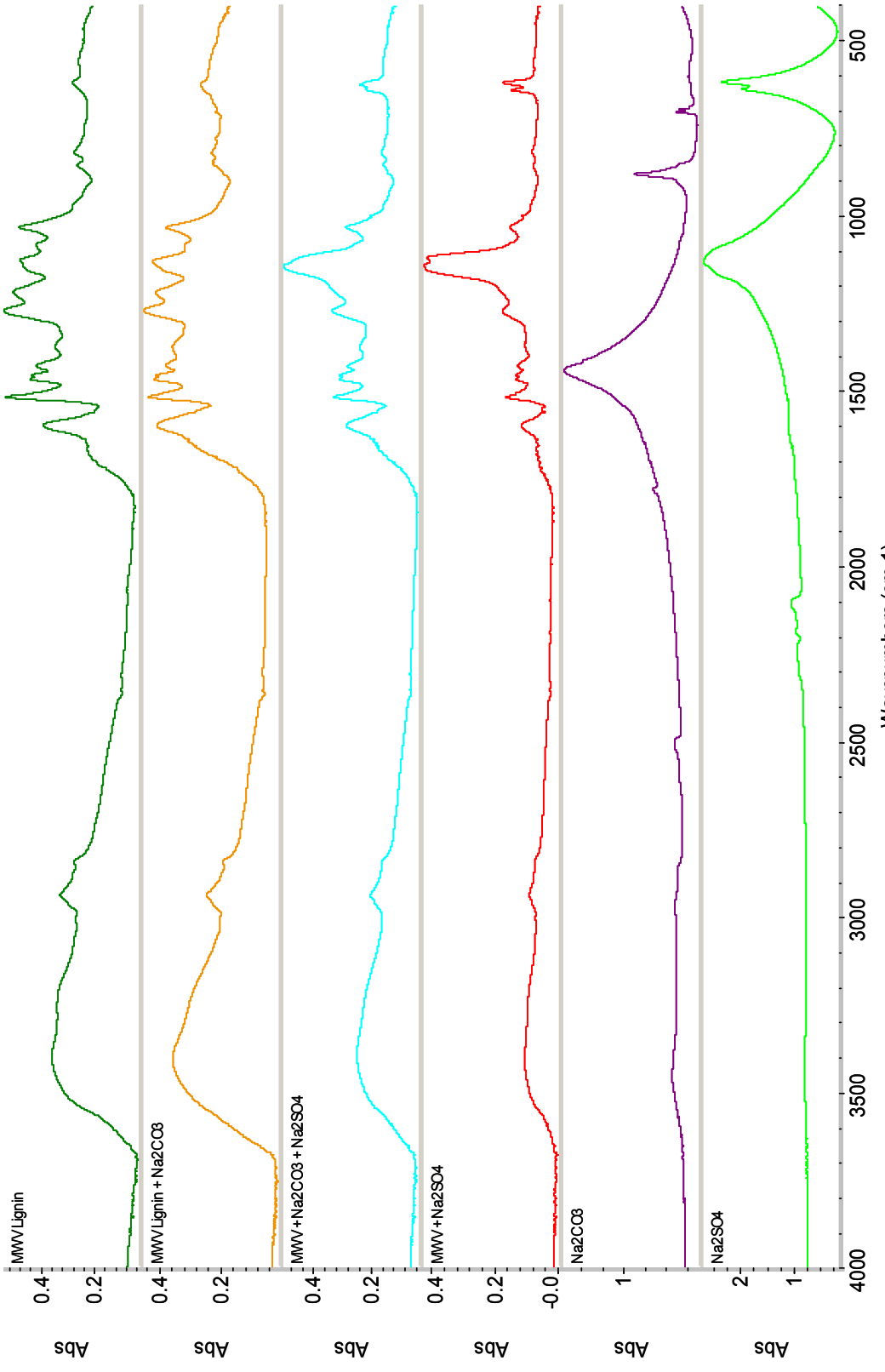

Figure 64: FTIR peaks of MWV lignin after the addition of Na_2CO_3 and Na_2SO_4

Figure 65 shows spectral changes after Na_2CO_3 addition to the SA lignin. The peaks at 1463, 1452 and 1421 cm^{-1} disappear and a new peak appears at 1440 cm^{-1}. This peak change was not visible for MWV lignin after Na_2CO_3 addition. It suggests that addition of Na_2CO_3 changes the structure of SA lignin differently than that of MWV lignin.

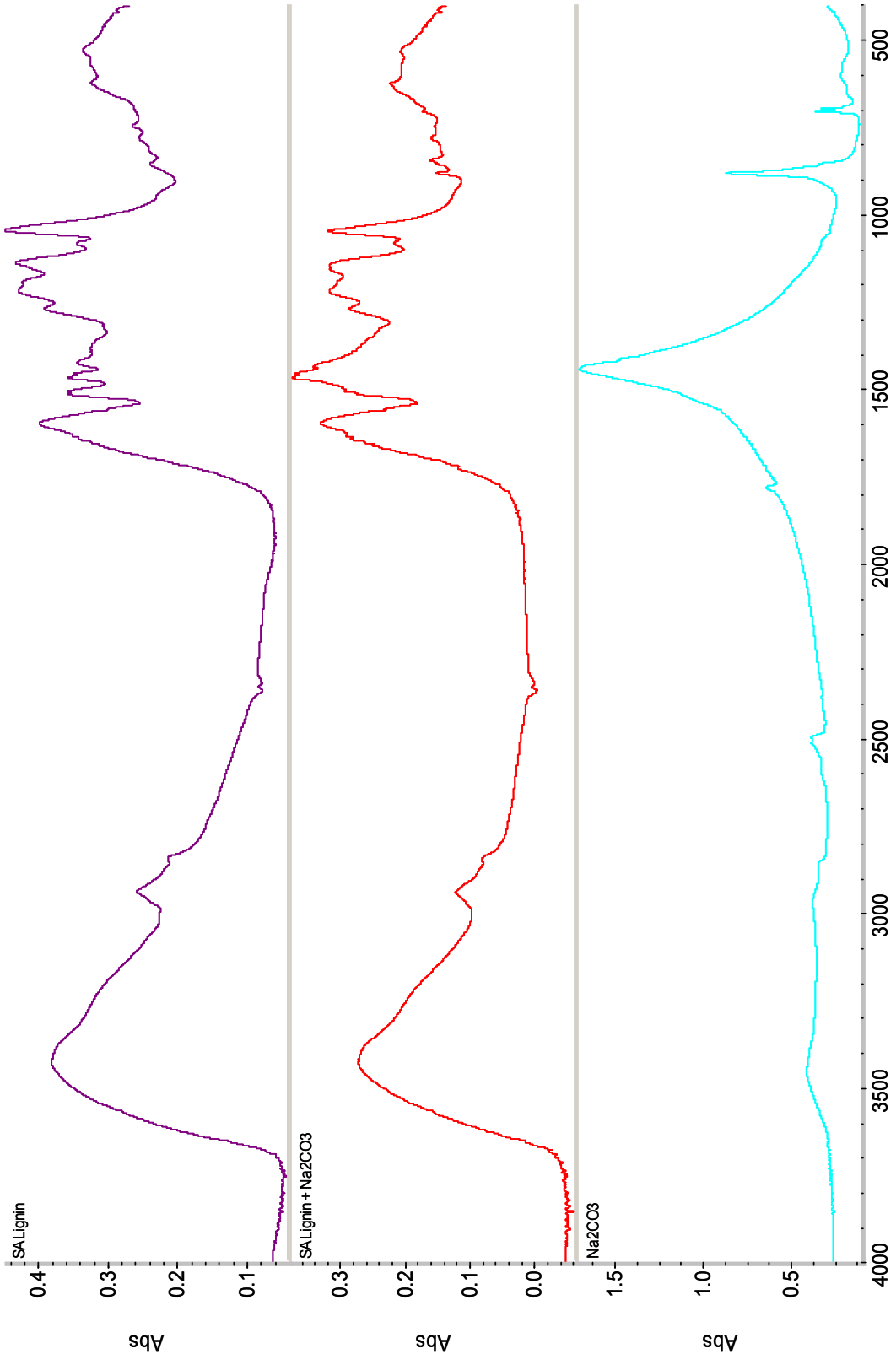

Figure 65: FTIR peaks of SA lignin after the addition of Na_2CO_3

5.3.2 Lignin pyrolysis results:

The thermal degradation of both lignin samples was studied between 150 °C and 800 °C. The samples were heated from room temperature to the holding temperature under nitrogen. The samples were held for 0.5 hour at the maximum temperature. After the reaction, the residues were cooled down to the room temperature under nitrogen and analyzed by FTIR spectroscopy to study the structural changes in lignin with the change of temperature. Figure 66 shows the FTIR spectra of residues of MWV lignin pyrolysis with change in temperature between 150 °C and 800 °C.

Up to a temperature of 320 °C there is not much change in the peaks of the pyrolyzed lignin residue. As seen in the TGA curve, the mass loss starts at close to 200 °C and the mass decreases gradually up to 600 °C. The maximum mass loss rate is experienced at 380 °C. After 600 °C, the mass loss rate decreases and very little mass changes occur with further increase in temperature.

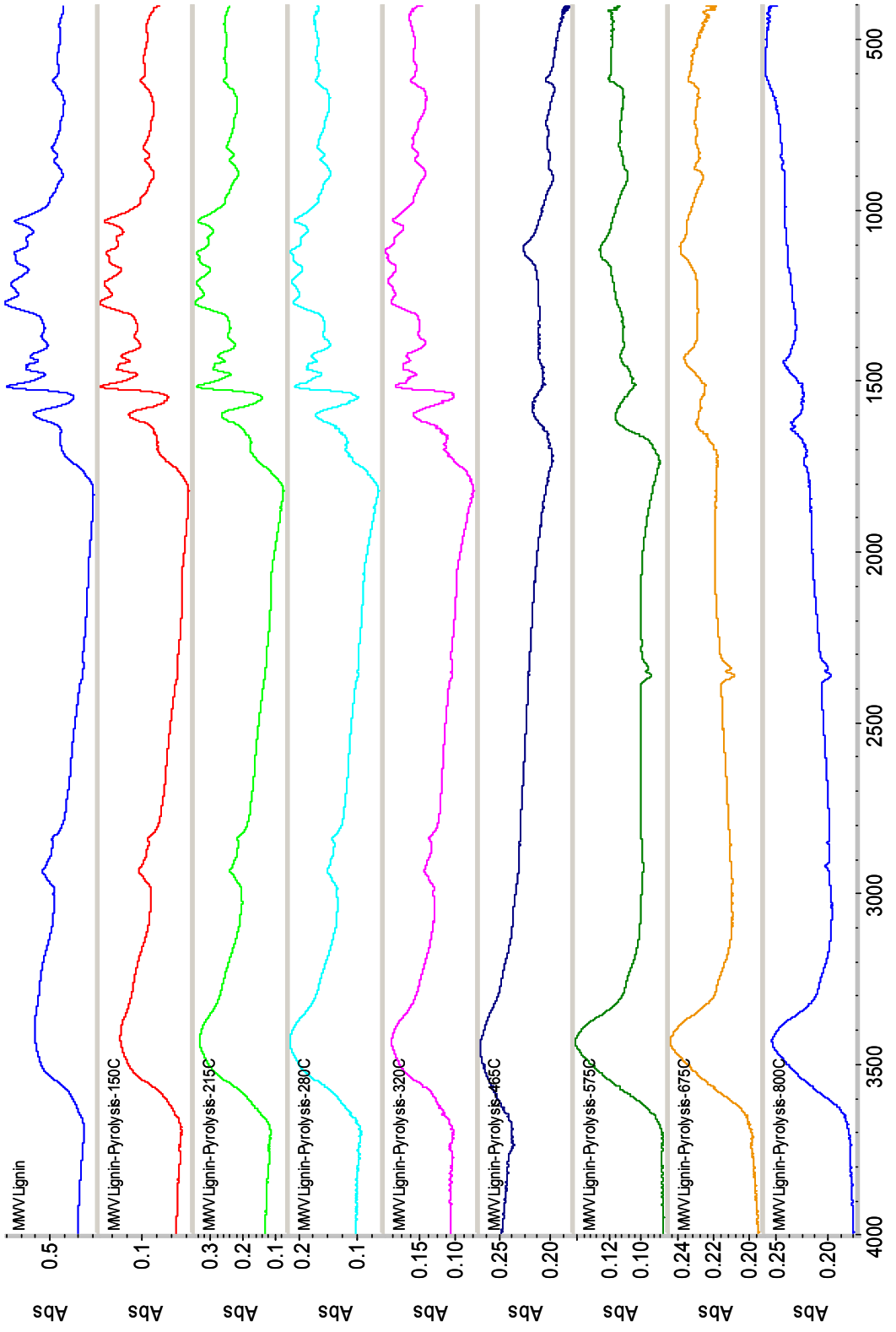

Figure 66: FTIR peaks of residues after MWV lignin pyrolysis at different temperatures

As seen in Figure 66, as the temperature increases above 320 °C, the OH stretching at (3381-3426 cm^{-1}) and aliphatic stretching CH (2843-3000 cm^{-1}) decreases. Bilba et al. also noticed similar behavior during the thermal degradation of sugar cane bagasse [70]. They found that a sample pyrolyzed at 300 °C showed a decrease in the intensities of bands characteristic of OH stretching and CH stretching. The FTIR results show that major changes in intensity are observed after 320 °C and a number of peaks disappear at 465 °C. With the increase in temperature beyond 320 °C the aromatic vibration at 1596 cm^{-1} vanishes. The band at 1515 cm^{-1} and 1460 cm^{-1} decreases with temperature and disappears at 465 °C.

After 575 °C, the changes in the spectra are small and the structure seems to be reaching stability. As seen in the TGA runs after 600 °C, the mass loss rate decreases and very little mass loss takes place upon further heating. At 800°C most of the peaks in the fingerprint region disappear and the spectrum looks very different than those at lower temperatures.

The peaks generated during heating MWV lignin in pyrolysis were compared with the peaks of Na_2SO_4 and Na_2CO_3 [Figure 67]. With temperature increase, the organic signals disappear and peaks of different salts start appearing. The Na_2SO_4 peak appears at 465 °C and continues up to 675 °C and disappears at 800 °C. The Na_2CO_3 peak appears at 675 °C and remains at 800 °C.

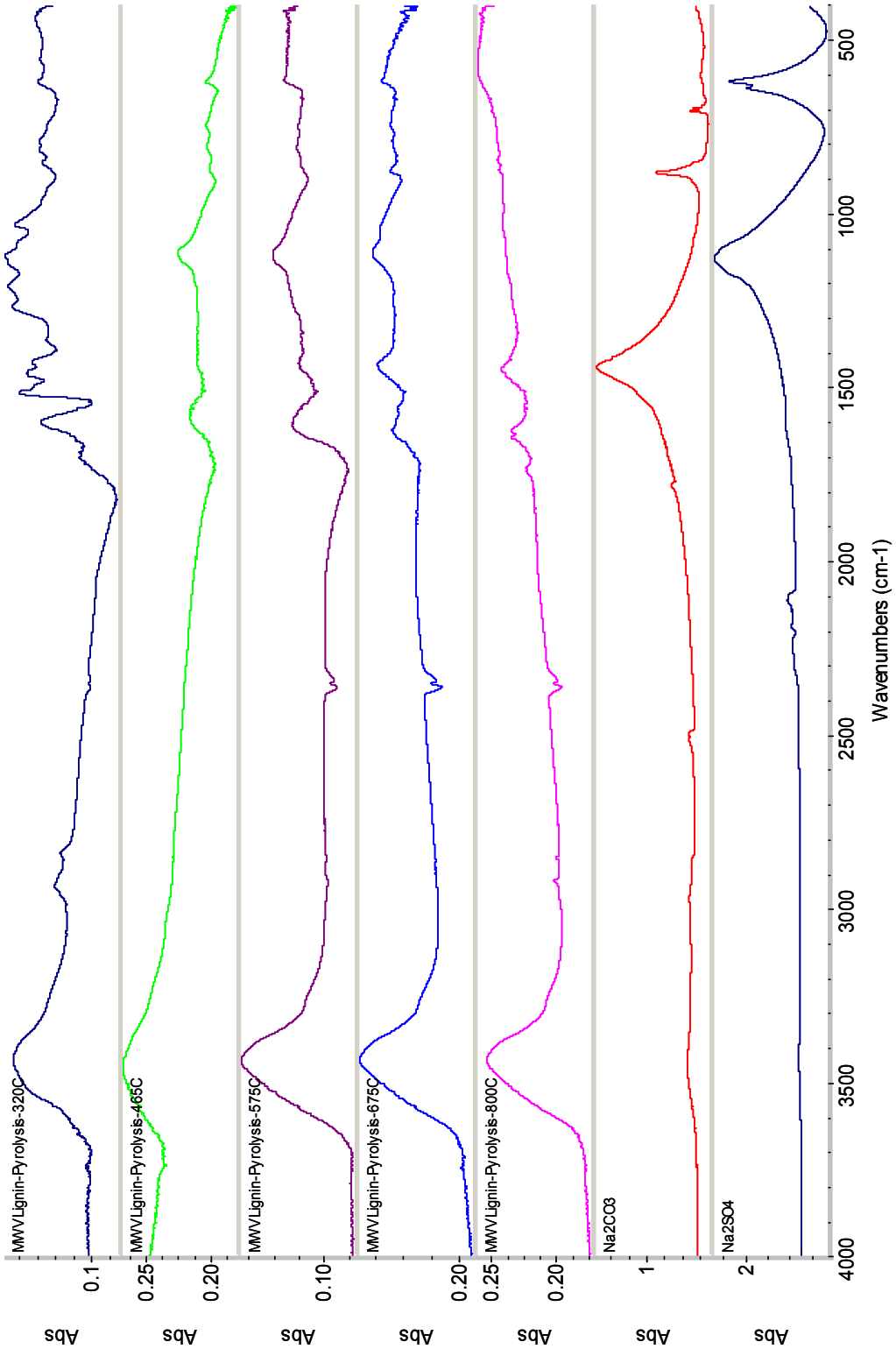

Figure 67: Comparison of FTIR peaks of residues and alkali salts after MWV lignin pyrolysis at different temperatures

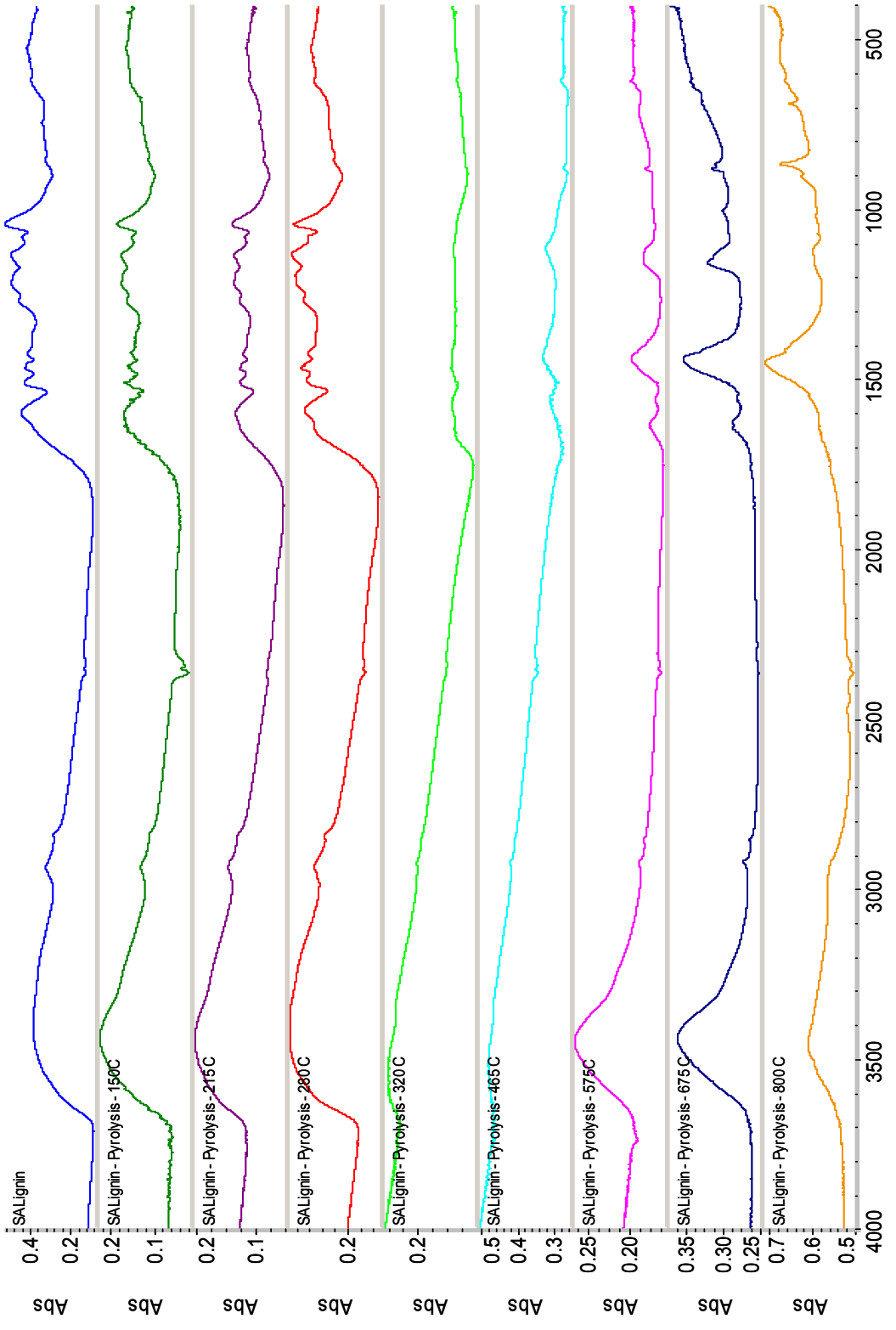

Figure 68: FTIR peaks of residues after SA lignin pyrolysis at different temperatures

Figure 68 shows the FTIR peaks of pyrolyzed SA lignin at different temperatures. SA and MWV lignin differ in their elemental composition and ash content. The FTIR bands show that up to 270 °C any modifications in the lignin structure are not apparent. With increase in temperature beyond 280 °C, significant change in FTIR bands are observed. With further heating, peaks starts disappearing at 320 °C. This behavior of SA lignin pyrolysis is different than that of MWV lignin pyrolysis for which the lignin peaks start disappearing at 465 °C. SA lignin has more ash than MWV lignin and the results suggest that the organics disappear earlier in SA lignin than in MWV lignin.

The TGA study of SA lignin showed that the mass change with temperature increase can be divided in two main parts. The mass loss for the first part starts at 200 °C and continues gradually until 575 °C. The maximum mass loss rate is observed at 320 °C, which is earlier than that for MWV lignin, which achieves the maximum mass loss rate at 380 °C.

The higher-ash SA lignin shows earlier devolatilization than MWV lignin. Significant peak disappearance starts to be seen at 320 °C which is earlier than the 465 °C observed for MWV lignin. With further increase in temperature beyond 575 °C, secondary mass loss takes place and continues up to 800 °C for SA lignin. The mass loss zones represent primary and secondary reactions, respectively. For SA lignin more overall mass loss takes place than for MWV lignin, which results in lower char yield for SA lignin.

The aromatic vibration bands at 1596 cm^{-1} and 1504 cm^{-1} decrease with increasing temperature and disappear at 320 °C. The C-H stretching peak at 1463 cm^{-1} decreases with higher

temperature and vanishes beyond 320 °C. A new band at 1117 cm^{-1} appears and increases with temperature. At 465 °C, the SA lignin also shows an appearance of the 1438 cm^{-1}peak. The peak height increases with increasing temperature. A third peak emerges at 876 cm^{-1} at 465 °C and it too shows an increase in peak height with further heating. The SA lignin does not lead to the emergence of a peak at 465 °C at 1621 cm^{-1} as was observed for MWV lignin pyrolysis.

The SA lignin spectra at different temperatures were also compared to the spectra of Na_2SO_4 and Na_2CO_3 [Figure 69]. New peaks of Na_2SO_4 and Na_2CO_3 start appearing at 465 °C. The Na_2CO_3 peak intensity increases up to 800 °C, while that of Na_2SO_4 decreases. For MWV lignin the Na_2SO_4 peak disappears at 575 °C but is present until 800 °C for SA lignin pyrolysis. The higher amount of ash in the SA lignin results in the presence of organic salts even at higher temperature. For SA lignin the Na_2CO_3 peak was stronger than for MWV lignin.

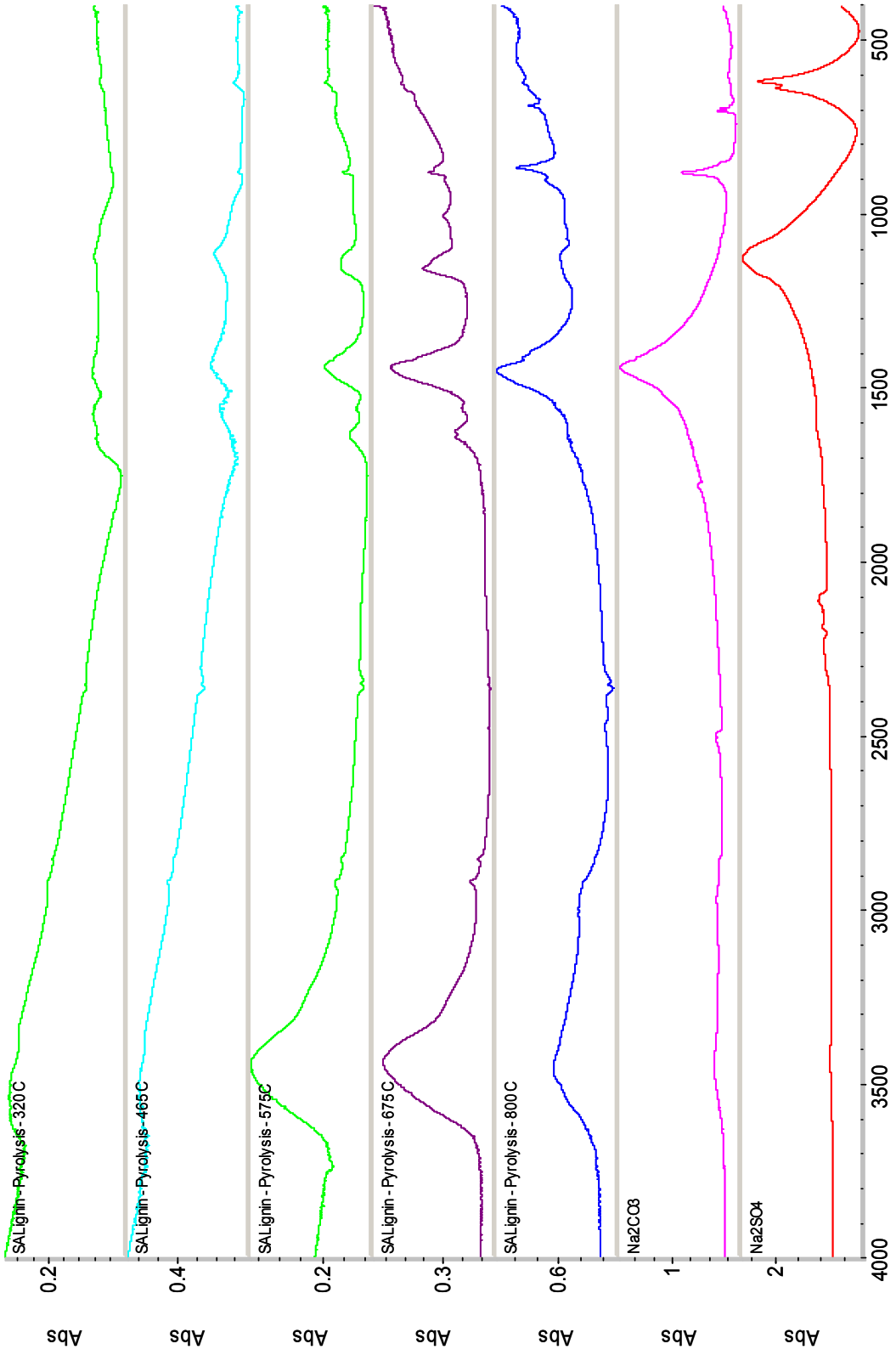

Figure 69: Comparison of FTIR peaks of residues and alkali salts after SA lignin pyrolysis at different temperatures

5.3.3 Lignin gasification results:

Lignin residues after gasification at different temperatures were also studied using the FTIR. Figures 70 and 71 show the FTIR peaks for gasification of MWV lignin and SA lignin, respectively. The FTIR peaks for both the lignins were quite similar to the peaks observed during pyrolysis. During gasification the effect of CO_2 atmosphere on the appearance and disappearance behavior of peaks was small.

As with pyrolysis runs, there are few spectral changes, up to 280 °C. Further increase of temperature reduces the spectral detail. For MWV lignin after 320 °C significant changes in peak behavior are observed and some of the peaks disappear at 465 °C.

SA lignin residues heated beyond 280 °C show significant changes in their spectra. After further heating, the major peaks disappear at 320 °C and two peaks emerge at 1438 cm^{-1} and 876 cm^{-1} at 465 °C. These peaks increase in height with increasing temperature and they were seen during pyrolysis as well. The band at 1117 cm^{-1} which appeared during pyrolysis was not evident.

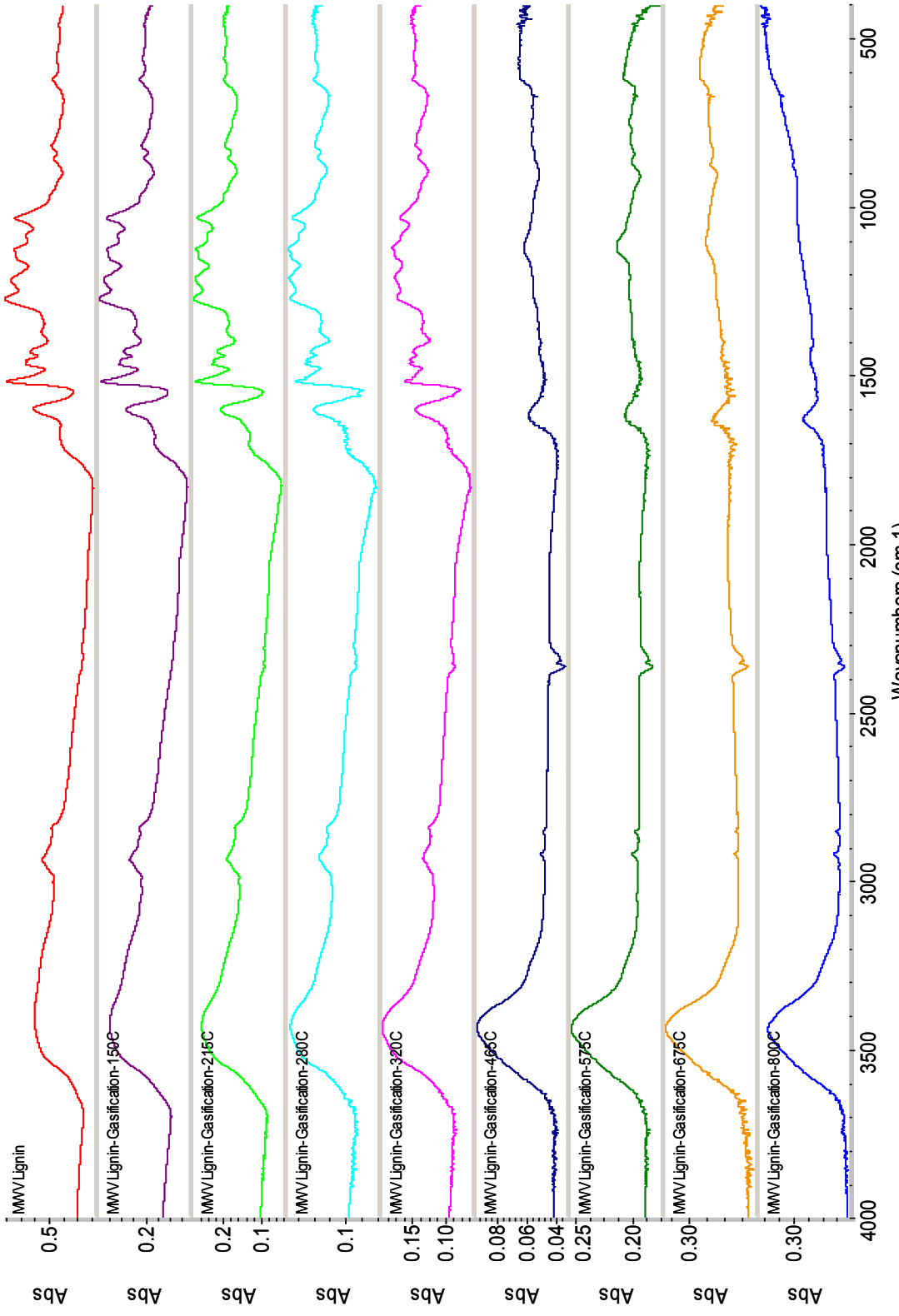

Figure 70: FTIR peaks of residues after MWV lignin gasification at different temperatures

As seen in Figure 70, during MWV gasification, a number of peaks disappear when MWV lignin reaches a temperature of 465 °C. A peak starts at 1621 cm^{-1} at 465 °C and continues to 800 °C. SA lignin does not show similar peak at 1621 cm^{-1}. As with pyrolysis, the SA lignin goes through major structural change up to 320 °C while MWV lignin needs a temperature of 465 °C for the same effect to occur.

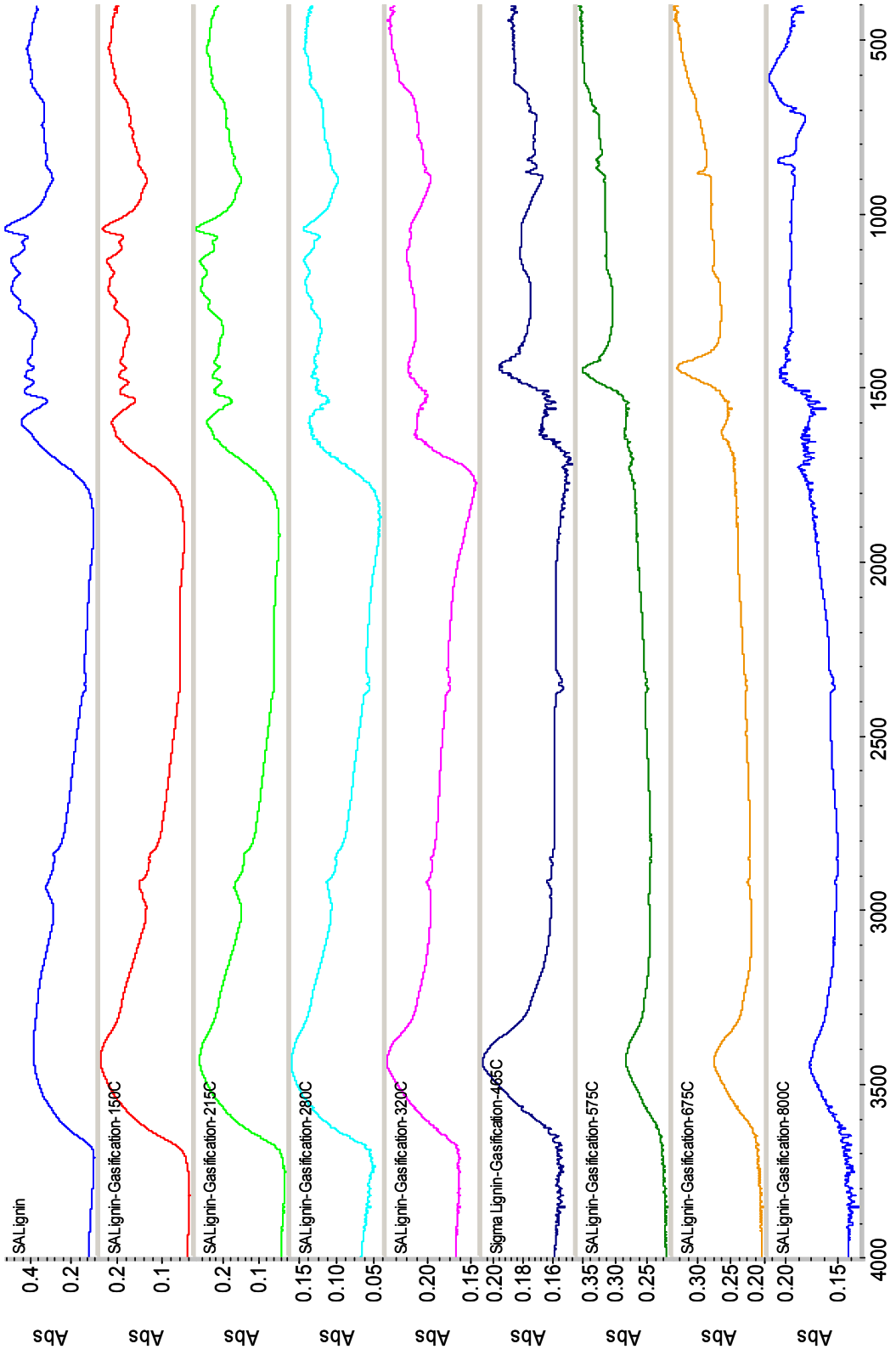

Figure 71: FTIR peaks of residues after SA lignin gasification at different temperatures

Figure 72 and 73 show the comparison of MWV lignin and SA lignin gasification spectra with the spectra of Na_2SO_4 and Na_2CO_3. Gasification of MWV lignin shows emergence of a Na_2SO_4 peak starting at 465 °C until 675 °C. Similar behavior was observed during MWV pyrolysis. Na_2CO_3 peaks did not appear during gasification as it did during pyrolysis from 675 °C to 800 °C.

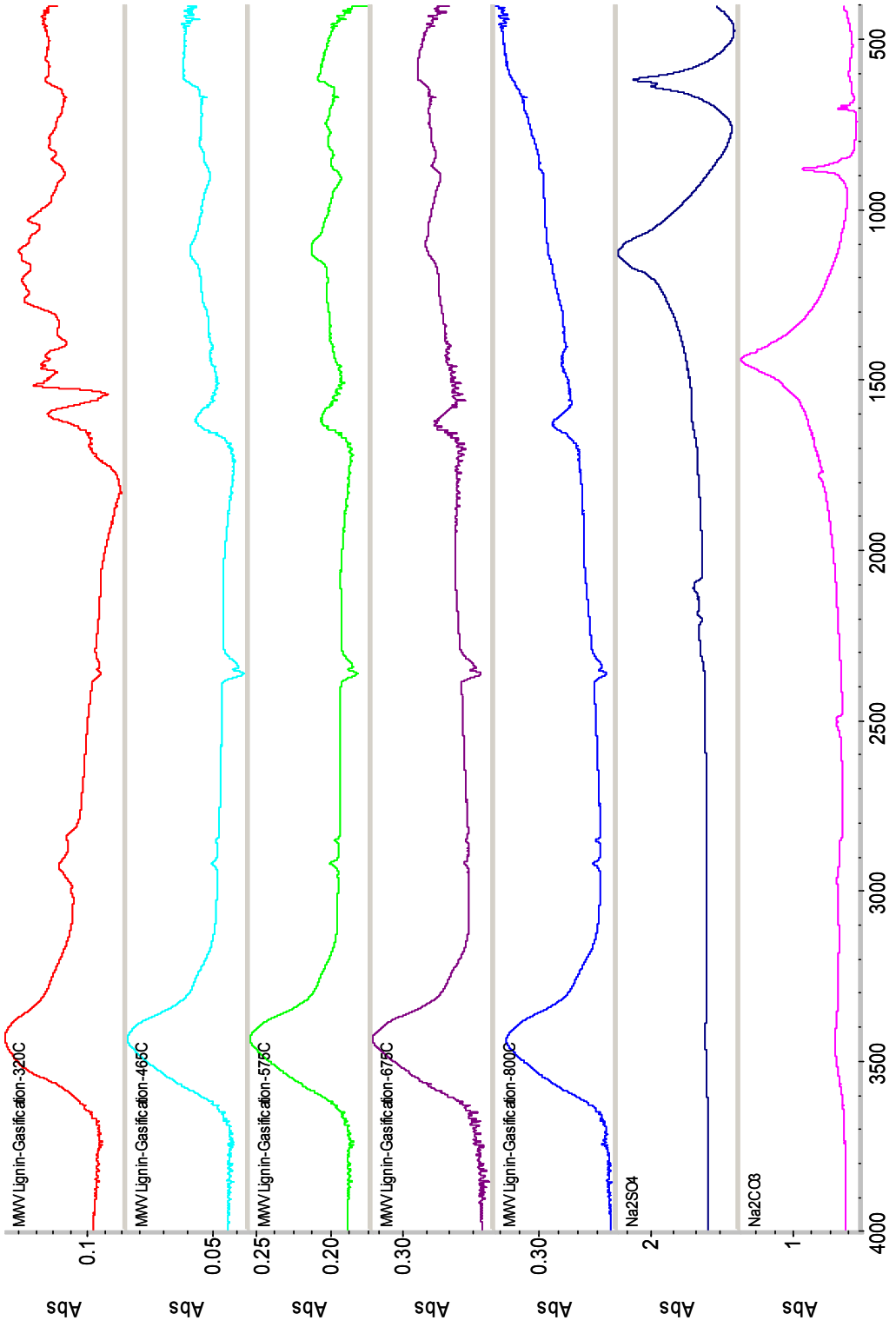

Figure 72: Comparison of FTIR peaks of residues and alkali salts after MWV lignin gasification at different temperatures

Figure 73 shows that during SA gasification, a strong Na_2CO_3 peak appears at 465 °C until 800 °C. For SA pyrolysis similar peaks appeared between 465 °C and 800 °C. SA lignin gasification did not show a Na_2SO_4 peak as was seen for SA pyrolysis between 465 °C to 800 °C.

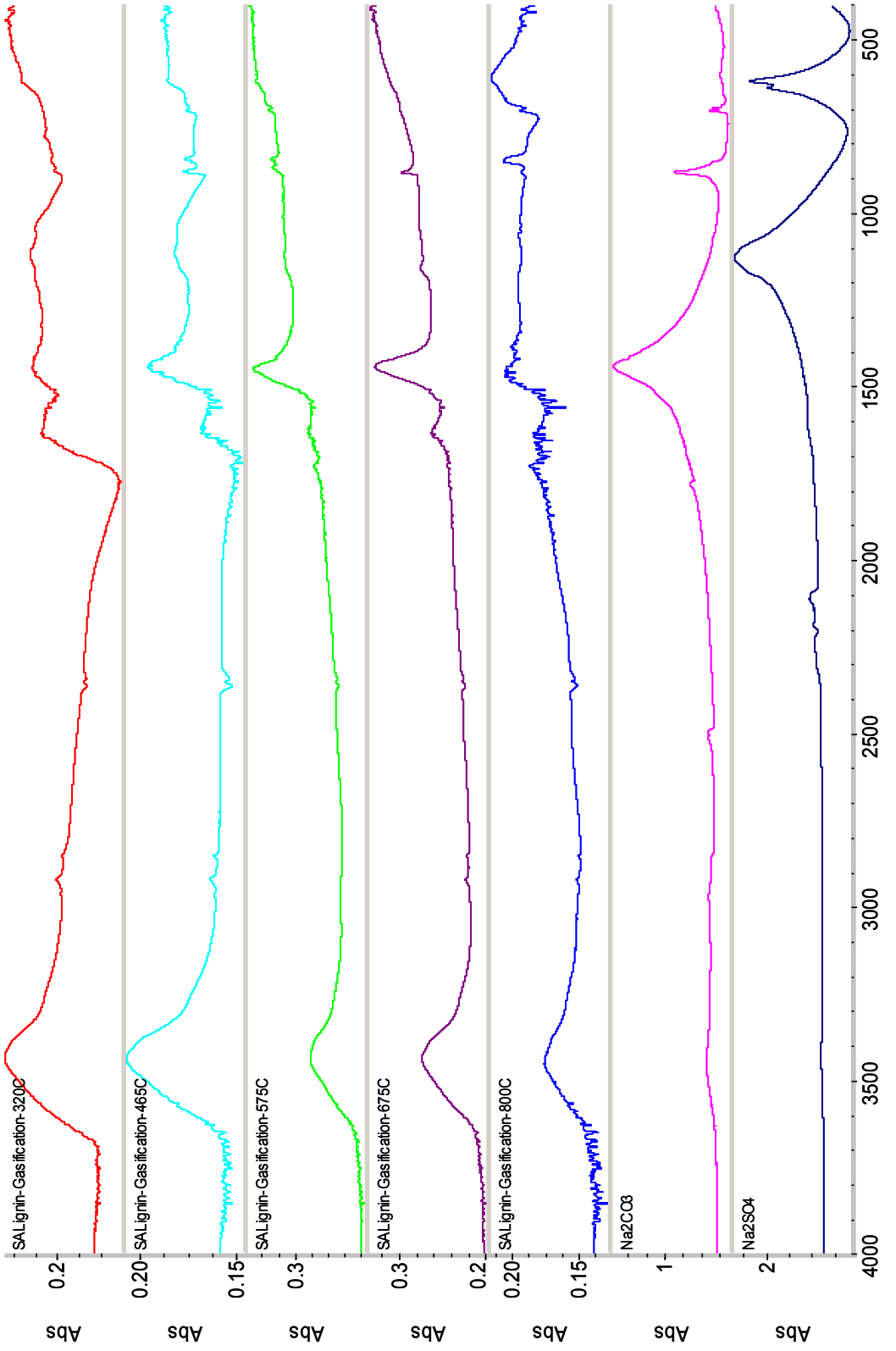

Figure 73: Comparison of FTIR peaks of residues and alkali salts after SA lignin gasification at different temperatures

The FTIR study showed that spectra of both lignins have similarities as well differences. For MWV lignin, significant peak disappearance starts at 320 °C while for SA lignin peak disappearance needs a higher temperature of 465 °C. For MWV lignin pyrolysis, the Na_2SO_4 peak appears at 465 °C and continues up to 675 °C, and for SA lignin it also starts at 465 °C but continues up to 800 °C. During pyrolysis, MWV lignin and SA lignin both show the Na_2CO_3 peak between 675 °C and 800 °C. The intensity of Na_2CO_3 peaks of SA lignin was higher than that of MWV lignin. MWV lignin also showed the Na_2SO_4 peak between 465 °C and 675 °C during gasification but it was not present during SA lignin gasification.

5.4 Study of kinetic parameters:

The kinetic study of biomass pyrolysis and gasification is necessary for the efficient production of fuel gases, chemicals and energy. The knowledge of kinetics helps in designing the equipment and process correctly. Thermogravimetric analysis provides a feasible way to accomplish preliminary kinetic studies on the thermal decomposition of solids [71]. This method is fast and is used for the determination of kinetics of degradation and other reactions.

There are numerous methods for weight loss measurements of biomass pyrolysis and gasification available in the literature but there is a lack of systematic classification of biomass fuels based on thermogravimetric analysis and general methods to interpret such measurements. There are quantitative differences between thermogravimetric characteristics of different biomasses. They are affected by several factors such as biomass species, the geographical origin, the age or the specific part of the plant. Different experimental apparatus and conditions also cause differences in the results.

Biomass pyrolysis and gasification are complex processes and involve different reactions at different temperatures. There is no single kinetic model explaining universally the rates for the thermal degradation of biomass [72].

The mass-loss curves generated during TGA runs allows the determination of the degree of conversion during pyrolysis and gasification at different heating rates. Different methods are

used to find kinetic parameters such as activation energy, reaction order and the pre-exponential factor.

Two different approaches were used to calculate kinetic parameters here: a differential method and an integral method.

5.4.1 Differential method:

In this method, a differential equation represents the thermal degradation of lignin at a given heating rate. Other researchers have also used the same method to study kinetic parameters of lignin and biomass thermal degradation [72, 73]. The general thermal decomposition taking place when a sample of lignin is heated in a TGA can be represented by Eq (17).

$$A(s) \rightarrow B(s) + C(g) \quad \textbf{(17)}$$

The rate of reaction can be expressed as dx/dt

$$dx/dt = k\, f(x) \quad \textbf{(18)}$$

where f(x) is a function related with conversion and depends on the reaction mechanism. x is degree of conversion, t is reaction time and k is the reaction rate coefficient.

x is defined as

$$x = (w_0-w_t)/(w_0-w_\infty) \quad \textbf{(19)}$$

where w_0 is initial mass of sample, w_t is the instantaneous mass of sample at time t and w_∞ is the final mass of the sample at the end of the process.

For simple nth order reactions, the function f(x) can be defined as Eq (20).

$$f(x) = (1-x)^n \quad \textbf{(20)}$$

As per the Arrhenius equation, the rate constant is defined at Eq (21),

$$k = A\exp(-E/RT) \quad \textbf{(21)}$$

where A is the pre-exponential (frequency) factor, E is the activation energy, R is the gas constant, and T is the reaction temperature.

After substituting values of k and f(x), the rate of reaction equation becomes

$$dx/dt = A\exp(-E/RT)(1-x)^n \quad \textbf{(22)}$$

The non-isothermal heating rate is defined as Eq (23)

$$\beta = dT/dt \quad \textbf{(23)}$$

With constant heating rate, the rate equation (22) can be written as

$$dx/dT = (A/\beta) \exp(-E/RT)(1-x)^n \quad \textbf{(24)}$$

After rearranging, Eq (24) is converted to

$$\ln(dx/dT) - n\ln(1-x) = \ln(A/\beta) - E/RT \quad \textbf{(25)}$$

The plot of $\ln(dx/dT) - n\ln(1-x)$ versus $1/T$ gives a straight line for a value of reaction order n. $(-E/R)$ is the slope of the line and $\ln(A/\beta)$ is the y intercept. The slope of the line is used to calculate the activation energy E. All the calculations were done assuming first order reaction model.

5.4.1.1 MWV lignin kinetic parameters:

The MWV lignin kinetic study was done using the differential method. Figure 74 shows a plot of $\ln(dx/dT) - n\ln(1-x)$ versus $1/T$ for pyrolysis kinetics of MWV lignin between 230 ºC – 395 ºC. The pyrolysis reaction starts after 205 ºC and this temperature range gives a straight line for the kinetic study. The plot for gasification kinetics between 730 ºC – 775 ºC for MWV lignin is shown in Figure 75 using the differential method. The TGA results showed that gasification for

MWV lignin takes place after heating up to 700 ºC and continues during extended holding at a temperature of 800 ºC.

From the slopes, the calculated values of the activation energy for pyrolysis and gasification are 34 kJ/mol and 214 kJ/mol respectively. These values show that there is a big increase in the value of activation energy from pyrolysis to gasification for MWV lignin. Calculated parameters from the differential method are listed in Table 9 and are compared with those from the integral method. All the kinetic plots are shown in Appendix A.

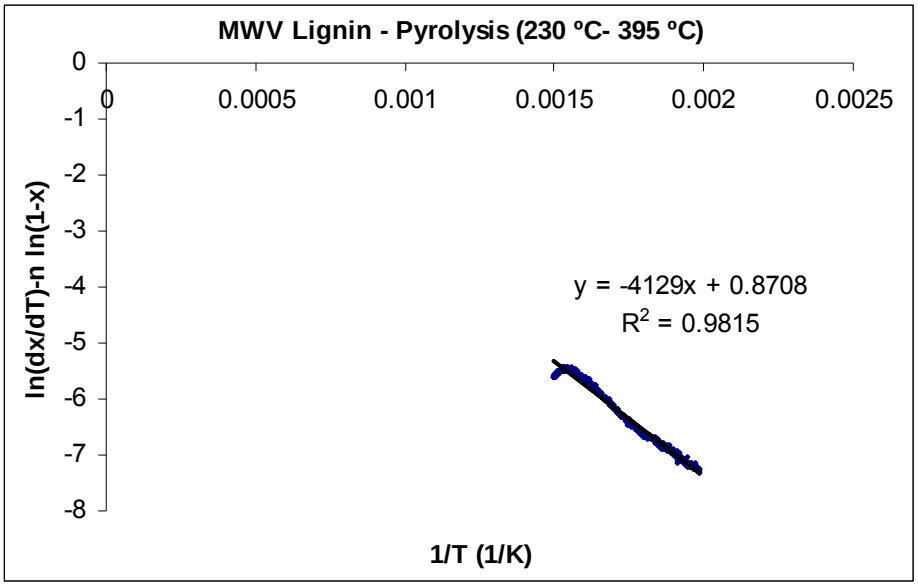

Figure 74: Kinetic plot using the differential method for MWV lignin pyrolysis between 230 ºC – 395 ºC

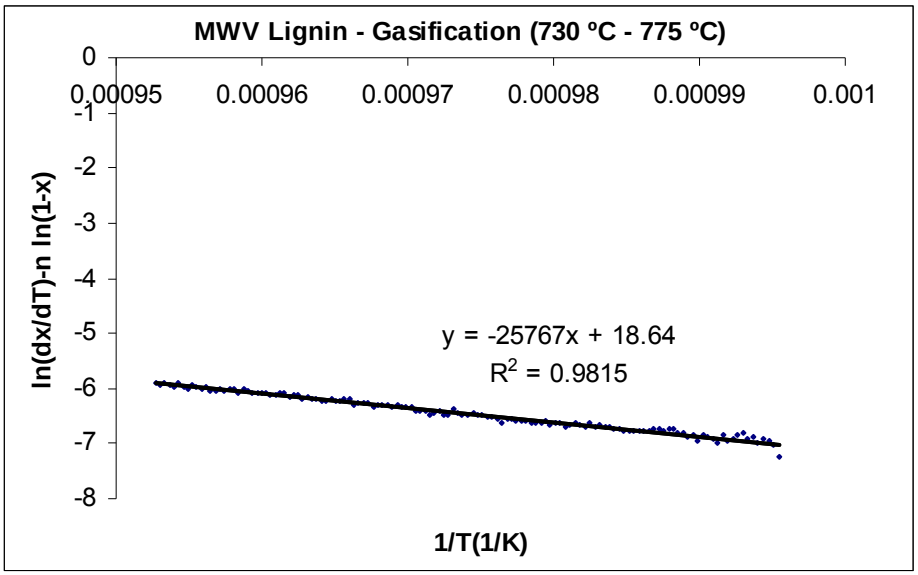

Figure 75: Kinetic plot using the differential method for MWV lignin gasification between 730 ºC – 775 ºC

Kinetic plots were also made for MWV lignin after addition of Na_2CO_3 for pyrolysis and gasification reactions. Figure 78 and 79 [Appendix A] represents ln(dx/dT) – nln(1-x) versus 1/T curves for pyrolysis and gasification reaction after Na_2CO_3 addition between the temperatures of 230 ºC – 380 ºC and 680 ºC – 780 ºC respectively.

The activation energy values for MWV lignin pyrolysis and gasification with Na_2CO_3 addition were 27 kJ/mol and 220 kJ/mol respectively. These results also show that the activation energy is higher for gasification than for pyrolysis. The devolatilization activation energy is slightly lower with Na_2CO_3 addition than without Na_2CO_3 addition. The gasification energy remained the same within experimental errors.

5.4.1.2 SA lignin kinetic parameters:

SA lignin kinetic parameters were also calculated with the differential method after plotting ln(dx/dT) – nln(1-x) versus 1/T curves for pyrolysis phases I and II. Phase I refers to the devolatilization reactions. SA lignin showed a secondary reaction after 680 ºC and kinetic parameters were calculated for this phase II. For SA lignin, gasification does not take place until the sample is kept for an extended holding time at 800 ºC. For this reason the activation energy and pre-exponential factor were not calculated for gasification.

Figures A.1.3 and A.1.4 [Appendix A] show the kinetic plots for pyrolysis phases between 230 ºC – 330 ºC (I) and 650 ºC – 740 ºC (II) respectively. The values of the activation energy were found to be 63 kJ/mol and 113 kJ/mol for pyrolysis phases I and II. The pyrolysis phase II shows higher activation energy than the phase I. The activation energy for SA lignin devolatilization was higher than that for MWV lignin devolatilization.

Figures A.1.5 and A.1.6 [Appendix A] show the ln(dx/dT) – nln(1-x) versus 1/T curves for pyrolysis – phases I and II, respectively for SA lignin after Na_2CO_3 addition. Values obtained for pyrolysis I and II phase activation energy are 50 kJ/mol and 184 kJ/mol. Also with this lignin, the addition of Na_2CO_3 decreased the activation energy for devolatilization (pyrolysis phase I).

5.4.2 Integral method:

In another approach, an integral method was used to obtain kinetic parameters. This approach has been previously used by different researchers for kinetic studies [74-77].

For non isothermal conditions,

$$g(x) = \int_{T_0}^{T} (A/\beta)\exp(-E/RT)dT \approx \int_{0}^{T} (A/\beta)\exp(-E/RT)dT \quad \textbf{(26)}$$

This equation can be integrated by the Coats- Redfern method [78].

$$\int_{0}^{T} e^{-E/RT}dT \approx \frac{RT^2}{E}(1-2RT/E)e^{-E/RT} \quad \textbf{(27)}$$

$$\ln\frac{g(x)}{T^2} = \ln[\frac{AR}{\beta E}(1-2RT/E)] - E/RT \quad \textbf{(28)}$$

For most conditions energies 2RT/E is << 1 and can be neglected.

Eq (28) can be rewritten as [74],

$$\ln\frac{g(x)}{T^2} = \ln\left(\frac{AR}{\beta E}\right) - E/RT \quad \textbf{(29)}$$

or

$$\ln G(x) = -E/RT + \ln\left(\frac{AR}{\beta E}\right) \quad \textbf{(30)}$$

where

for n = 1 $$G(x) = -\frac{\ln(1-x)}{T^2} \quad \textbf{(31)}$$

for n ≠ 1 $$G(x) = \frac{1-(1-x)^{1-n}}{(1-n)T^2} \quad \textbf{(32)}$$

For a given reaction order, G(x) varies linearly with 1/T and the slope gives the value of the activation energy E. The pre-exponential factor A can be calculated from the intercept. All the results were obtained assuming first order reaction kinetics for both MWV and SA lignin.

5.4.2.1 MWV lignin kinetic parameters:

Kinetic parameters were also calculated using the integral method and were compared with those of the differential method. When comparing both methods, results showed some similarity as well as differences. lnG(x) vs. 1/T was plotted for the pyrolysis reaction between 230 ºC – 395 ºC and showed a straight line [Figure 76]. The calculated value of activation energy was 33 kJ/mol. In the case of gasification reaction between 730 ºC – 775 ºC, a steep slope was obtained [Figure 77]. The activation energy for MWV lignin gasification was 353 kJ/mol. When compared to the results from the differential method, the calculated activation energy using the integral method was very similar for the pyrolysis phase but higher for the gasification stage.

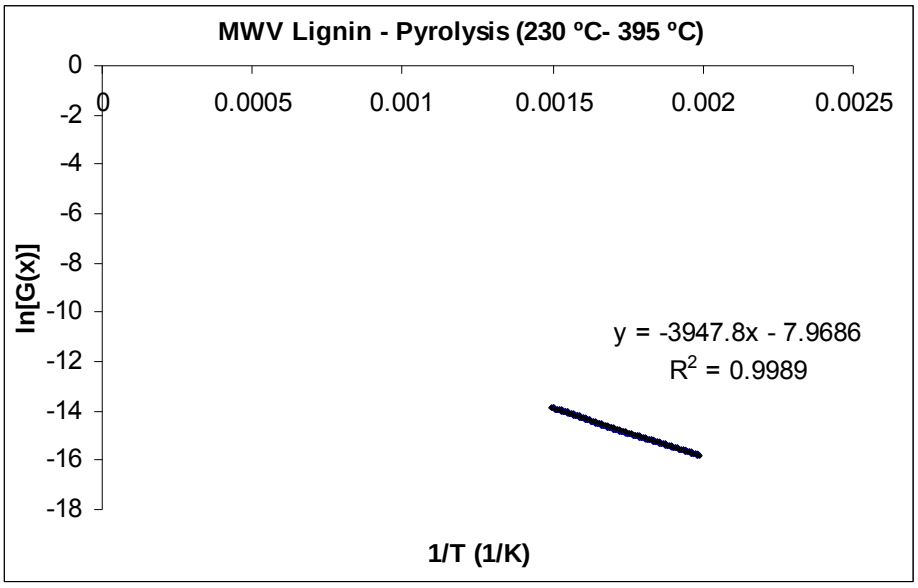

Figure 76: Kinetic plot using integral method for MWV lignin pyrolysis between 230 ºC – 395 ºC

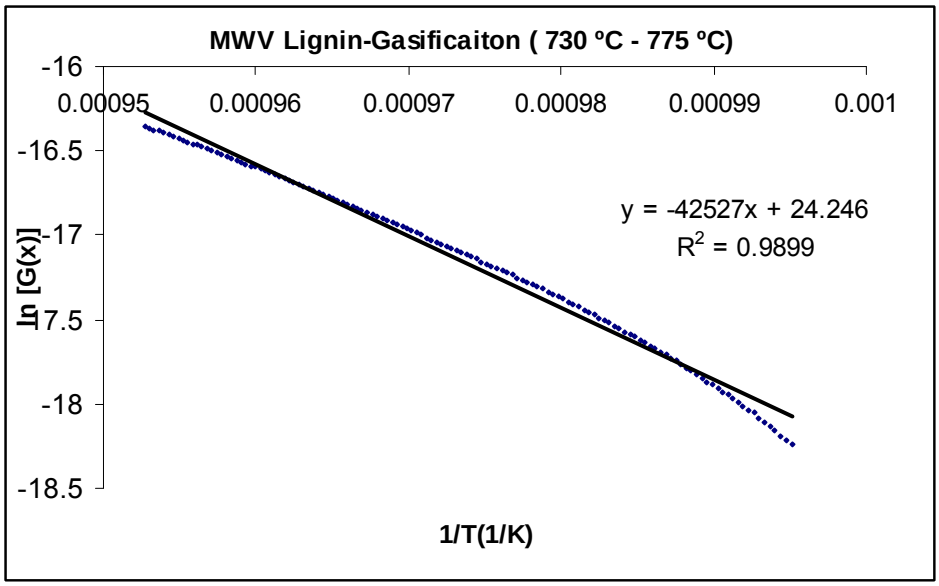

Figure 77: Kinetic plot using the integral method for MWV lignin gasification between 730 ºC – 775 ºC

Kinetic plots for pyrolysis and gasification with the addition of Na_2CO_3 were linear. Figures A.2.1 and A.2.2 [Appendix A] show the kinetic plots for pyrolysis and gasification reactions for the temperature range between 230 ºC – 380 ºC and 730 ºC – 775 ºC respectively. The calculated values of the activation energy were found to be 28 kJ/mol and 381 kJ/mol for pyrolysis and gasification respectively. With this material as well, both the differential and the integral method gave similar activation energies but for the gasification activation energy, the integral method gave significantly higher activation energy than the differential method. The integral method also suggested that the addition of Na_2CO_3 slightly decreased the devolatilization activation energy.

5.4.2.2 SA lignin kinetic parameters:

Kinetic plots for SA lignin using the integral method were linear for devolatilization and secondary pyrolysis phases. Figures A.2.3 and A.2.4 [Appendix A] show the kinetic plots for phase I and II of pyrolysis respectively. For the phase I pyrolysis the activation energy was 39 kJ/mol and the phase II pyrolysis gave a value of 238 kJ/mol. As also seen earlier, the pyrolysis phase II showed a higher value of activation energy than the pyrolysis phase I using the integral method. However, the activation energies by the differential and the integral methods were quite different.

Figures A.2.5 and A.2.6 show the kinetic curves for SA lignin + Na_2CO_3 pyrolysis phase I and II. For the pyrolysis phase I, the graph was not as linear as other graphs and gave a lower activation energy value [Figure A.2.5]. The curves gave activation energy values of 13 kJ/mol

for the phase I and a higher value of 273kJ/mol for the phase II. The impact of Na_2CO_3 addition on the activation energies was the same as obtained by the differential method (decrease in the activation energy for phase I pyrolysis and an increase for phase II pyrolysis) though the activation energies by the two methods were quite different.

Table 9 shows the kinetic parameters during different temperature ranges using the differential and integral methods.

Table 9: Activation energy and pre-exponential factor values for SA lignin and MWV lignin using differential and integral methods

		Activation Energy (kJ/mol)		A (s^{-1})	
Sample	**Temperature Range**	**Differential Method**	**Integral Method**	**Differential Method**	**Integral Method**
MWV Lignin	230 ºC – 395 ºC (Pyrolysis)	34	32	0.79	0.45
	730 ºC – 775 ºC (Gasification)	214	353	$4.1*10^{7}$	$4.8*10^{14}$
MWV Lignin + Na_2CO_3	230 ºC – 380 ºC (Pyrolysis)	27	27	0.20	0.17
	650 ºC – 740 ºC (Gasification)	220	381	$4.7*10^{8}$	$6.0*10^{16}$
SA Lignin	230 ºC – 330 ºC (Pyrolysis – I)	63	39	$9.7*10^{2}$	5.4
	680 ºC – 740 ºC (Pyrolysis – II)	113	238	$2.7*10^{2}$	$2.4*10^{10}$
SA Lignin + Na_2CO_3	230 ºC – 330 ºC (Pyrolysis – I)	50	13	0.17	$7.6*10^{-3}$
	680 ºC – 740 ºC (Pyrolysis – II)	183	273	$1.34*10^{7}$	$1.6*10^{12}$

Results obtained from the present study are compared with results from previous pyrolysis studies of lignin by different researchers [Table 10].

Table 10: Activation energy and pre-exponential factor values for lignin pyrolysis in the current and previous studies

Studies	**Sample**	**Temperature Range**	**Activation Energy (kJ/mol)**	**A (s^{-1})**
Present (Differential Method)	MWV Lignin SA Lignin SA Lignin	230 ºC – 395 ºC 230 ºC – 330 ºC 650 ºC – 740 ºC	34 63 113	0.79 $9.7*10^{2}$ $2.7*10^{2}$
Present (Integral Method)	MWV Lignin SA Lignin SA Lignin	230 ºC – 395 ºC 230 ºC – 330 ºC 650 ºC – 740 ºC	32 39 238	0.45 5.4 $2.4*10^{10}$
Ferdous et al. [38]	Alcell Lignin Kraft Lignin	272 ºC – 532 ºC 234 ºC – 503 ºC	129 – 361 80 – 158	$10^{11} – 10^{22}$ $10^{7} – 10^{9}$
Liu et al. [77]	Fir Lignin Birch Lignin	149 ºC – 492 ºC 154 ºC – 427 ºC	72 – 136 87 – 141	$10^{7} – 10^{9}$ $10^{8} – 10^{12}$
Wang et al. [79]	Lignin from Alfa Aesar Company	100 ºC – 600 ºC	120 – 197	$10^{6} – 10^{11}$
Cordero et al. [71]	Eucalyptus Kraft Lignin	200 ºC – 900 ºC	36.7	0.655
Murgan et al. [42]	Alcell Lignin	71 ºC – 259 ºC	8 – 68	$10^{3} – 10^{26}$

The present study found the values of activation energy to range from 32 kJ/mol to 34 kJ/mol and the values of the pre-exponential factor to range between 0.45 s^{-1} – 0.79 s^{-1} for MWV lignin at low temperatures. For phase I pyrolysis, the SA lignin showed activation energies to range from 39 kJ/mol to 63 kJ/mol with pre-exponential factors of 5.4 s^{-1} – 9.7*10^2 s^{-1}. For SA lignin II phase, the activation energy ranged between 113 kJ/mol to 238 kJ/mol and the pre-exponential factor between 2.7*10^2 s^{-1} and 2.4*10^{10} s^{-1}.

There have been a number of studies of kinetic parameters of lignin pyrolysis. Cordero et al. [71] used a first-order overall rate equation for the entire conversion and obtained kinetic energy and pre-exponential factor of 36.7 kJ/mol and 0.655 s^{-1} respectively. Liu et al. [77] studied fir and birch lignin pyrolysis and found that the reaction at lower temperature has an activation energy of 70-90 kJ/mol and about 135 – 142 kJ/mol at higher temperature. They also found that the activation energies of birch lignin pyrolysis are higher than those of fir lignin. In the present study results using both the differential and integral methods suggest that the activation energy at higher temperature is higher than that at lower temperature.

Ferdous et al. [38] calculated the activation energy for kraft lignin to be between 80 – 158 kJ/mol in the temperature range of 234 ºC – 503 ºC. Murgan et al. [42] studied Alcell lignin and calculated the activation energy in the range of 8 – 68 kJ/mol between 71 ºC – 259 ºC. Wang et al. [79] did a TG study of lignin from Alfa Aesar Company and found activation energy ranged between 120 kJ/mol. to 197 kJ/mol.

Rodriguez-Mirasol et al. [23] studied the partial CO_2 gasification of eucalyptus kraft lignin in the temperature range from 750 ºC – 900 ºC and found activation energy to range from 212 kJ/mol to 239 kJ/mol. In an another study Rodriguez-Mirasol et al. [80] found the activation energy in the range of 216 – 241 kJ/mol for CO_2 gasification of kraft lignin char.

The differential and integral methods give comparable results at low temperatures but at higher temperatures much variation was experienced. For the higher temperature range, both the methods give higher activation energy than at lower temperatures. Previous studies have also suggested that the activation energy increases with increase in the temperature range.

For the differential method, with the addition of Na_2CO_3 the activation energy decreased at lower temperature but increased at higher temperature. Also for the integral method, the activation energy decreased with the addition of Na_2CO_3 during devolatilization phase but increased during phase II pyrolysis and gasification stages. Using the integral method, the calculated values of activation energy during secondary pyrolysis and gasification stages were quite high. The values for the gasification activation energy by the integral method here were higher than those found in previous studies. Based on the present study, the differential method gives overall values of the kinetic parameters that are more consistent with previous studies. However, both methods gave similar impacts of the addition of Na_2CO_3 on the activation energies.

CHAPTER VI

CONCLUSIONS

This thesis studied the pyrolysis and gasification of lignin using two different reactors, a LEFR and a TGA. The study also included the effect of alkali addition on pyrolysis and gasification of lignin using a TGA. Changes in lignin structure with increase in temperature were studied using an FTIR. The kinetic parameters were also calculated and compared using differential and integral methods for pyrolysis and gasification in the TGA.

Gasification studies of primary sludge and artificial sludges mixed with filler showed limited reproducibility and a better feeding system is needed for consistent results. After gasification, unbleached liner shows more fixed C remaining than bleached pulp does, which is attributed to the higher lignin content in unbleached liner. Filler addition to the pulps did not show any significant effect on the gasification rate.

SA lignin has higher char yield than MWV lignin at both the temperatures, 800 °C and 1000 °C in the LEFR experiments. During MWV lignin gasification, the char yield decreases from 32% to 27% at 1s as the temperature is increased from 800 °C to 1000 °C. The gasification of SA lignin shows a decrease in char yield from 62% to 57% over the same temperature increase.

There is not much difference between pyrolysis and gasification experiments in the LEFR. Most of the organic decomposition of lignin takes place during initial devolatilization and the additional small decrease in char yield occur because of the reactions of inorganics present in the

sample. Primary devolatilization is complete during the initial residence time of 0.3 – 0.5 seconds, and the maximum possible residence time of 1.5 second is too short for appreciable gasification to occur. As a longer residence time is required for substantial gasification to take place, the LEFR is unsuitable for lignin gasification studies beyond the initial devolatilization at these temperatures. Both lignins show swelling and change in particle morphology during gasification.

During TGA studies, the MWV lignin gives approximately 46% final char yield at both the temperatures, 800 °C and 1000 °C, and SA shows a decrease in the char yield from 40% to 36% with increasing in temperature. For both lignins, primary pyrolysis starts at about 200 °C and the reaction rate progressively increases with temperature and reaches a maximum. SA lignin shows a maximum mass loss rate at 320 °C, which is a lower temperature than that of MWV lignin, which achieves maximum its mass loss rate at 380 °C. For both lignins, the pyrolysis reaction rate decreases up to 600 °C, above which only SA lignin undergoes a secondary mass loss. Na_2CO_3 present in high ash SA lignin is responsible for the secondary reactions.

During gasification both the lignins show a secondary mass loss region which is due to carbon gasification reactions. CO_2 suppresses the Na_2CO_3 decomposition reaction and a higher amount of ash and sodium in the SA lignin does not lead to a higher reaction rate. Secondary gasification reactions during MWV lignin gasification start at 650 °C and continues through 800 °C. After the initial slow secondary reaction significant SA lignin gasification does not begin until the sample has been held at 800 °C for some time.

The results showed that Na_2CO_3 addition had both positive and negative effect on the reaction rate. The addition of Na_2CO_3 made the primary pyrolysis reaction occur at a lower rate but enhanced the rate for the secondary reaction. MWV lignin with Na_2CO_3 addition corresponding to the difference in the Na content between the two lignins experienced a higher reaction rate at 600 – 800 °C than did either the MWV or the SA lignin. It suggests that all Na in SA lignin is not present as Na_2CO_3. Na_2CO_3 addition to MWV lignin increases the gasification rate immediately with no delay in the gasification as was experienced with the original SA lignin. It shows that Na catalyzes the gasification rate.

The presence of Na_2CO_3 in the SA lignin does not explain the differences during gasification between the low-ash MWV lignin and the high-ash SA lignin. Na_2CO_3 increased the gasification rate already at temperatures below 800°C whereas gasification was suppressed in the high-ash lignin.

The addition of different amounts of Na_2CO_3 shows that the gasification rate increases proportionally to the amount of added Na. For carbon pyrolysis and gasification Na_2SO_4 is a more efficient catalyst than Na_2CO_3. Results with varying amounts of CO_2 suggest that above a certain value, the gasification rate is not affected by CO_2 concentration.

The FTIR study showed that the spectra of both lignins have similarities as well as differences. For MWV lignin and SA lignin, the loss of spectral features starts at 320 °C and 465 °C, respectively. This change corresponds to the maximum mass loss rate of the lignins. There were limited differences between the FTIR peaks from pyrolysis and gasification of both the lignins.

Study of kinetic parameters showed that both differential and integral methods gave a higher activation energy at high temperature than at lower temperatures. The activation energy for MWV lignin was between 32 kJ/mol - 34 kJ/mol for initial devolatilization phase I and between 214 kJ/mol – 353 kJ/mol for gasification. SA lignin pyrolysis phase I showed activation energies in the range of 39 kJ/mol to 63 kJ/mol; the pyrolysis phase II gave 113 kJ/mol to 238 kJ/mol

The differential and integral methods gave comparable results at low temperatures but showed variations at higher temperatures. For both methods, the activation energy decreases with the addition of Na_2CO_3 during the devolatilization phase but increases during phase II pyrolysis and gasification stages. The differential method shows overall more consistent results than the integral method.

APPENDIX A

KINETIC PLOTS

Kinetic plots of MWV lignin and SA lignin:

A.1: Differential method

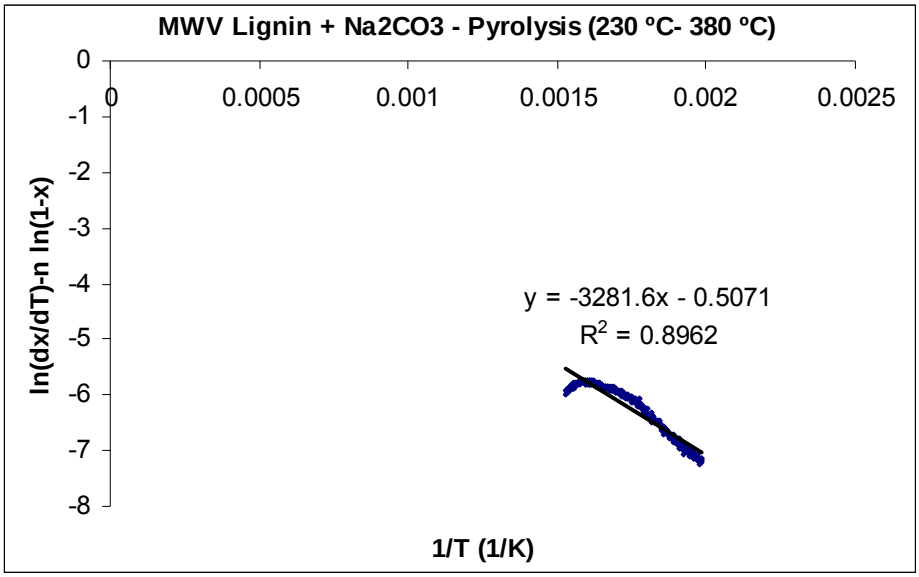

Figure A.1.1: Kinetic plot using the differential method for MWV lignin + Na_2CO_3 pyrolysis between 230 ºC – 380 ºC

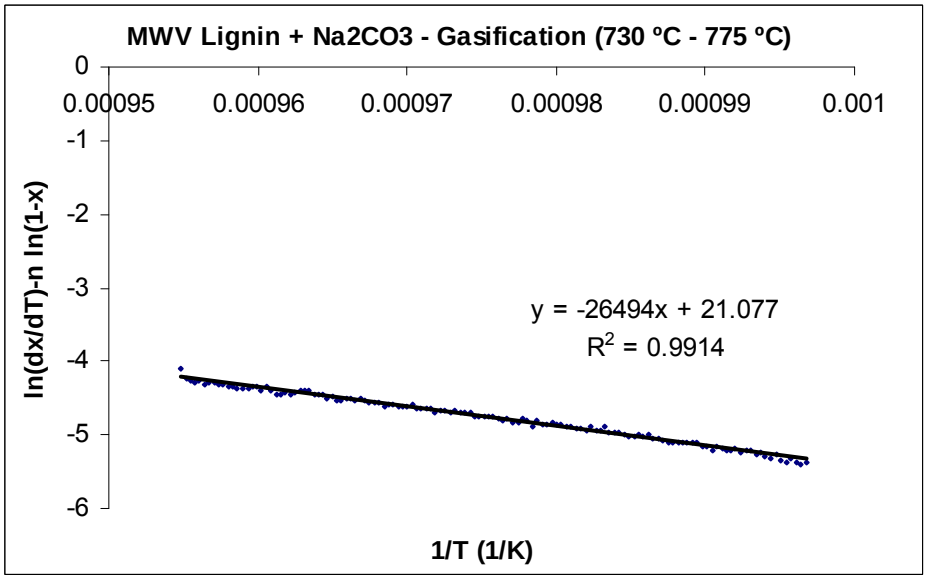

Figure A.1.2: Kinetic plot using the differential method for MWV lignin + Na_2CO_3 gasification between 730 ºC – 775 ºC

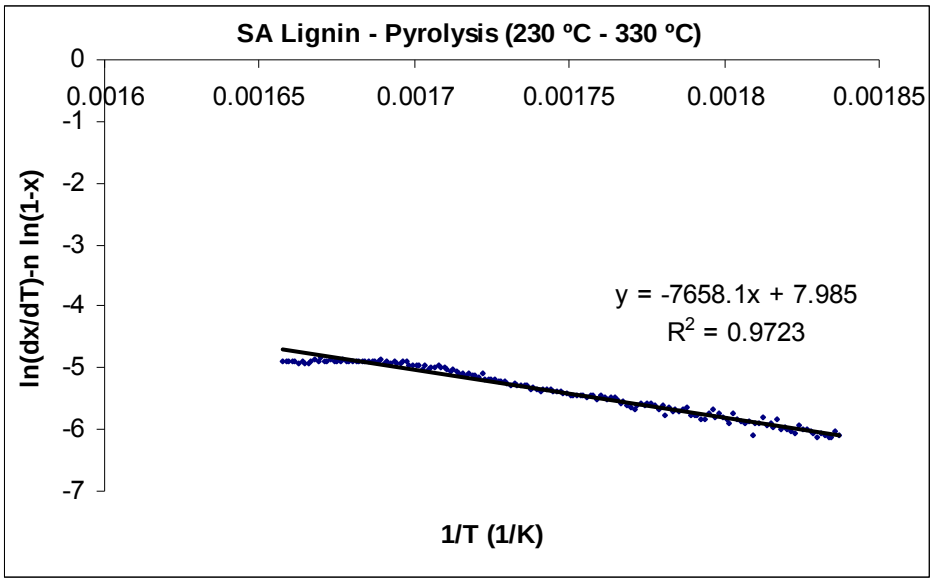

Figure A.1.3: Kinetic plot using the differential method for SA lignin pyrolysis – phase I between 230 ºC – 330 ºC

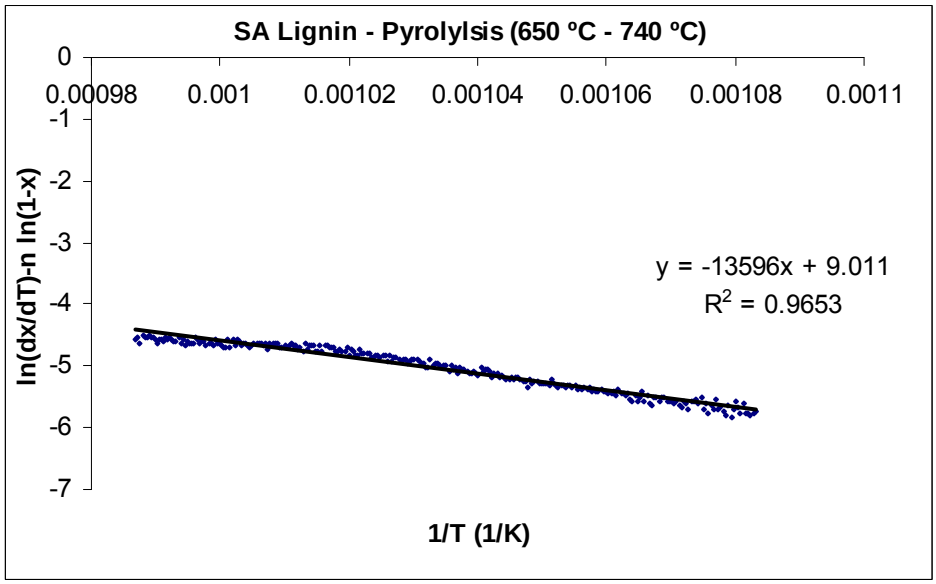

Figure A.1.4: Kinetic plot using the differential method for SA lignin pyrolysis – phase II between 650 ºC – 740 ºC

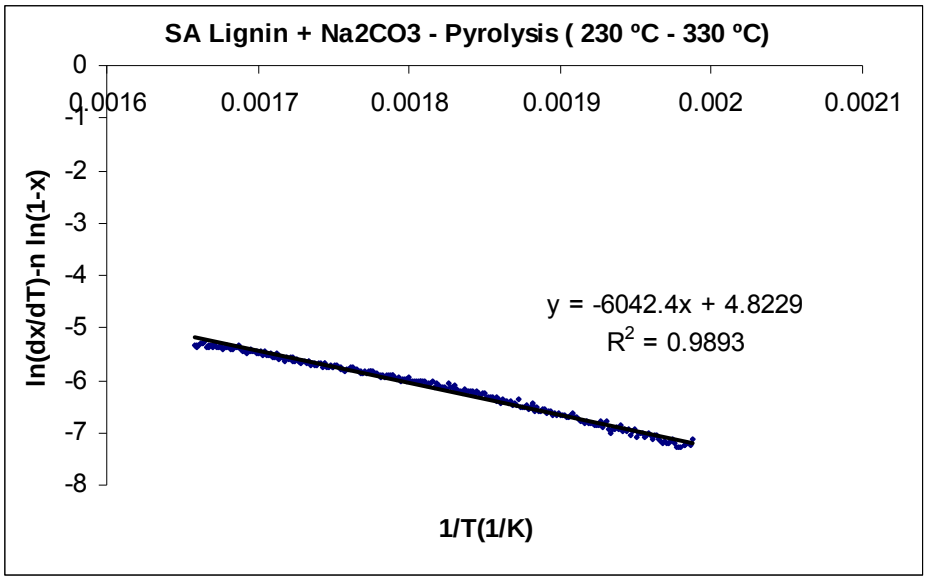

Figure A.1.5: Kinetic plot using the differential method for SA lignin + Na_2CO_3 pyrolysis – I phase between 230 ºC – 330 ºC

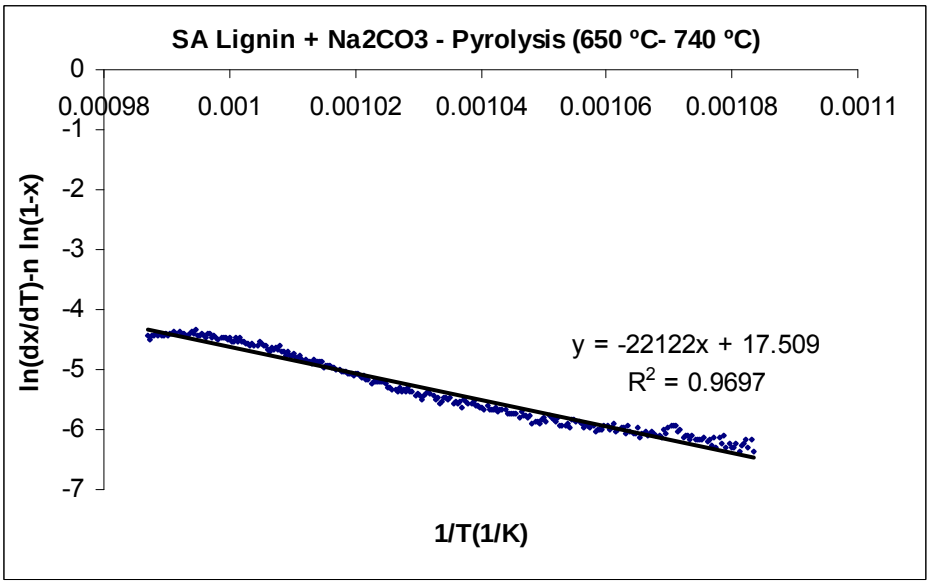

Figure A.1.6: Kinetic plot using the differential method for SA lignin + Na_2CO_3 pyrolysis – II phase between 650 ºC – 740 ºC

A.2 Integral Method:

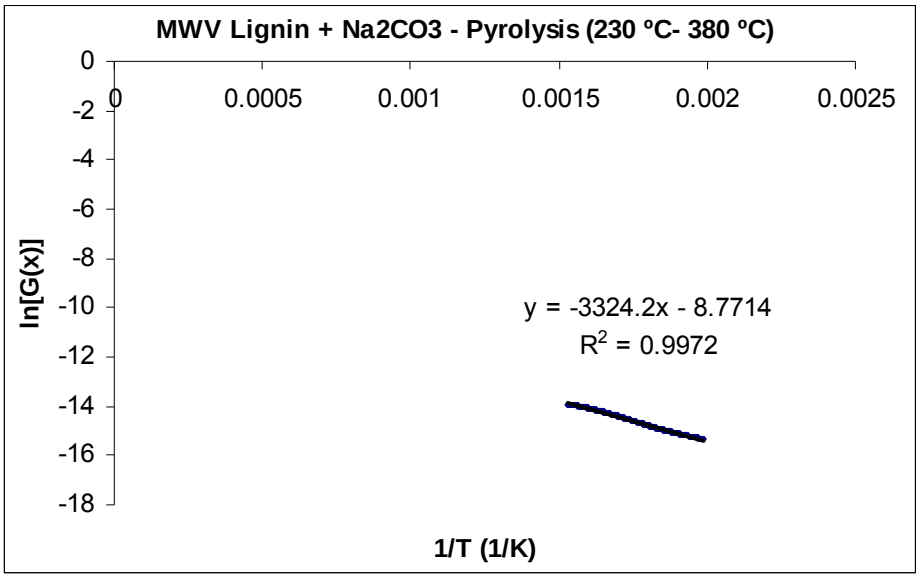

Figure A.2.1: Kinetic plot using the integral method for MWV lignin pyrolysis + Na_2CO_3 between 230 ºC – 380 ºC

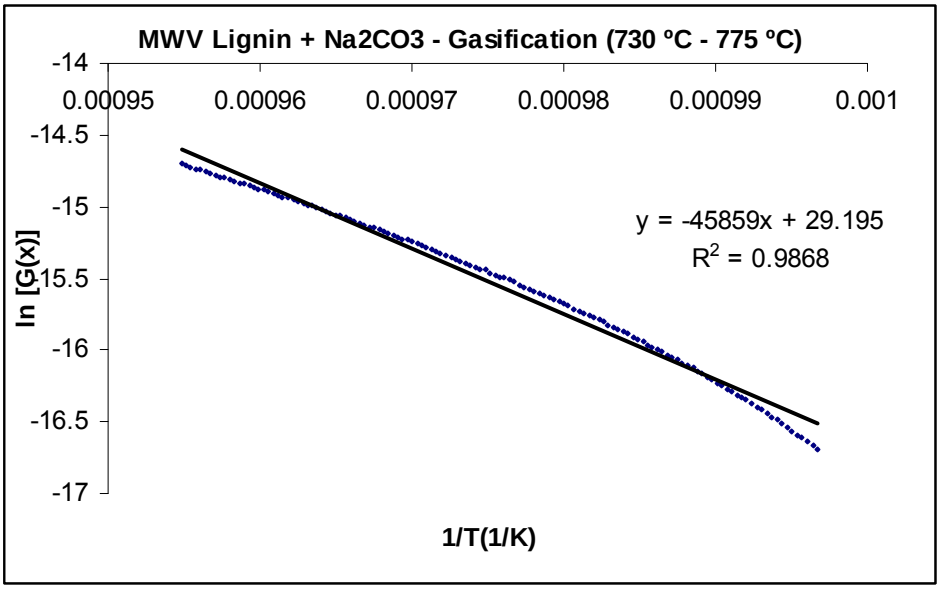

Figure A.2.2: Kinetic plot using the integral method for MWV lignin gasification + Na_2CO_3 between 730 ºC – 775 ºC

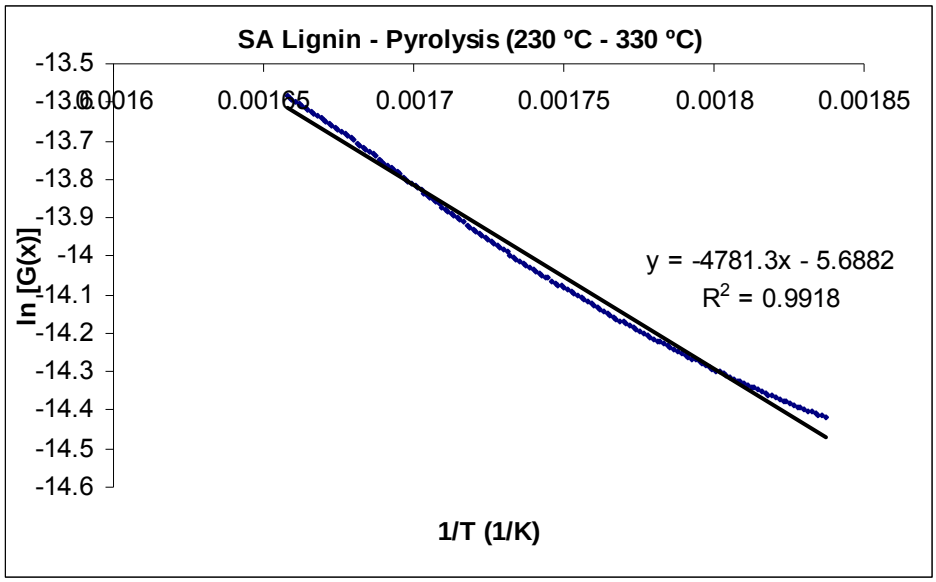

Figure A.2.3: Kinetic plot using the integral method for SA lignin pyrolysis – I phase between 230 ºC – 330 ºC

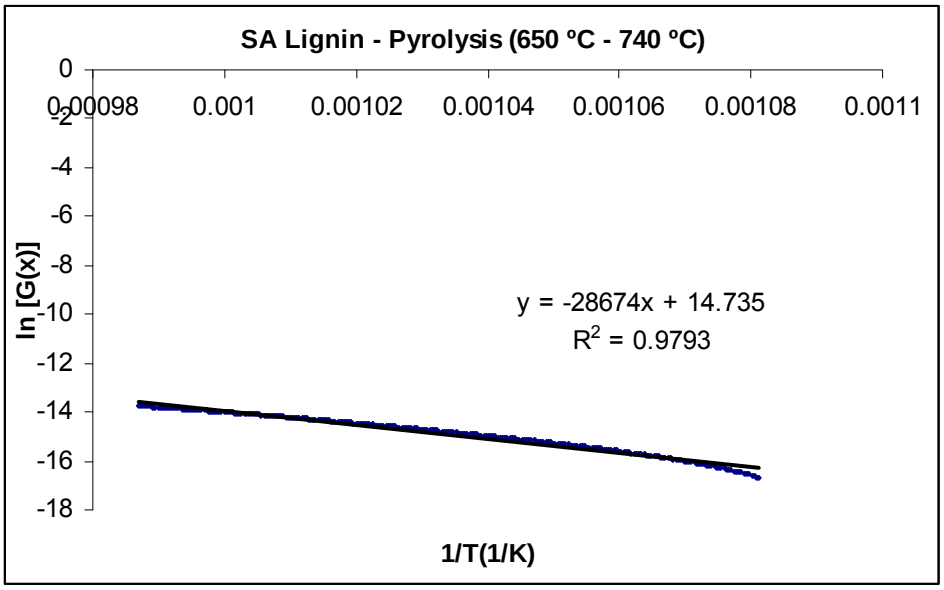

Figure A.2.4: Kinetic plot using the integral method for SA lignin pyrolysis – II phase between 650 ºC – 740 ºC

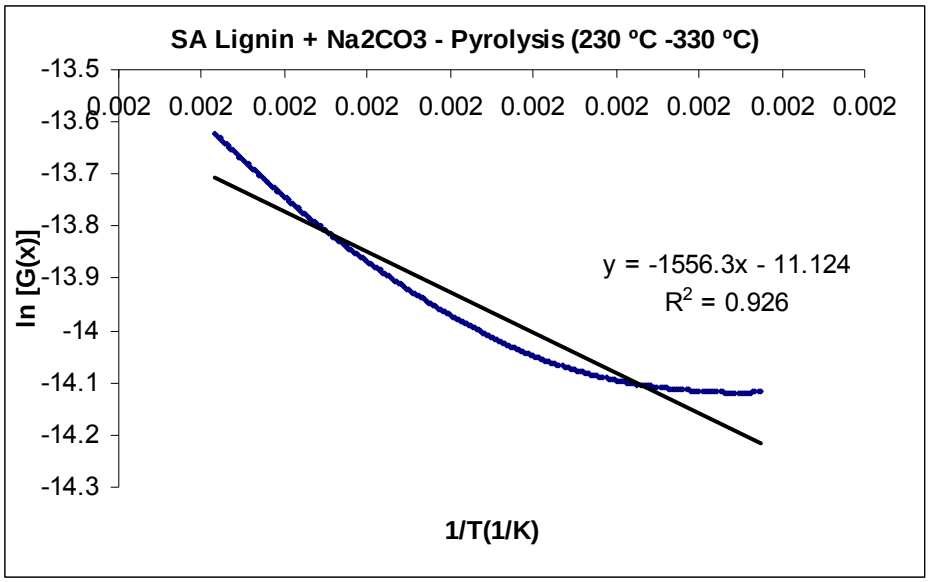

Figure A.2.5: Kinetic plot using integral method for SA lignin + Na_2CO_3 pyrolysis – II phase between 230 ºC – 330 ºC

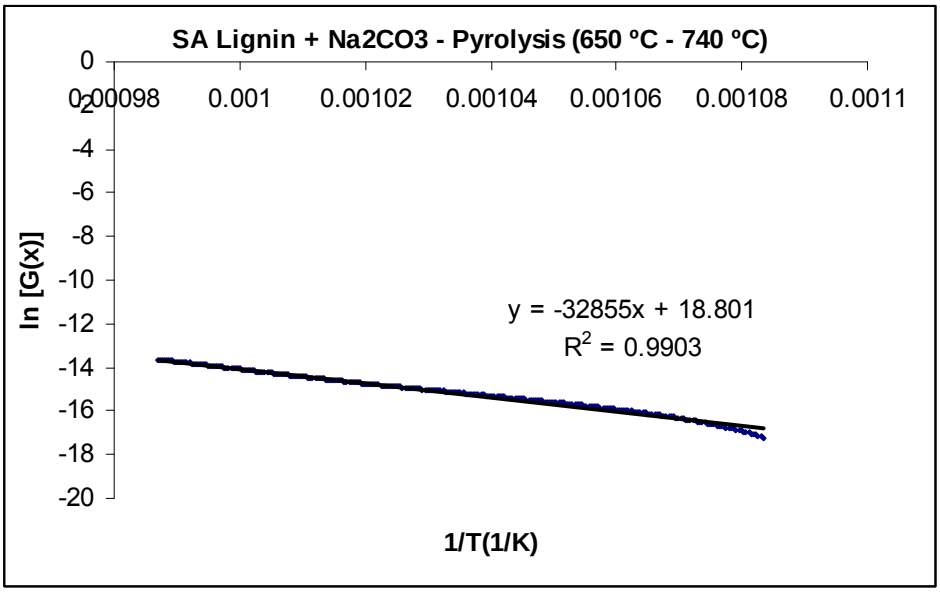

Figure A.2.6: Kinetic plot using the integral method for SA lignin + Na_2CO_3 pyrolysis – II phase between 650 ºC – 740 ºC

REFERENCES

1. Reed, T.B. and Gaur S., S*urvey of Biomass Gasification 2001, 2nd edition*, National Renewable Energy Laboratory, BEF Press, 2001

2. Reed, T. B. *Biomass Gasification, Principles and Technology*, Noyes Data Corporation, New Jersey, 1981.

3. Sricharoenchaikul, V., *Fate of carbon-containing compounds from gasification of Kraft black liquor with subsequent catalytic conditioning of condensable organics*, Ph.D. Thesis, Georgia Institute of Technology, Atlanta, 2001.

4. Rezaiyan, J., and Cheremisinoff N. P., *Gasification Technologies, A Primer for Engineers and Scientists*, ed. Heinemann, H., CRC Press, Taylor & Francis Group, Boca Raton, FL, 2005.

5. Belgiorno V., Feo De G., Rocca Della and Napoli R. M. A., Energy from gasification of solid wastes, *Waste Management*, 2003, 23, 1-15.

6. Whitty, K., *Pyrolysis and Gasification Behavior of Black Liquor under Pressurized Conditions*, Ph.D. Thesis, Abo Akademi, Finland, 1997.

7. http://www.cogeneration.net/IntegratedGasificationCombinedCycle.htm

8. Hayashi, J.-I., Takashashi, H., Iwatsuki, M., Essaki, K., Tsutsumi, A. and Chiba, T., Rapid conversion of tar and char from pyrolysis of a brown coal by reactions with steam in a drop-tube reactor, *Fuel* 2000, *79*, 439-447.

9. Gil, J., Caballero, M. A., Martin, J. A., Aznar, M. P. and Corella, J., Biomass Gasification with Air in a Fluidized Bed: Effect of the In-Bed Use of Dolomite under Different Operation Conditions. *Industrial & Engineering Chemistry Research,* 1999, 38, 4226 – 4235.

10. Jorapur, R. and Rajvanshi A. K., Sugarcane Leaf-Bagasse Gasifiers for Industrial Heating Applications, *Biomass Bioenergy,* 1997, 13, 141-146.

11. Drift A.Doorn, J. and Vermeulen, J.W., Ten residual biomass fuels for circulating fluidized-bed gasification, *Biomass Bioenergy,* 2001, 20, 45-56.

12. Gil, J., Aznar, M.P., Caballero, M.A., Frances, E. and Corella, J., Biomass Gasification in Fludized Bed at Pilot Scale with Steam-Oxygen Mixtures, Product Distribution for Very Different Operating Conditions, *Energy Fuels*, 1997, 11, 1109-1118.

13. Delgado, J., Aznar, M. P. and Corella, J., Calcined Dolomite, Magnesite, and Calcite for Cleaning Hot Gas from a Fluidized Bed Biomass Gasifier with Steam: Life and Usefulness. *Industrial & Engineering Chemistry Research*, 1996, 35, 3637-3643.

14. Smook, G.A., *Handbook for pulp and paper technologists*, ed. M. J. Kocurek, TAPPI and CPPA, Montreal, Quebec, Canada, 1982.

15. http://www.fos.su.se/~magnuss/conclusions.html

16. Tejado, A., Pena, C., Labidi, J., Echeverria J. M. and Mondragon, I., Physico-chemical characterization of lignins from different sources for use in phenol-formaldehyde resin synthesis, *Bioresource Technology*, 2007, 98, 1655 – 1663.

17. Sharma, R. K., Wooten, J. B., Baliga, V. L., Lin, X., Chan, W. G. and Hajaligol M. R., Characterization of chars from pyrolysis of lignin, *Fuel*, 2004, 83, 1469 – 1482.

18. Guerra, A., Filpponen, I., Lucia, L. A. and Argyropoulos, D. S., Comparative evaluation of three lignin isolation protocols for various wood species, *Journal of Agricultural and Food Chemistry*, 2006, 54, 9696-9705.

19. Ikeda, T., Holtman, K., Kadla, J., Chang H. and Jameel, H. Studies on the effect of ball milling on lignin structure using a modified DRFC method., *Journal of Agricultural and Food Chemistry*, 2002, 50, 129 – 135.

20. Wu, S. and Argyropoulos, D. S., An improved method for isolating lignin in high yield and purity, *Journal of Pulp and Paper Science*, 2003, 27, 671 – 677.

21. http://www.lignin.org/01augdialogue.html

22. Adams, T. N., Frederick, W. J., Grace, T. M., Hupa, M., Iisa, K., Jones, A. K. and Tran, H., *Kraft Recovery Boiler*, Tappi Press, Atlanta, Georgia, 1997.

23. Rodriguez-Mirasol J., Cordero T. and Rodriguez J.J., Activated carbons from CO_2 partial gasification of eucalyptus Kraft lignin. *Energy & Fuels*, 1993, 7, 133-138.

24. Rodriguez-Mirasol J., Cordero T. and Rodriguez J. J., Preparation and characterization of activated carbons from eucalyptus Kraft lignin, *Carbon*, 1993, 31, 87-95.

25. Eriksson, H. and Harvey, S., Black liquor gasification – consequences for both industry and society, *Energy*, 2004, 29, 581 – 612.

26. Kamm, B., Gruber, P.R. and Kamm, M. *Biorefineries – Industrial Processes and Products,* Status Quo and Future Directions Vol 2, Wiley-VCH Verlag GmbH & Co. KGaA, Weinheim, Germany, 2006.

27. Kamm, B., Gruber, P.R. and Kamm, M., *Biorefineries – Industrial Processes and Products,* Status Quo and Future Directions Vol 1, Wiley-VCH Verlag GmbH & Co. KGaA, Weinheim, Germany, 2006.

28. Heiningen, A. V., Converting a kraft pulp mill into an integrated forest biorefinery [IFBR], *Department of chemical and biological engineering*, University of Maine, Orono, ME, USA. http://www.forestbioproducts.umaine.edu/ForestBiorefinery.pdf

29. Wise, L.E., *Wood Chemistry*, American Chemistry Society Monographs, Series No. 97, 1946.

30. Nowakowski, D. J., Jones, J., Brydson, R. M. D. and Ross, A. B., Potassium catalysis in the pyrolysis behaviour of short rotation willow coppice, *Fuel*, 2007, 86, 2389 – 2402.

31. Raveendran, K., Ganesh, A. and Khilar, K.C., Pyrolysis characteristics of biomass and biomass components, *Fuel*, 1996, 75, 987-998.

32. Yang, H.,Yan, R., Chen, H., Zheng, C., Lee, D. H. and Liang, D. T., In-Depth Investigation of Biomass Pyrolysis Based on Three Major Components: Hemicellulose, Cellulose and Lignin, *Energy and Fuel*, 2006, 20, 388-393.

33. Srivastava, V.K. and Jalan, R. K., Predictions of concentration in the pyrolysis in the yrolysis of biomass materials – I, *Energy Conversion and Management*, 1994, 35, 1031-1040.

34. Boutin, O., Ferrer, M. and Lede, J., Radiant flash pyrolysis of cellulose – Evidence for the formation of short life time intermediate liquid species, *Journal of Analytical and Applied Pyrolysis*, 1998, 47, 13-31.

35. Wei, L., Xu, S., Zhang L., Zhang, H., Liu, C., Zhu, H. and Liu, S., Characteristics of fast pyrolysis of biomass in a free fall reactor, *Fuel Processing Technology*, 2006, 87, 863-871.

36. Dominguez, J. C., Oliet, M., Alonso, M. V., Gilarranz, M. A. and Rodriguez, F., Thermal tability and pyrolysis kinetics of organosolv lignins obtained from Eucalyptus globulus, *Industrial Crops and Products*, 2008, 27, 150 – 156.

37. Gosselink, R.J.A., Jong, E. D., Guran, B. and Abacherli, A., Co-ordination network for lignin-standardisation, production and applications adapted to market requirements, (Eurolignin), *Industrial Crops and Products*, 2004, 20, 121-129.

38. Ferdous, D.; Dalai, A. K. Bej, S. K. and Thrigh, R. W., Pyrolysis of Lignins: Experimental and Kinetics Studies, *Energy & Fuels*, 16, 1405-1412.

39. Ferdous, D., Dalai, A. K., Bej, S. K., Thrigh, R. W and Bakhshi N.N., Production of H_2 and medium Btu gas via pyrolysis of lignins in a fixed-bed reactor, *Fuel Processing Technology*, 2001, 70, 9-26.

40. Caballero, J. A., Font R. and Marcilla A., Study of the primary pyrolysis of Kraft lignin at high heating rates: yields and kinetics, *Journal of Analytical and Applied Pyrolysis*, 1996, 36, 159 – 178.

41. Caballero, J. A., Font R., Marcilla A. and Garcia A.N., Flash pyrolysis of Klason lignin in a Pyroprobe 1000. *Journal of Analytical and Applied Pyrolysis,* 1993, 27, 221 – 244.

42. Murugan, P., Mahinpey, N., Johnson, K. E. and Wilson, M., Kinetics of the pyrolysis of lignin using thermogravimetric and differential scanning calorimetry methods, *Energy & Fuels*, 2008 , 22, 2720 – 2724.

43. Fushimi. C., Araki, K., Yamaguchi, Y. and Tsutsumi, A., Effect of Heating Rate on Steam Gasification of Biomass with a Thermogravimetric Reactor. 1. Reactivity of Char. *Industrial and Engineering Chemistry Research*, 2003, 42, 3922-3928.

44. Fushimi, C., Araki, K., Yamaguchi, Y. and Tsutsumi, A. Effect of Heating Rate on Steam Gasification of Biomass. 2. Thermogravimetric-Mass Spectrometric (TG-MS) Analysis of Gas Evolution. *Industrial and Engineering Chemistry Research*, 2003, 42, 3929-3936.

45. Pasquali C. E. L. and Herrera, H., Pyrolysis of lignin and IR analysis of residues, *Theromchimica Acta*, 1997, 293, 39-46.

46. Willner T., Brunner G. Pyrolysis Kinetics of Wood and Wood components, *Chemical Engineering & Technology*, 2005, 28, 1212 – 1225.

47. Guzman, J. A., Olivares, M. and Saavedra, A., Study of thermal degradation of lignin derivatives, in Grassi, G., Delmon, G., Molle, J.F.; Zibetta (Eds.), *Biomass for Energy and Industry, 4th E.C. Conference* – 1987, 1024-1030.

48. Gustafsson, C. and Richards, T., Pyrolysis kinetics of washed precipitated lignin, *Bioresources*, 2009, 4(1), 26 – 37.

49. Matsukata, M., Kikuchi, E. and Morita, Y., A new classification of alkali and alkaline earth catalysts for gasification of carbon, *Fuel*, 1992, 71, 819 – 823.

50. McKee, D.W., Gasification of graphite in carbon dioxide and water vapor-the catalytic effects of alkali metal salts, *Carbon*, 1982, 20, 59 – 66.

51. Wigmans, T., Doorn, J. V. and Moulijn, J. A., Temperature-programmed desorption study of Na_2CO_3-containing activated carbon, *Fuel*, 1983, 62, 190 – 195.

52. Wigmans, T., Goebel, G. C. and Moulijn, J. A., The influence of pretreatment conditions on the activity and stability of sodium and potassium catalysts in carbon-steam reactions, Carbon, 1983, 21, 295 - 301.

53. Mudge, L. K., Sealock, L.J. Jr. and Weber, S.L., Catalyzed steam gasification of biomass, *Journal of Analytical and Applied Pyrolysis*, 1979, 1, 165-175.

54. Biagini, E., Barontini, F. and Tognotti, L., Devolatilization of biomass components studied by TG/FTIR technique, *Industrial and Engineering Chemistry Research*, 2006, 45, 4486 – 4493.

55. Sricharoenchaikul, V., Hicks, A. L. and Frederick, W. J., Carbon and char residue yields from rapid pyrolysis of kraft black liquor, *Bioresource Technology*, 2001, 77, 131-138.

56. Sricharoenchaikul, V., Frederick and W. J., Agrawal, P., Carbon distribution in char residue from gasification of kraft black liquor, *Biomass and Bioenergy*, 2003, 25 , 209-220.

57. Flaxman, R. J. and Hallett, W. L. H., Flow and particle heating in an entrained flow reactor, *Fuel*, 1987, 66, 607-611.

58. Willard, H.H., Merritt, L.L. Jr., Dean, J. A. and Settle, F. A. Jr., *Instrumental Methods of Analysis,* 7th edition, Wadsworth Publishing Company, Belmont, California, 1988.

59. SSC 5200 Series, *Comprehensive Brochure on Thermal Analysis System*, SII – Seiko Instruments.

60. Frederick, W. J., Iisa, K., Lundy, J. R., O'Conner, W. K., Reis, K., Scott, A. T., Sinquefield, S. A., Sricharoenchaikul, V. and Vooren, C.A.V., Energy and materials recovery from recycled paper sludge. *TAPPI Journal*, 1996, 79 -6, 123-131.

61. Young, C., *Pressure effects on black liquor gasification*, Ph.D. Thesis, Georgia Institute of Technology, Atlanta, 2006.

62. R.T. Hallen, L.T. Sealock, R. Cuello and A.V. Bridgwater In: J.L. Kuester, Editor, *Research in Thermochemical Biomass Conversion*, Elsevier Applied Science, London 1988, 157.

63. El- Saied, H. and Nada, A. M. A., The thermal behavior of lignin from wasted black pulping liquors, *Polymer Degradation and Stability*, 1993, 40, 417-421.

64. Sun, R. C., Tomkinson, J. and Jones, G. L., Fractional characterization of ash-AQ lignin by successive extraction with organic solvent from oil palm EFB fibre, *Polymer Degradation and Stability*, 2000, 68, 111-119.

65. Kapteijn, F., Meijer, R. and Moulijn, J. A., Kinetics and Mechanism of the Alkali Catalyzed Gasification of Carbon, *International Conference on Coal Science Proceedings*, Sept 16-20, 1991, University of Newcastle-upon-Tyne, UK; Butterworth: Oxford, 1991, 295-298.

66. Fredrick, W. J., Wag, K. J. and Hupa, M. M., Rate and Mechanism of Black Liquor Char Gasification with CO_2 at Elevated Pressure, *Industrial Engineering Chemistry Research*, 1993, 32, 1747 – 1753.

67. Baker, E. G. and Mudge, L. K., Mechanism of catalytic biomass gasification, *Journal of Analytical and Applied Pyrolysis*, 1984, 6, 285-297.

68. Mudge, L. K., Baker, E. G., Mitchell, D. H. and Brown, M. D., Catalytic steam gasification of biomass for methanol and methane production, *Journal of Solar Energy Engineering*, 1985, 107, 89 – 92 .

69. Hergert, H.L., *Infrared Spectra*, in Sarkanen, K.V. and Ludwing, C.H. (Eds.). *Lignins: Occurance, Formation, Structure and Reaction*, Wiley – Interscience, New York, 1971, 268-272.

70. Bilba, K. and Ouensanga, A., Fourier Transform infrared spectroscopic study of thermal degradation of sugar cane bagasse, *Journal of Analytical and Applied Pyrolysis*, 1996, 38, 61 – 73.

71. Cordero, T., Rodriguez-Maroto, J. M., Rodriguez-Mirasol J. and Rodriguez, J.J, On the kinetics of thermal decomposition of wood and wood components; *Thermochimica Acta*, 1990, 164, 135-144.

72. Munir, S., Daood, S. S., Nimmo, W., Cunliffe, A. M. and Gibbs, B. M., Thermal analysis and devolatilization kinetics of cotton stalk, sugar cane bagasse and shea meal nitrogen and air atmospheres, *Bioresource Technology*, 2009, 100, 1413-1418.

73. Zhang, X., Xu, M., Sun, R. and Sun, L., Study of biomass pyrolysis kinetics, *Journal of Engineering for Gas Turbine and Power*, 2006, 128, 493 – 496.

74. Yang, H., Yan, R., Chin, T., Liang, D. T., Chen, H. and Zheng, C., Thermogravimetric Analysis – Fourier Transform Infrared Analysis of palm oil waste pyrolysis, *Energy and Fuels* 2004, 18, 1814 – 1821.

75. Fang, M.X., Shen, D. K., Li, Y.X., Yu, C. J., Luo, Z. Y. and Cen, K. F., Kinetic study on pyrolysis and combustion of wood under different oxygen concentrations by using TG-FTIR analysis, *Journal of Analytical and Applied Pyrolysis,* 2006, 77, 22 – 27.

76. Chen, J.H. and Li, C. R., *Thermal Analysis and Application*, Science Press: Beijing, China, 1985, 10.

77. Liu, Q., Wang, S., Zheng, Y., Luo, Z. and Cen, K., Mechanism study of wood lignin pyrolysis by using TG-FTIR analysis, *Journal of Analytical and Applied Pyrolysis*, 2008, 82, 170 -177.

78. Coats, A. W. and Redfern, J. P., Kinetic Parameters from Thermogravimetric Data, *Nature*, 1964, 201, 68-69.

79. Wang, G., Li, W., Li, B. and Chen, H., TG study on pyrolysis of biomass and its three components under syngas, *Fuel*, 2008, 87, 552 – 558.

80. Rodriguez-Mirasol, J., Cordero, T. and Rodriguez, J. J., CO_2-Reactivity of eucalyptus kraft lignin chars, *Carbon*, 1993, 31, 53-61.